ACSNANO

www.acsnano.org

REVIEW

Emerging Strategies in Stimuli-Responsive Prodrug Nanosystems for Cancer Therapy

Chendi Ding,[Δ] Chunbo Chen,[Δ] Xiaowei Zeng, Hongzhong Chen,* and Yanli Zhao*

Cite This: *ACS Nano* 2022, 16, 13513−13553

Read Online

ACCESS | Metrics & More | Article Recommendations

ABSTRACT: Prodrugs are chemically modified drug molecules that are inactive before administration. After administration, they are converted *in situ* to parent drugs and induce the mechanism of action. The development of prodrugs has upgraded conventional drug treatments in terms of bioavailability, targeting, and reduced side effects. Especially in cancer therapy, the application of prodrugs has achieved substantial therapeutic effects. From serendipitous discovery in the early stage to functional design with pertinence nowadays, the importance of prodrugs in drug design is self-evident. At present, studying stimuli-responsive activation mechanisms, regulating the stimuli intensity *in vivo*, and designing nanoscale prodrug formulations are the major strategies to promote the development of prodrugs. In this review, we provide an outlook of recent cutting-edge studies on stimuli-responsive prodrug nanosystems from these three aspects. We also discuss prospects and challenges in the future development of such prodrugs.

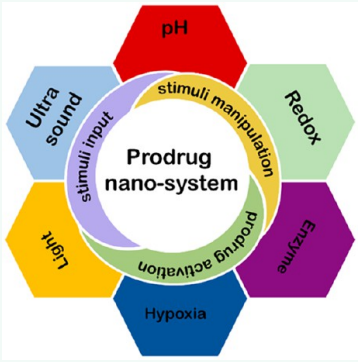

KEYWORDS: *biomedical nanotechnology, cancer therapy, controlled release, drug delivery, nanomedicine, nanoscale prodrugs, on-demand activation, stimuli responsiveness*

Recent decades have witnessed the explosion of advanced cancer therapies, including surgery, chemotherapy, radio therapy, gene therapy, photodynamic and photothermal therapies (PDT/PTT), and immunotherapy. Among them, chemotherapy has been widely adopted in clinical use as an effective therapeutic technique. Despite great progress worldwide, there are still serious drawbacks for chemotherapy, such as a lack of specificity and systemic toxicity. A series of strategies have been explored to overcome these drawbacks, including the fabrication of various drug delivery systems to load chemotherapy drugs and the construction of stimuli-responsive activable prodrugs. Although the drug delivery systems have been extensively investigated and utilized in the laboratory and the clinic, they still need further upgrade to overcome low drug loading content, premature drug leakage, and insufficient drug release.

Prodrugs are derivatives of drug molecules in which the activity of the drugs is temporarily blocked by modifying the active sites to alleviate toxicity in normal tissues and improve bioavailability. Currently, prodrugs account for approximately 10% of marketed drugs worldwide.[1] When prodrugs accumulate at the tumor site and are activated with endogenous (e.g., enzymes, reducing environment, reactive oxygen species (ROS), acidity, and hypoxia)[2] or exogenous stimuli (e.g., light and ultrasound),[3,4] they can be converted to active forms for enhanced toxicity. With the participation of these stimuli, especially exogenous stimuli, the prodrug activation process can be combined with many advanced therapeutic methods, including PDT and immunotherapy, to achieve synergistic cancer treatment. Due to on-command activation at the tumor tissues, prodrugs exhibit higher specificity than parent drugs to improve the chemotherapy performance, leading to better therapeutic outcomes and fewer side effects. Most chemotherapy drugs suffer from poor water solubility, having a short circulation lifetime because of the intrinsic hydrophobicity. In comparison, the prodrugs often show enhanced aqueous solubility. The self-assembly of macromolecular prodrugs or amphiphilic prodrugs can lead to nanosized particles, which not only endow the chemotherapy drugs with better pharmacokinetics due to improved dispersity in water but also enhance the drug accumulation efficacy at the tumor tissues by the enhanced permeability and retention (EPR) effect.[5] Through the formation of the prodrugs, the water solubility and *in vivo* circulation time of the drugs are improved, the side effects of chemotherapy are alleviated, and the specificity and performance are enhanced.

Received: June 1, 2022
Accepted: August 26, 2022
Published: September 1, 2022

https://doi.org/10.1021/acsnano.2c05379
ACS Nano 2022, 16, 13513−13553

Table 1. Examples of Recently Developed Prodrugs in Clinical Trials and in Market

prodrug products	action mechanisms	therapeutic objectives	status	ref
MLN9708 (ixazomib citrate)	ester linkage hydrolysis induced activation	lymphoma, triple-negative breast cancer	in market	6
fosaprepitant dimeglumine	phosphatase induced activation	non-small-cell lung cancer with alleviated nausea	in market	7
uridine triacetate	esterase induced prodrug activation	colon cancer	in market	8
aldoxorubicin	acid-responsive hydrazone linker cleavage	soft tissue sarcomas	phase III	9
TH-302	hypoxia-responsive prodrug activation	pancreatic ductal adenocarcinoma, head and neck squamous cell carcinoma	phase III	10
AST-3424	aldo-keto reductase-responsive prodrug activation	liver, non-small-cell lung, and gastric cancer	phase II	11

Scheme 1. Schematic Illustration of Stimuli-Responsive Activation Process of Prodrug Nanosystems and Various Kinds of Stimuli for Prodrug Activation

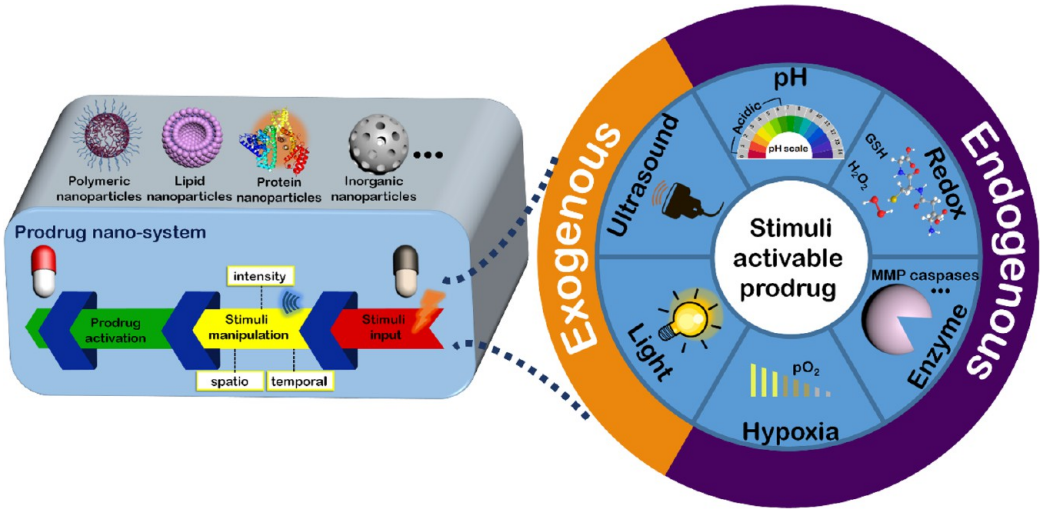

Scheme 2. (A) pH Values in Blood, Tumor Microenvironment, Endosome, and Lysosome and (B) Representative Acid-Activable Chemical Structures

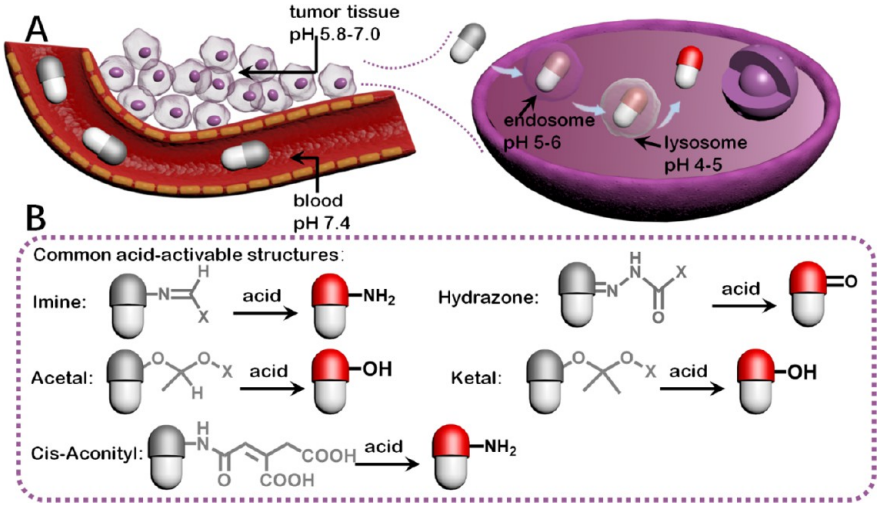

For oncology-related prodrugs, their arrival brings a series of benefits including improved pharmacological properties and clinical efficacy and alleviated side effects. Examples are summarized in Table 1.[6−11]

At present, investigating stimuli-responsive activation mechanisms, regulating the stimuli intensity *in vivo*, and designing nanoscale prodrug formulations have greatly improved the development of prodrugs (Scheme 1). In this review, we discuss recent progress in developing stimuli-responsive prodrug nanosystems for cancer therapy from these three aspects. Based on different types of stimuli-responsiveness, the prodrug activation mechanisms are summarized in each subsection, and the methods of precisely controlling stimuli are reviewed. The preparation methods of such prodrugs into nanoscale formulations are also discussed. Finally, challenges accompanying the rapid development of stimuli-responsive prodrug nanosystems and the future prospects are provided. We hope this review will provide

https://doi.org/10.1021/acsnano.2c05379
ACS Nano 2022, 16, 13513−13553

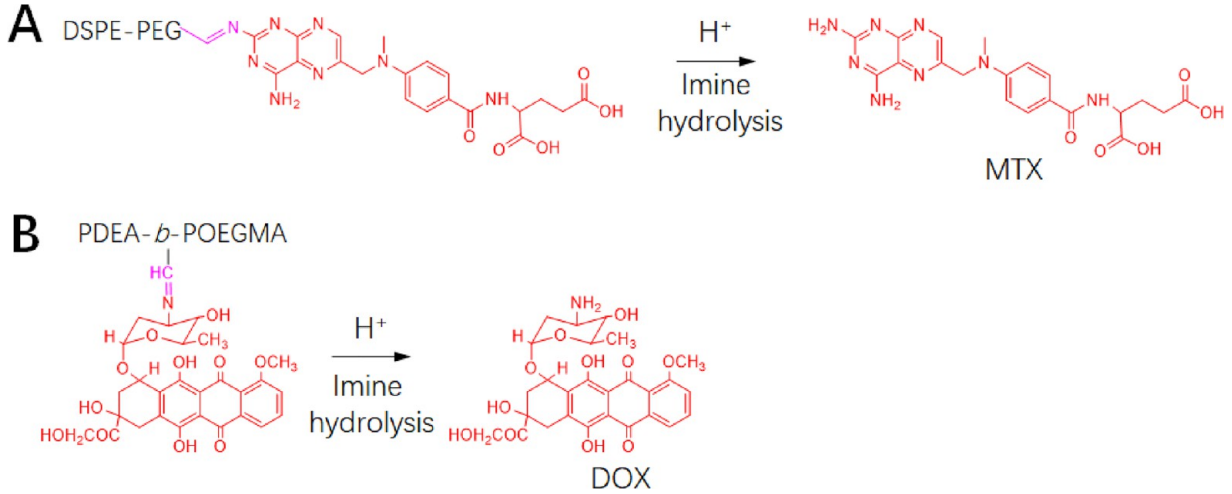

Figure 1. Imine functionalized prodrugs for acid-triggered anticancer therapy. (A) Structure of MTX prodrug with imine linkage. The structures were redrawn according to ref 16. (B) Schematic design of imine functionalized DOX prodrug for acid-responsive chemotherapy and PTT. The structures were redrawn according to ref 17.

design guidance for researchers to advance further progress on stimuli-responsive prodrugs.

pH-ACTIVABLE PRODRUGS

pH-Responsive Chemical Structures for Developing Prodrugs. It is well-known that the pH in tumor tissues is lower than that in normal tissues because of the high conversion rate of glucose to lactic acid, the generation of CO_2 in cancer cells, and abnormal vascular type proton pumps in solid tumors.[12] For normal tissues, the pH is approximately 7.4, while in tumor tissues, pH ranges from 5.8 to 7.0. The microenvironment inside the subcellular organelles is much more acidic than the extracellular tumor tissues. The pH of the cytoplasm is about 7.0, while the pH is much lower in the endosomes and lysosomes, which are 5−6 and 4−5, respectively (Scheme 2A).[13,14] This discrepancy is one of the earliest identified tumor characteristics, and therefore, pH-responsive tumor therapy has been intensively developed. Many chemical bonds such as ester and amide linkers can be hydrolyzed under this acidic environment to activate the prodrug and slowly release the parent drug.[15] However, considering more targeted drug delivery purposes, the pH-sensitive functional groups are considered better triggers for fabricating the drug delivery systems for cancer therapy, such as protonable components, acid-labile chemical bonds (Scheme 2B), and acid-unstable inorganic materials. Like the drug delivery systems, acid-labile chemical bonds including *ortho*-ester, hydrazone, acetal/ketal, imine, and *cis*-aconityl have been utilized to construct pH-sensitive prodrugs due to acidic activation linker cleavage cascaded chemical structure transformation. Under the acidic environment, the acid-labile chemical bonds undergo cleavage to convert the prodrugs to their original forms.

Imine. Imine bonds are formed by the condensation of aldehydes or ketones with amine compounds and are cleaved in an acidic environment, which contributes to the development of acid-degradable nanomaterials and endows prodrugs with an acid-activable feature. Theoretically, drugs containing amino groups can be designed as imine functionalized prodrugs. For example, methotrexate (MTX), a hydrophilic folic acid antagonist, has an amino group at the 4-position of the pteridine, which can react with an aldehyde group to produce an acid-labile imine linker. Hou et al. proposed that MTX could be integrated on amphiphilic polymer through this strategy for constructing a nanoscale prodrug (Figure 1A).[16] The amphiphilic MTX prodrug was then coassembled with an epirubicin (EPI)−phospholipid derivative for combinational therapy. The MTX unit had two actions: targeting folate receptors on tumor cells and cancer cell killing function. Compared with the control sample without the imine bond, the nanoscale prodrug showed apparent acid-accelerated MTX release at pH 5.0 with an accumulated release ratio of 80% in 48 h. Along with the disassembly of the nanosystem, EPI was also released concomitantly, leading to an antiproliferation effect on HeLa cells. Doxorubicin (DOX) also has an amino group that can be converted to imine. Cui et al. conjugated DOX to an amphiphilic polymer scaffold via an aromatic imine linkage (Figure 1B).[17] Near-infrared fluorescence dye IR780, a highly efficient photothermal therapeutic agent, was also loaded into the polymer micelles through $\pi-\pi$ stacking between DOX and IR780. In the tumor microenvironment, the polymer micelles exhibited obvious shrunken diameters, facilitating deep penetration of this nanosystem. An *in vitro* drug release study indicated that acid stimulus triggered a marked release of DOX due to hydrolysis of the imine linkage. In addition, with laser irradiation, synergistic PTT−chemotherapy induced tumor growth suppression. Finally, histological analysis of major organs confirmed the biosafety of this nanoscale prodrug.

Hydrazone. Using the hydrazone bond is another strategy to functionalize carbonyl groups in drug molecules and has been extensively used to conjugate anticancer drugs to carrier materials for constructing pH-activable prodrugs. Hydrazone linkages can be obtained by replacing the oxygen atom of the ketone or aldehyde with a hydrazine group, which exhibits a much faster hydrolysis rate in the acidic environment than in the neutral physiological environment. When an acid stimulus is applied, the hydrazone is protonated, followed by hydrolysis to give free hydrazide compounds, as well as carbonyl compounds. Because the carbonyl group is an active site of DOX, the activity of DOX will be blocked after modification of the carbonyl group. In the past decades, the hydrazone linkage has also been widely employed to fabricate prodrugs, especially for DOX. DOX can be designed as the hydrophobic part in an

https://doi.org/10.1021/acsnano.2c05379
ACS Nano 2022, 16, 13513−13553

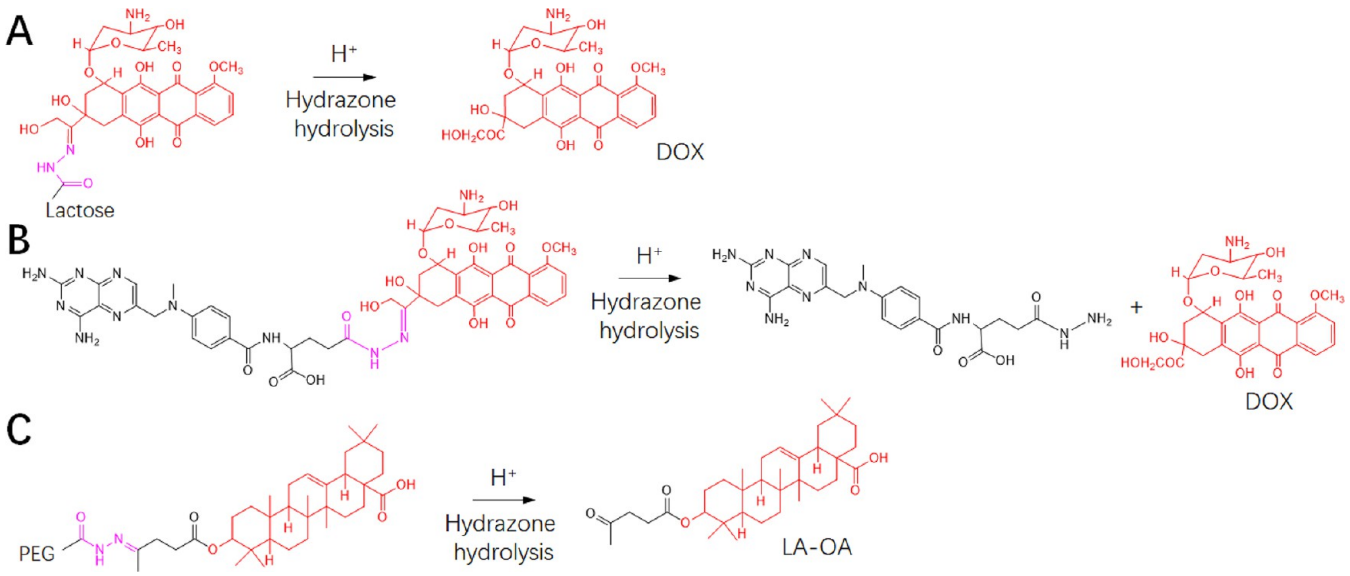

Figure 2. Prodrugs containing hydrazone linkage for acid-responsive activation. (A) Structure of DOX−lactose conjugated amphiphilic prodrug and working mechanism of the acid-triggered activation. The structures were redrawn according to ref 18. (B) Hydrazone-based MTX−DOX prodrug and action mechanism of acid-responsive activation for cancer therapy. The structures were redrawn according to ref 19. (C) Hydrazone functionalized PEG−OA macromolecule and schematic illustration of pH-induced OA activation. The structures were redrawn according to ref 20.

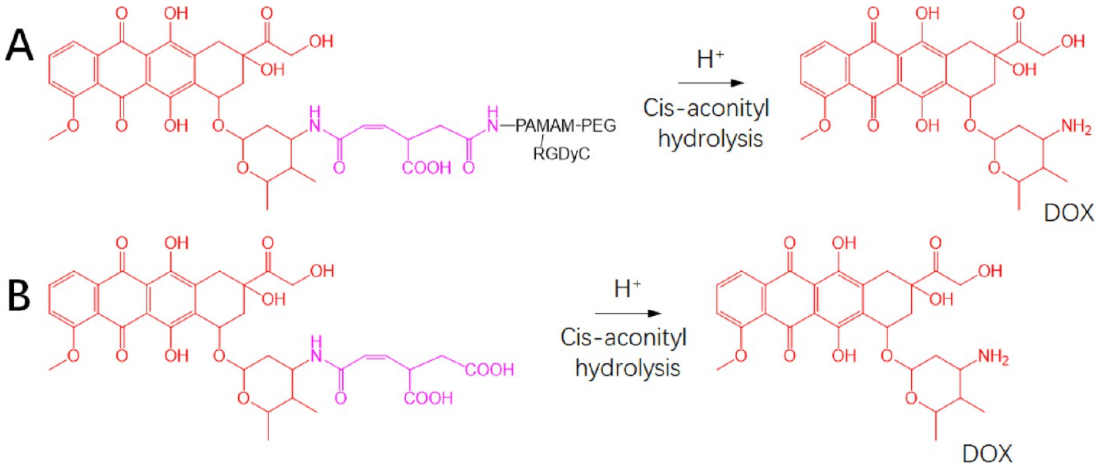

Figure 3. Structures and working mechanisms of *cis*-aconityl functionalized prodrugs for acid-responsive activation. (A) Dendritic DOX prodrug caged by the *cis*-aconityl linkages. The structures were redrawn according to ref 22. (B) Negatively charged *cis*-aconityl modified DOX prodrugs for physical encapsulation via electrostatic and hydrophobic interactions. The structures were redrawn according to ref 23.

amphiphilic self-deliverable molecule. For instance, Yan et al. reported an acid-activable DOX prodrug using a hydrazone linked DOX and a targeting ligand lactose to obtain an amphiphilic molecule (Figure 2A).[18] After self-assembly in water, this prodrug nanoparticle exhibited an average diameter of 172 nm, which met the EPR standard, integrating both passive and active tumor targeting. Under pH 5.5, the DOX−lactose prodrug was rapidly hydrolyzed to release free DOX, demonstrating the great possibility that this nanoscale prodrug can be activated after entering tumor cells. In comparison, a negligible amount of free DOX was detected under neutral conditions. As a result, *in vivo* anticancer studies showed that this prodrug nanoparticle exhibited a tumor inhibition effect in SMMC-7721 tumor-bearing mice. Xu et al. designed a carrier-free prodrug nanosystem for combination chemotherapy (Figure 2B).[19] MTX can be decorated with the hydrazine moiety on the carboxyl position. Then the DOX molecule as a hydrophobic segment can be attached via hydrazone linkage to an afford amphiphilic prodrug for further assembly into nanoparticles. The prodrug showed pH-dependent DOX release behavior, with 87% of DOX released in 72 h at pH 5.0. Camptothecin (CPT) was also covalently attached to MTX via a disulfide bond. This nanosystem combines three chemotherapeutics with different mechanisms of action to produce a synergistic effect in killing tumor cells, as evidenced by the suppression effect in xenograft-tumor-bearing mice. The hydrazone bond can also integrate drug molecules on a carrier scaffold. Zhao et al. devised an acid-responsive prodrug delivery nanoparticle based on hydrazone structure. They developed a hydrazone-based oleanolic acid (OA) conjugated at the end of a poly(ethylene glycol) (PEG) segment through the formation of a hydrazone bond (Figure 2C).[20] The obtained PEG−OA macromolecule was amphiphilic, allowing further encapsulation of MTX during the formation of micellar

https://doi.org/10.1021/acsnano.2c05379
ACS Nano 2022, 16, 13513−13553

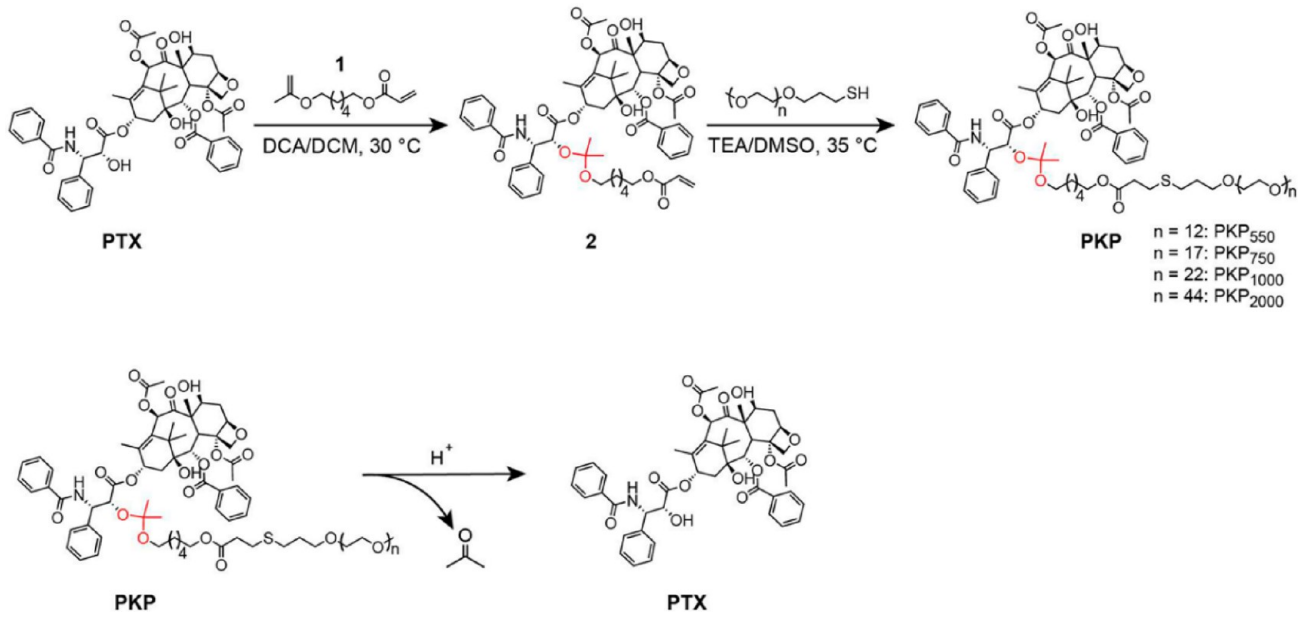

Figure 4. Acetal-based acid-activable PTX prodrugs. Reproduced with permission from ref 25. Copyright 2020 Elsevier.

nanostructure. Apart from antitumor function, the OA component also alleviates the hepatotoxicity of this system since it is introduced as a hepatoprotective compound.[21] At pH 5.0, this nanoscale prodrug was degraded due to acid-accelerated hydrazone cleavage, simultaneously releasing OA and MTX.

cis-Aconityl. With carbonyl and amine groups, DOX has been intensively developed as an acid-responsive prodrug by forming acid-labile bonds. The modification of the amine group on DOX with a *cis*-aconityl linkage is an effective strategy to prepare and acid-responsive DOX prodrug, as *cis*-aconityl can be rapidly hydrolyzed and cleaved in a mildly acidic tumor microenvironment (pH 6.5−4.5). Jiang et al. reported a dendritic DOX prodrug with the *cis*-aconityl linkage (Figure 3A).[22] A polyamidoamine dendrimer was modified with three functional components: Arg-Gly-Asp (RGD) peptides were employed as a targeting moiety, a PEG segment prolonged blood circulation, and DOX was conjugated on the dendrimer as a therapeutic agent through *cis*-aconityl linkages. The pH-dependent release was tested under four different pH conditions, 7.4, 6.5, 5.5, and 4.5. Negligible drug release from this dendritic prodrug was observed over 96 h at 7.4 pH, while increase in the release percentage was observed as the pH value decreased. About 63.55 ± 3.03% of DOX was released at the pH value of 4.5, indicating the effective acid-triggered prodrug activation. This system's *in vivo* antitumor performance was also confirmed using B16 tumor-bearing mice. Based on synergetic electrostatic and hydrophobic interactions, Zhang et al. fabricated a nanoparticle for pH-triggered DOX delivery by using a slightly positively charged polyelectrolyte polymer and a negatively charged *cis*-aconityl functionalized DOX (Figure 3B).[23]

Acetal and Ketal Groups. Acetal and ketal are frequently employed as acid-responsive linkages. Under acid conditions, the oxygen of the acetal group is protonated to activate the adjacent carbon, which favors attack from water molecules, resulting in the cleavage of the acetal to the corresponding aldehyde and alcohol. Theoretically, the hydroxyl functional groups in drug molecules or drug delivery materials can be modified into acetal or ketal structures, thus possessing acid-responsiveness. Fréchet et al. reported that their hydrolysis behavior can be finely tuned by altering the chemical structures.[24] Guo et al. also reported that the hydrolysis kinetics of a PEGylated paclitaxel (PTX) prodrug based on ketal could be adjusted by varying the length of the PEG segment (Figure 4).[25] The rate of prodrug hydrolysis increased with the growing length of PEG. A longer PEG block resulted in a weak and loose outer shell for promoting the penetration of protons to degrade the ketal linkages, which finally affected the cytotoxicity and pharmacokinetics of the obtained prodrug nanoparticles. Therefore, they are considered as promising linkers for designing pH-responsive therapeutics. However, they are primarily used for constructing acid-degradable materials[26,27] due to lack of synthetic methods, and acetal/ketal containing prodrugs are less reported. As a paradigm, Guo et al. reported a series of isomeric glycoside-based prodrugs containing asymmetric ketal linkers.[28] The prodrugs were synthesized by reacting etoposide with isopropenyl 2,3,4,6-tetra-*O*-benzyl-α- or β-D-glucopyranoside, and the glucose moiety was restored by removing the protecting benzyl groups through hydrogenolysis. The obtained prodrug molecules were amphiphilic and could self-assemble into nanoparticles without extra excipients. The anomeric and positional configurations had considerable impact on the acid-responsiveness of the prodrug nanoparticles: the 3″-positional β-anomeric prodrug exhibited the most acid-sensitivity and was the most cytotoxic against A549 cells among other congeners. In additional studies, pH-sensitive ketal linkers were developed to modify hydroxyl-containing anticancer drugs such as gemcitabine (GEM),[29] which can also be activated in a mild acid milieu, exhibiting antitumor therapeutic effect in tumor-bearing mice models.

Silyl Ether. Silyl ether groups were originally used as protecting groups for alcohols. Since they are easily cleavable under acid conditions, DeSimone et al. reported a series of silyl ether-based acid-activable prodrugs.[30,31] They modified the anticancer drug GEM with a silyl ether group to obtain an asymmetric bifunctional silyl ether structure.[30] Therefore, the

https://doi.org/10.1021/acsnano.2c05379
ACS Nano 2022, 16, 13513−13553

Scheme 3. Hyper-reductive and Hyper-oxidative Features Co-exist in Tumor Cells, as Reductive GSH and ROS Levels Are Upregulated[a]

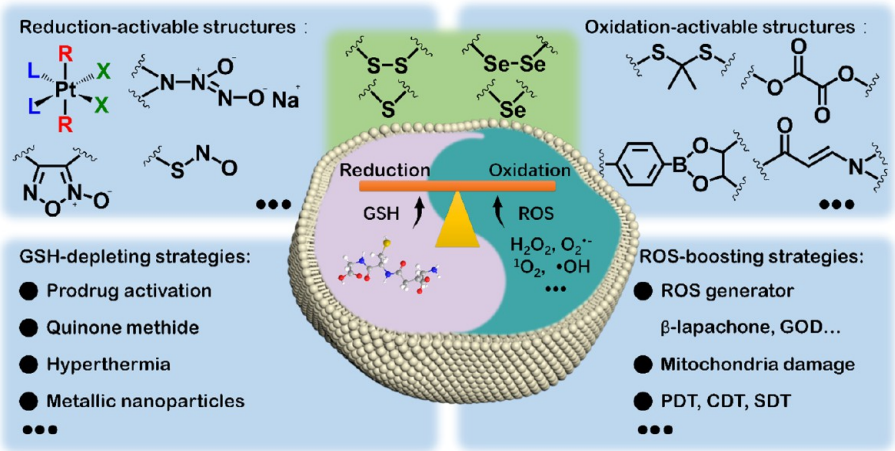

[a]Common reduction-activable and oxidation-activable structures are summarized. GSH-depleting strategies and ROS-boosting methods are also summarized for increasing the therapeutic index of redox-activable prodrugs.

water-soluble GEM can be covalently conjugated to a hydrogel particle. The hydrolysis-based drug release behavior can be adjusted by altering the substituents on the silicon atom. Based on this synthetic strategy, they also constructed an antibody–drug conjugate by coupling the monoclonal antibody (mAb) trastuzumab to GEM through a silyl ether linkage, which can release GEM in parental form at endosomal pH, indicating that silyl ether linkages are promising for constructing acid-activable prodrugs.

ortho-Ester. Many other chemical structures have been confirmed to exhibit acid-responsive cleavability, including *ortho*-esters,[32] oxime groups,[33] and phenylboronate esters.[34] In addition to being explored as acid-degradable materials, recently, researchers have managed to expand the scope of acid-activable prodrugs with these structures. For instance, Tang et al. reported that *ortho*-esters could be developed for acid-activable prodrugs.[32] For this purpose, an *ortho*-ester compound with an amino group was reacted with the anticancer agent indomethacin (IND) to obtain an acid-cleavable IND dimer, which could be further assembled into nanostructures and could encapsulate another therapeutic unit, DOX. It was found that IND suppressed the expression of multidrug resistance protein 1, promoting the therapeutic effect of DOX by reversing multidrug resistance. This nanosystem was designed to disassemble in endosomes and lysosomes, releasing IND and DOX after acid-induced *ortho*-ester hydrolysis. The acid-responsive release behavior was tested at pH 7.4 and 5.0; both ^{1}H NMR analysis and release kinetics data verified the pH-dependent behavior. Compared with free DOX treated ones, MCF-7/ADR tumor-bearing nude mice treated with nanoparticle injection showed better tumor suppression response. It is important to note that these above-mentioned acid-labile chemical bonds are not self-immolative structures. In other words, the cleavage of these linkers may not fully recover prodrug to their parental forms.

Acid-Intensifying Strategies for Prodrug Activation. Although the acidic microenvironment is one of the earliest studied physiological characteristics of tumors, related tumor therapies suffer deeply from tumor heterogeneity,[35] which also accounts for the hindrance of clinical translation for acid-activable prodrugs. Having the delivered therapeutic nanoplatform in a sufficiently acidic tumor environment is the key to ensuring stable efficacy. Glucose oxidase (GOx), known as an efficient biocatalyst, can accelerate the conversion of glucose into hydrogen peroxide (H_2O_2) and gluconic acid, and thus has been extensively applied for starvation therapy and chemodynamic (CDT) therapy. It was reported by the Huang research group that GOx loaded Janus γ-Fe_2O_3/SiO_2 nanoparticles efficiently consumed intracellular glucose, generating H^+ and H_2O_2.[36] The Fe^{2+} involving Fenton reaction is pH-dependent, with an optimum reaction pH range of 2–4. On the other hand, the generation of Fe^{2+} and Fe^{3+} also relied on the acid dissolution of γ-Fe_2O_3. After mixing with glucose, the GOx loaded nanoparticle was found to increase the H_2O_2 level and decrease the pH value of the test solution. GOx was also used to increase acidity to degrade hydrogel carrier materials, as reported by Zhang et al.[37] However, related strategies for more reliable activation of acid-responsive prodrugs have not been reported yet.

REDOX-ACTIVABLE PRODRUGS

The abnormal cancer metabolism and inflammatory microenvironment result in the loss of redox homeostasis in the solid tumor microenvironment, such as elevated levels of ROS and an abnormal thiol/disulfide redox state.[38] This fact has led to a therapy concept based on such a prominent discrepancy between healthy and cancerous cells as a triggering mechanism for prodrug activation. After decades of research, there is a great deal of versatility in redox responsive structures that have been developed for prodrug design, such as the disulfide bond, which is reduction-responsive degradable, and boronic ester, which can be cleaved in response to H_2O_2. Despite the great potential behind this drug activation mechanism, its application has not yet overcome the clinical transition hurdle. Redox-responsive prodrugs are divided into two categories: reduction-responsive and the oxidation-responsive types (Scheme 3). In this section, we will discuss recent progress in redox-activated prodrugs and analyze the corresponding strategies to manipulate the intensity of these stimuli.

Reduction-Responsive Chemical Structures for Developing Prodrugs. As mentioned above, one of the reasons for the reducing milieu inside tumor cells is the high thiol/

https://doi.org/10.1021/acsnano.2c05379
ACS Nano 2022, 16, 13513–13553

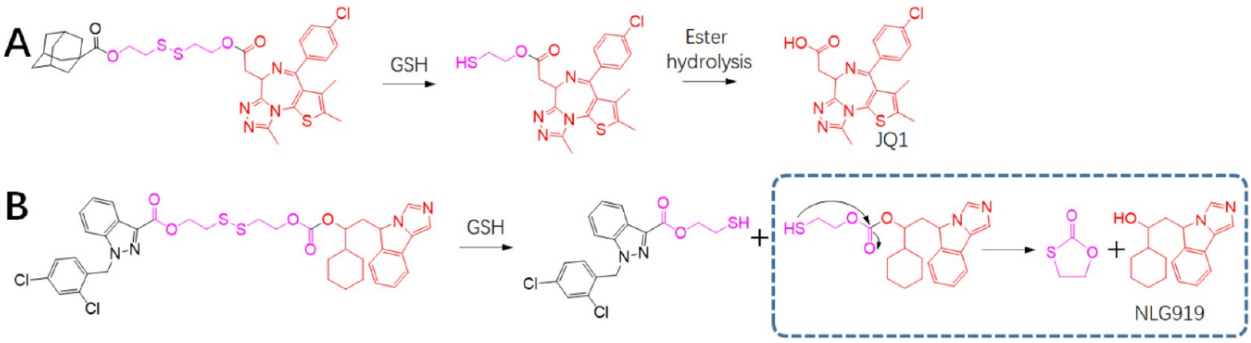

Figure 5. Reduction-activable prodrugs based on GSH-cleavable disulfide linkages: (A) JQ1 covalently conjugated with adamantane through disulfide. The structures were redrawn according to ref 41. (B) Dimer prodrug LND-NLG919 constructed by linking LND and NLG919 together through disulfide bonds. The structures were redrawn according to ref 44.

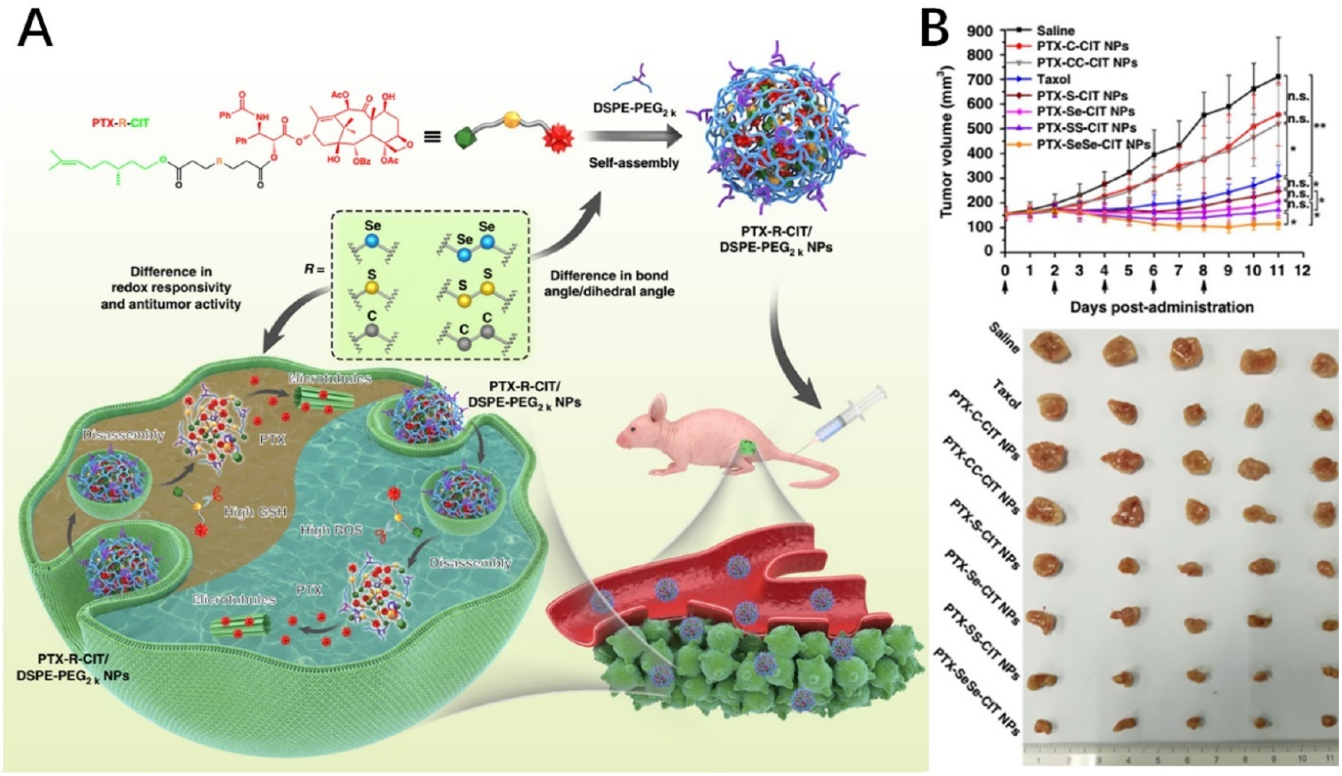

Figure 6. (A) Sulfur, selenium, and carbon bond-bridged PTX−citronellol prodrug nanoassemblies for cancer therapy. (B) *In vivo* anticancer performance of each group. Reprinted with permission under a Creative Commons Attribution 4.0 International License from ref 45. Copyright 2019 The Authors.

disulfide ratio or other kinds of cellular antioxidant species. In particular, glutathione (GSH), an important tripeptide containing a thiol group, is among the most advantageous stimuli for activating prodrugs. The concentration of GSH (2−10 mM) in cancer cells is 10^4-fold higher than that in the extracellular environment; the GSH content level in tumor tissues is also 4-fold higher than that in healthy tissues.[39]

Disulfide. One of the most extensively studied structures that respond to high GSH concentration is the disulfide bond. Featuring excellent reversible properties, disulfide structures have widely been developed as self-immolative linkers for reduction-activable prodrugs so that the original structure of the parent drug could be completely restored via 1,4-elimination, 1,6-elimination, or intramolecular cyclization cascade reaction.[40] In recent work, Yu et al. used disulfide linkers to construct a GSH-activable prodrug of JQ1, which is a bromodomain-containing protein 4 inhibitor (Figure 5A).[41] An adamantine moiety was conjugated to the other side of the disulfide linkage, allowing for the loading of JQ1 prodrug into β-cyclodextrin (β-CD) functionalized hyaluronic acid through supramolecular host−guest interaction. Adamantine modified photosensitizer pyropheophorbide a (Ppa) was also loaded in the same way to induce photoimmunotherapy by PDT. Release studies in the presence of GSH (10 mM) showed that total release of JQ1 was achieved in 48 h due to the cleavage of disulfide linkers. The obtained nanosystem accumulated in the tumor region with high efficacy on account of the targeting function of the carrier material hyaluronic acid. Under near-infrared (NIR) light, the co-delivered Ppa produced ROS and induced immunogenicity, allowing the infiltration of $CD8^+$ cytotoxic T cells. The activated JQ1 further regulated the immune microenvironment by silencing

https://doi.org/10.1021/acsnano.2c05379
ACS Nano 2022, 16, 13513−13553

the oncogene c-Myc signaling, restraining glycolysis, and downregulating programmed death ligand 1 (PD-L1) expression to avoid PDT-mediated immune invasion. In another study of disulfide self-immolative linker-based prodrugs, Yu et al. constructed a JQ1−NLG919 heterodimer prodrug to promote cancer immunotherapy by downregulating BRD4 and suppressing indoleamine-2,3-dioxygenase 1 (IDO-1).[42] This prodrug was then coated with an acid-responsive Ppa-containing amphiphilic polymer, which provided PDT under NIR irradiation and tumor-specific degradation. JQ1 and NLG919 were synchronously activated owing to the GSH-mediated disulfide degradation. In 4T1 and CT26 tumor models, the experimental results verified that this combination therapy considerably suppressed tumor growth and overcame immune resistance. In follow-up work, the disulfide-modified JQ1 prodrug also exhibited promising tumor immune microenvironment modulation in combination use with autophagy inhibitor doxycycline.[43]

In another study of disulfide self-immolative linker-based prodrugs, Tang et al. constructed a lonidamine (LND)−NLG919 dimer prodrug to simultaneously disrupt the energy metabolism and immune escape of tumor tissues (Figure 5B).[44] The parental form of NLG919 could be restored through intramolecular cyclization cascade reaction, while for LND, an additional step of ester hydrolysis was needed to get back to its original form completely. The dimer prodrugs were encapsulated in F127 micelles to improve the pharmacokinetic performance of the prodrug. Inside cancer cells, the LND component damaged mitochondria and inhibited glycolysis for energy production, and the cleavage of disulfide linkages consumed GSH, leading to accumulation of ROS, which jointly induced immunogenic cell death. The released NLG919 further alleviated the immunosuppressive microenvironment by downregulating regulatory T cells to boost antitumor effect. As revealed by *in vivo* antitumor experiments, compared to the single drug group, the combination therapy of the LND−NLG919 prodrug nanoparticle group exhibited better tumor inhibition therapeutic efficacy.

Diselenide. As a close analog of sulfur, the element selenium also belongs to the chalcogen family and constructs important biomolecules, such as selenocysteine, to maintain a regular redox state. Compared to the disulfide linkage, the diselenide bond simultaneously responds to dual-redox stimuli; if the disulfide linker is replaced with diselenide within a prodrug molecule, the activation dynamics of prodrug will definitely change. Sun et al. recently studied the impact of sulfur, selenium, and carbon linkages on prodrug assemblies (Figure 6A).[45] Although thioether, disulfide, selenoether, and diselenide bonds possess similar structures, the differences in the atomic structures of carbon, sulfur, and selenium result in differences in bond length, angle, and energy, which further leads to different chemical properties. The selenium-containing structures responded to oxidative stimulus more positively than the sulfur-containing linkers since selenium is directly below sulfur in the periodic table of the elements. Selenoether bonds could be more easily transformed to selenoxide or selenone to facilitate the hydrolysis of ester bonds to release PTX molecules from the prodrug nanoassemblies. In terms of reduction-responsiveness, because selenium belongs to the fourth period and sulfur belongs to the third period, the sulfur atoms attract electrons more actively than selenium atoms; therefore, disulfide bonds are prioritized in being cleaved by reductive species compared to diselenide containing counterparts. The order of reduction induced drug release rate of these four linkers is -SS- > -SeSe- > -S- > -Se-. Whereas under the same reducing stimulus, the diselenide bonds were less broken than disulfide bonds, both the bond angle of diselenide and the dihedral angle of C−SeSe−C are very close to 90°, which provides sufficient structural stability and promotes stable self-assembly of prodrug molecules for longer circulation time. Based on dual-redox activation and better colloidal stability, the diselenide-bridged prodrug nanoassemblies exhibited the best antitumor effect in the *in vivo* experiment (Figure 6B). In an extension study, they fabricated a series of docetaxel (DTX) dimer prodrugs based on diselenide, disulfide, and dicarbide linkers.[46] The diselenide DTX prodrugs outperformed the other two counterparts in terms of antitumor efficacy. According to molecular dynamics simulations, the perpendicular arrangement of diselenide's bond angle and dihedral angle enhanced the flexibility of prodrug structures, promoted the self-assembling tendency of the diselenide-based prodrug molecules, and finally improved the stability and pharmacokinetic performance of diselenide-based DTX dimer prodrugs.

Pt(IV). In addition to the reduction-activable organic type of prodrugs, metal-based anticancer agents also play a crucial role in this field. As a representative of them, platinum anticancer drugs have achieved great clinical success. Most Pt(IV) prodrugs can be reduced to divalent state by the overexpressed reductive species (such as GSH) in the cancer cells. To accelerate clinical translation for early practical application, recent progress in this domain focused on the following issues: (1) optimizing the Pt(IV) structure by altering the ligands to modulate physicochemical parameters; (2) developing Pt(IV) nanoformulations to effectively improve the uptake of platinum drugs by tumors; (3) constructing synergistic therapeutic platforms with other anticancer agents for dual-threat to enhance the biological anticancer effect.

Rational ligand design improves the therapeutic efficacy of Pt(IV) prodrugs. In a recent work by Zhu et al., when a monochalcone moiety was introduced on the axial position of cisplatin Pt(IV) prodrug, the resulting monochalcoplatin could effectively accumulate in cisplatin-resistance cancer cells through a transporter-mediated active transport process and realize quick reduction-activation to induce cell apoptosis.[47] The reduction speed of this Pt(IV) prodrug is also astonishing. The E_p value of monochalcoplatin obtained by cyclic voltammetry was −0.85 V (vs Fc^+/Fc = +0.05 V), which demonstrates that monochalcoplatin can be easily reduced after entering into cancer cells. Treated with the reducing agent sodium ascorbate, half of monochalcoplatin Pt(IV) prodrug was reduced within 6 h. With improved tumor accumulation and activation speed, monochalcoplatin exhibited the most cytotoxic effect among other Pt(IV) species, as revealed by its extremely low IC_{50} values against A2780 and A549 cells (10 nM and 80 nM, respectively).

Recent research has focused on developing a nanovehicle strategy to provide Pt(IV) prodrug with a cloak barrier against reductive species during blood circulation to overcome instability and deactivation issues. Through covalent or noncovalent conjugation, Pt(IV) prodrugs have realized effective loading into multiple carrier materials. Our group also reported Pt(IV) delivery materials based on carbon dots.[48,49] The development of carrier material design expands their function; today, it is possible to construct a delivery nanoplatform with synergistic benefits of therapy capabilities. For example, Yu et al. reported that oxaliplatin based Pt(IV)

https://doi.org/10.1021/acsnano.2c05379
ACS Nano 2022, 16, 13513−13553

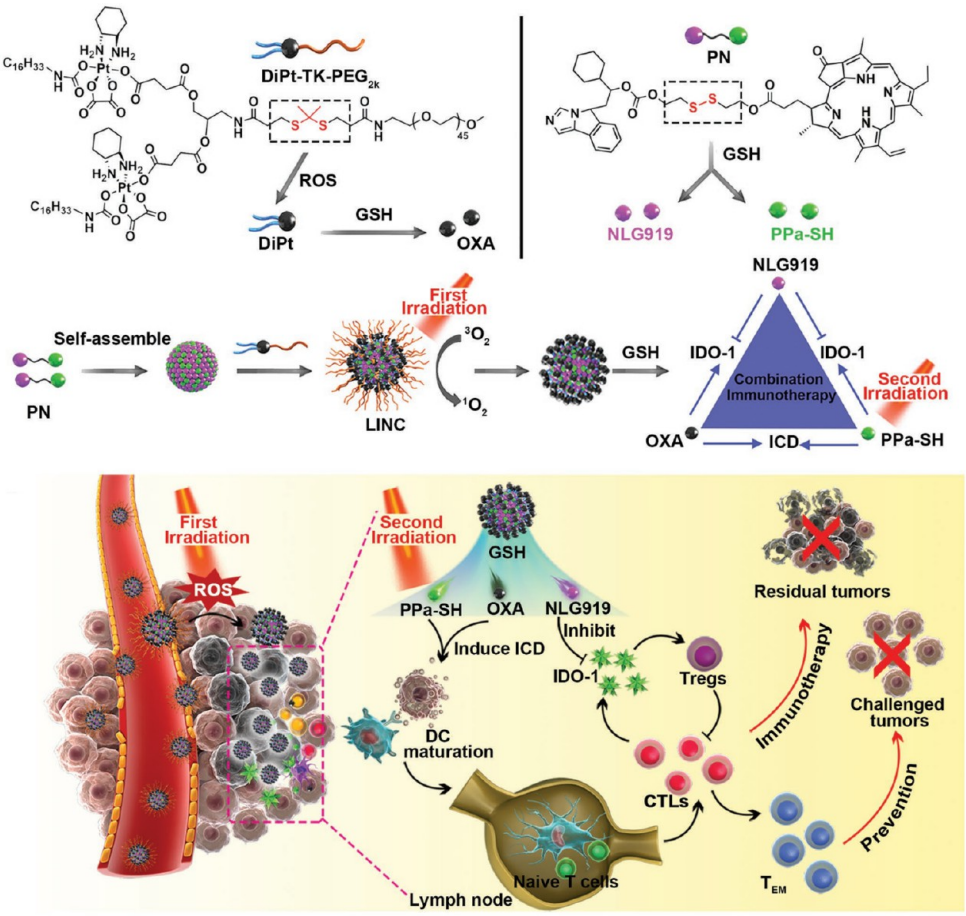

Figure 7. Schematic illustration of Pt(IV) prodrug based nanosystems: GSH induced Pt(IV) activation inhibited tumor growth and elicited immune response, and the co-delivered NLG919 reversed the immunosuppressive microenvironment to enhance the synergistic immunotherapy. Reproduced with permission from ref 50. Copyright 2019 WILEY-VCH.

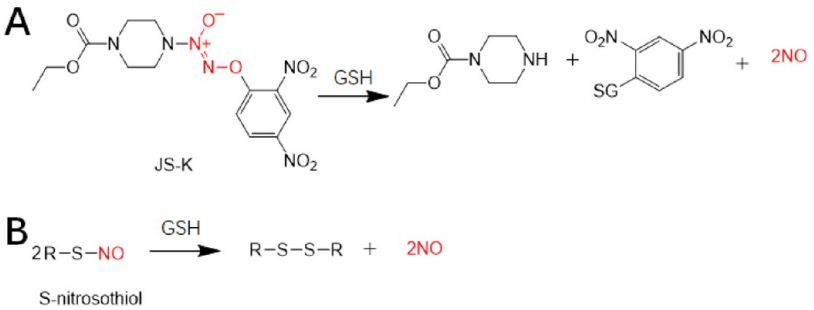

Figure 8. GSH-responsive NO release from reduction-activable NO prodrugs: (A) JS-K and (B) *S*-nitrosothiol.

prodrugs could be PEGylated with ROS-responsive thioketal linkages (Figure 7).[50] This amphiphilic polymer prodrug was subsequently loaded with a disulfide linked NLG919−Ppa heterodimer molecule. Upon NIR irradiation, the Ppa moiety induced the generation of ROS to cleave the thioketal linker, triggering the detachment of the PEG layer and facilitating the tumor retention of the nanosystem. In the presence of overexpressed GSH within the tumor, the oxaliplatin based Pt(IV) prodrug and disulfide-caged NLG919 prodrug were activated. The restored oxaliplatin inhibited tumor growth and elicited immunogenicity, while the released NLG919 reversed the immunosuppressive tumor microenvironment by inactivating IDO-1. The Pt(IV) based chemotherapy together with NLG919-mediated immunotherapy exhibited the highest antitumor efficacy in comparison with monotherapy control groups.

In another recent study that was also based on a self-assembly strategy to enhance cellular uptake of Pt(IV), Wang and co-workers constructed a cisplatin Pt(IV) prodrug with a peptide skeleton at the axial positions.[51,52] The peptide was incorporated for *in situ* self-assembly purposes and was decorated with a phosphate group and nonsteroidal anti-inflammatory drug, naproxen, at each end. Phosphatase in the tumor microenvironment cut off the phosphate groups, improving the hydrophobicity of Pt(IV) prodrugs, which finally self-assembled into well-defined nanofibers. Compared with free cisplatin, a higher level of Pt−DNA adducts was found in cisplatin-resistant HeLa cells due to its unique

https://doi.org/10.1021/acsnano.2c05379
ACS Nano 2022, 16, 13513−13553

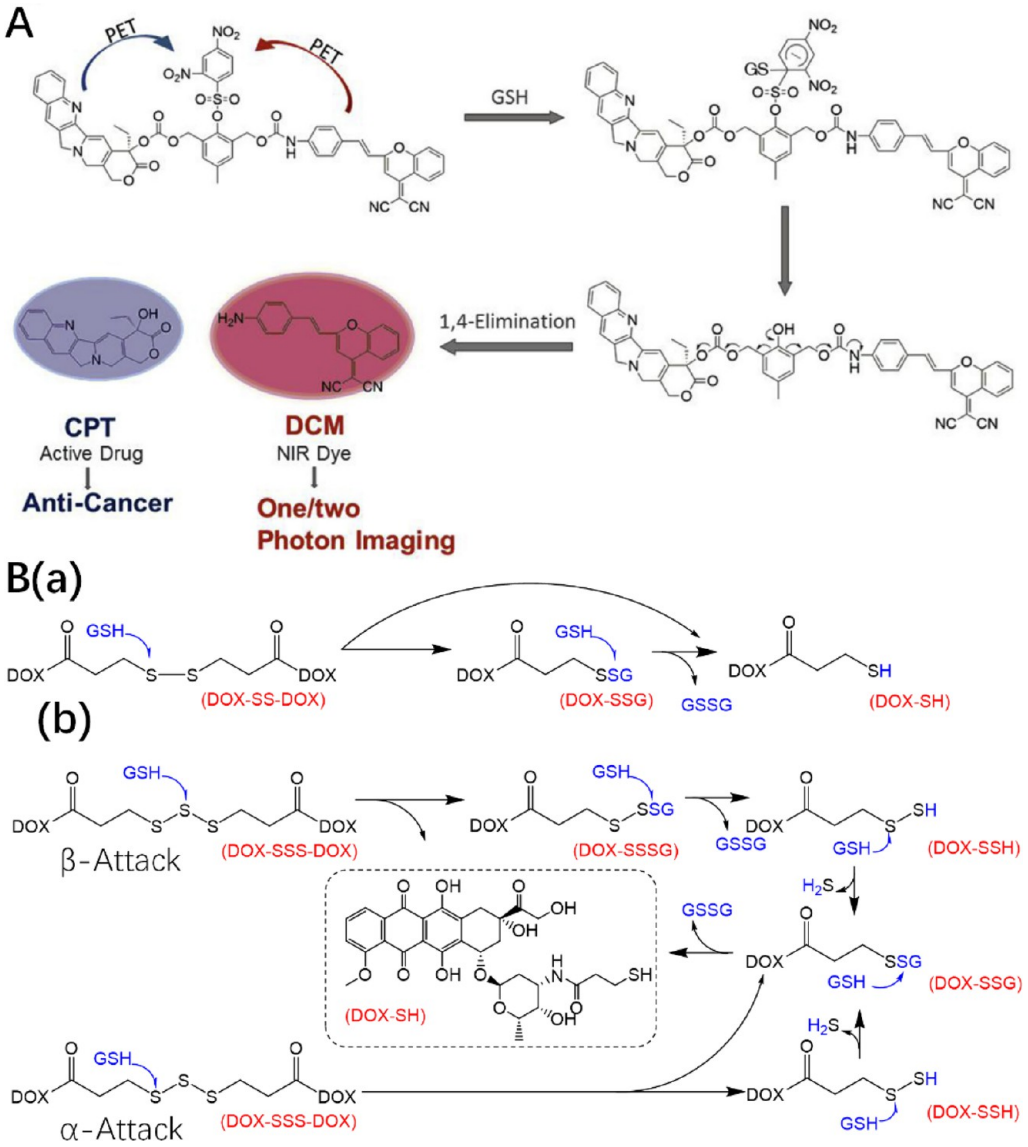

Figure 9. (A) Schematic illustration of GSH triggered CPT and NIR dye synchronous release based on self-immolative dendritic molecule. Reproduced with permission from ref 59. Copyright 2017 Elsevier. (B) GSH activation comparison between (a) disulfide and (b) trisulfide bridged DOX dimer. The structures were redrawn according to ref 60.

nanosized morphology and receptor-mediated endocytosis. The overexpressed GSH activated Pt(IV) inside cancer cells, and the released cisplatin with naproxen further induced apoptosis of cisplatin-resistant tumor cells through suppression of cyclooxygenase-2 (COX-2) and nuclear factor kappa B simultaneously.

Reduction-Activated NO Donors. Gas therapy has emerged as a promising strategy for treating cancers Therapeutic gas molecules such as nitric oxide (NO), carbon monoxide, and hydrogen sulfide can be considered as a special kind of drug; thus, their donor molecules can be counted as prodrugs. One of the key activation mechanisms is reduction-responsive NO release. Typical reduction-activable NO prodrugs include diazeniumdiolates (JS-K)[53] and *S*-nitrosothiols (Figure 8).[54] Research reported by Kong et al. revealed that the controllable NO release is vital for effective anticancer therapy.[53] They covalently attached a JS-K-type NO donor to an amphiphilic, pH-degradable polymer scaffold through click reaction, which guaranteed high NO capacity to induce apoptosis of cancer cells. DOX was also coloaded during the assembly. The Griess assay showed that NO release was obvious after co-incubation with GSH and 58.86% of NO was released from nanoparticles after 72 h. Together with acid-responsive DOX release, this nanoformulation exhibited effective *in vitro* antiproliferation and *in vivo* tumor suppression effects. In addition to directly killing tumor cells, NO works as a good sensitizer to enhance the efficacy of chemo-, radio-, and immunotherapy; the NO delivery platforms were often designed to carry other therapeutic agents. Ding et al. reported impressive progress: they fabricated a NO delivery polymeric nanoparticle by coordinating interaction between bidentate carboxyl groups in NO prodrugs and Fe^{3+}.[55] Reduction stimulus triggered on-demand NO release in a GSH concentration-dependent way. The iron ions mediated Fenton reaction together with Haber–Weiss cycle generated $^{\bullet}OH$ and $O_2^{\bullet-}$. In addition, NO participated in the chemodynamic process by reacting with $O_2^{\bullet-}$, producing $ONOO^-$. Thus, the NO, $^{\bullet}OH$, $O_2^{\bullet-}$, and $ONOO^-$ generated in this strategy contributed to the effective

https://doi.org/10.1021/acsnano.2c05379
ACS Nano 2022, 16, 13513−13553

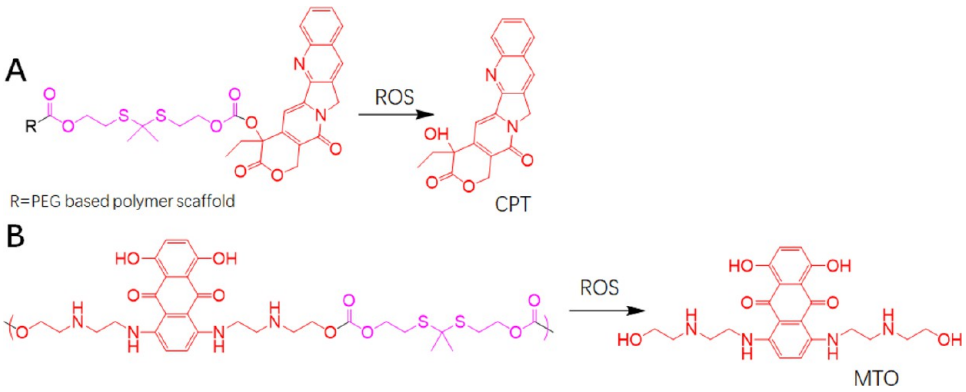

Figure 10. Oxidation-activated prodrugs based on thioketal linkages. (A) Thioketal modified CPT polyprodrug. The structures were redrawn according to ref 61. (B) Thioketal containing A-B type MTO polyprodrugs. The structures were redrawn according to ref 63.

antitumor performance. In a subsequent *in vivo* study, the NO−CDT combination therapy considerably inhibited tumor growth without body weight loss. For further development of these NO prodrugs, it is vital to think about the double-edged-sword effect of NO in cancer biology since NO promoted the proliferation of cancer cells at low concentrations. All the references discussed in this section did not consider NO concentration monitoring. In the future, it is urgent to figure out how to activate NO prodrugs immediately after they reach the targeted site to guarantee that NO is released in high concentration and to precisely measure the real-time intratumoral NO concentration to avoid it falling below the effective level.

Dinitrophenyl-Based Groups. Dinitrophenyl-based groups can respond to thiol, and the subsequent thiolysis process has been designed as a trigger for fluorescent imaging,[56] as an analyte probe,[57] and for therapeutic agent release.[58] Recently, Wu et al. exploited the GSH-rich tumor intracellular microenvironment, where the dinitrophenyl-based group 2,4-dinitrobenzenesulfonyl (DNS) can respond to the thiol group of GSH and trigger the activation of prodrug.[59] They designed a self-immolative dendritic platform for synchronously releasing CPT and dicyanomethylene-4*H*-pyran, a two-photon NIR fluorophore. Cascade reaction was initiated by the cleavage of DNS by the thiol group of GSH to release these two kinds of payloads (Figure 9A). Before reacting with GSH, the fluorescence signal of dicyanomethylene-4*H*-pyran was quenched by the carbamate linker; after the 1,4-elimination, the liberated dicyanomethylene-4*H*-pyran can report the simultaneously released CPT through one- or two-photon imaging. When applied on the HeLa and L929 cell lines, the prodrug exhibited a cancer cell killing effect, and the NIR signal can also be observed in the HeLa tumor-bearing mice.

Trisulfides. Trisulfides are considered as upgraded dynamic bonds compared to disulfides. With one more sulfur atom in its structure, the trisulfide is more flexible than disulfides. In their recent research, Yang and co-workers found that using trisulfide as a bridge linker for a dimeric prodrug facilitated the self-assembly stability of prodrug molecules, especially for DOX, which has been restricted by its rigid planar structure.[60] According to their simulation, the bond angles of trisulfides were close to 90°, which favored obtaining the stable self-assembly conformation. Thus, the DOX dimeric prodrug could be made into nanoparticles without the aid of surfactants and guaranteed high drug loading efficiency in the meantime. Compared to thioether and disulfide analogs, the trisulfide bridged DOX dimer was also more sensitive to GSH activation (Figure 9B). This is because the trisulfide bonds could be nucleophilically attacked by GSH at α-sulfur and β-sulfur simultaneously. In addition, the reduction potential of the trisulfide bond was also higher than that of the disulfide bond. With improved stability and GSH-sensitivity, the trisulfide group exhibited superior *in vivo* antitumor efficacy in 4T1 xenograft models.

Oxidation-Responsive Chemical Structures for Developing Prodrugs. Compared to normal tissues, the profuse tumor metabolism results in enhanced mitochondrial ROS generation, and the ROS levels in cancer cells (∼100 μM) and in normal cells (∼20 nM) differ by thousands of times. Therefore, ROS activable prodrugs thrived and have become an important therapeutic strategy. These prodrugs are mainly based on a series of ROS-responsive cleavable chemical structures, for example, diselenide and thioether bonds, which are incorporated to cage the parent chemotherapy drug, realize molecular rearrangements, and conjugate functional units.

Thioketal. Thioketal linkers undergo oxidation-induced cleavage in the presence of ROS. For thioketal-based prodrugs, cytotoxic agents were mostly connected through thioketal linkers as side chains of polyprodrugs[61] or as the hydrophobic part of amphiphilic prodrug nanoassemblies.[62] Ge et al. fabricated a ROS-activable polyprodrug through reversible addition−fragmentation chain-transfer polymerization (RAFT) of a thioketal containing CPT drug monomer (Figure 10A).[61] The carrier polymer scaffold contained 2-(pentamethyleneimino) segments, which could be protonated in the acidic tumor microenvironment and promote the uptake of nanoscale prodrugs. Thioketal caged CPT was activated after entering cancer cells, as verified by an *in vitro* drug release experiment that 10 mM H_2O_2 induced release of half of the CPT after 45.2 h. In addition to thioketal cleavage triggered drug release, they tuned the morphology of the nanoformulation by altering the nanoprecipitation conditions. Nanosphere and nanofiber-shaped micelles with similar cross-section diameters but different morphologies were prepared, which facilitated direct performance comparison of nanoscale prodrugs with different lengths in terms of circulation time in the body and tumor uptake. The shape of the nanoscale prodrug also influenced the CPT release kinetics in the sequence of spherical micelles > short filomicelles > long filomicelles. Notably, the short nanofiber micelles with 180 nm length exhibited the best *in vivo* therapeutic efficiency due to sufficient contact with cancer

https://doi.org/10.1021/acsnano.2c05379
ACS Nano 2022, 16, 13513−13553

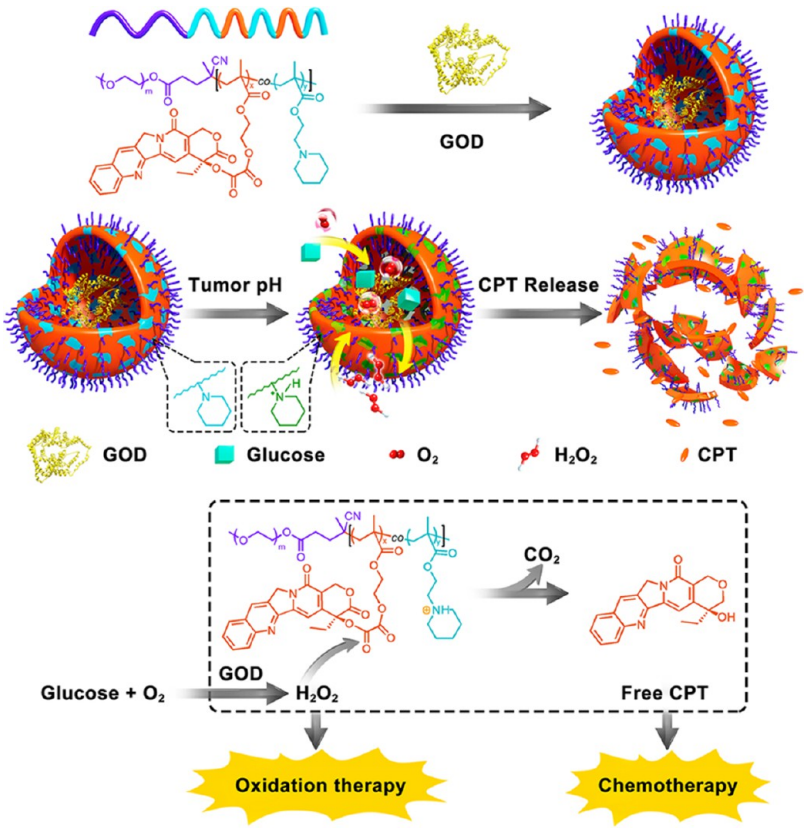

Figure 11. ROS activable prodrug based on oxalate ester linkage: Nanoreactor with H_2O_2-amplifying function was constructed by coassembly between amphiphilic CPT polymer prodrug and GOx. CPT was released in response to generated H_2O_2 to achieve synergistic oxidation and chemotherapy. Reproduced with permission from ref 64. Copyright 2017 American Chemical Society.

cells and subsequent cellular uptake. Compared with spherical micelles and longer filomicelles, the short filomicelles exhibited marked tumor inhibition in H22 tumor-bearing mice without substantial side effects. Recently, Farokhzad et al. devised a thioketal-based polyprodrug by condensation polymerization between mitoxantrone (MTO) and thioketal-containing monomer (Figure 10B).[63] Benefiting from the A-B type condensation polymer structure, the MTO loading ratio in the polymer chain is fixed. Upon treatment with oxidative species, MTO parent drugs were completely released within 6 h due to thioketal cleavage-induced backbone shattering. After further coassembly with iRGD-conjugated DSPE−PEG, the obtained nanoscale polyprodrug exhibited stable ROS-responsive release behavior and better tumor penetration. Both *in vitro* and *in vivo* experiments confirmed the antitumor performance of this nanoscale prodrug.

Oxalate Ester. Oxalate ester is another widely employed ROS-responsive cleavable linkage. The cleavage mechanism was revealed when oxalate ester reacted with H_2O_2 to form a cyclic peroxide intermediate that degraded into CO_2 upon being cleaved. For prodrug design, to realize *in situ* activation, the oxalate ester modified prodrugs are often accompanied by a H_2O_2-generating catalyst as a typical paradigm to strengthen responsiveness. For instance, Ge et al. encapsulated GOx into polymersome nanoreactors with oxalate ester linker CPT as pendant polymer side chain (Figure 11).[64] Piperidine moieties were copolymerized to increase the permeability of glucose when polymersome nanoreactors accumulated in tumor regions. When exposed to a medium with pH 6.8, the glucose oxidation reaction quickly improved H_2O_2 level, reaching 0.5 mM within 1 h. The CPT drug molecules were then released. Nearly 80% of CPT was released within one hour, which disintegrated the nanoreactor vesicular structure. During the treatment of A549 tumor-bearing mice, elevated H_2O_2 levels and CPT release behavior were detected in the tumor. The enhanced oxidative stress caused damage to the cellular membrane and DNA. Along with oxidation-cleaved CPT, the combined effect made the tumor almost disappear at the end of treatment. Mo et al. fabricated an oxalate ester modified polymer CPT prodrug and encapsulated a cancer stem-like cell differentiation-inducing agent, all-trans retinoic acid (ATRA), to afford hybrid prodrug nanoparticles against cancer stem-like cells.[65] The ATRA triggered mitochondrial generation of superoxide and promoted oxalate ester cleavage and CPT release. *In vitro* experimental results showed a concomitant prodrug activation after the release of ATRA, which substantiated that ROS levels are upregulated during the cancer stem-like cell differentiation process. The differentiation therapy and CPT release inhibited both the primary tumor and metastases in MCF-7 and 4T1 tumor-bearing mice.

Arylboronic Ester and Arylboronic Acid. Arylboronic ester or arylboronic acid structures can be transformed into phenol and boric ester or acid in response to ROS, especially H_2O_2. Like other ROS-responsive prodrugs, the key aspect improving activation sensitivity is incorporating ROS-inducing species or antioxidant depleting substances. Arylboronic ester or arylboronic acid linkers have their own advantages: during the activation process the intermediate quinone methide (QM) consumes GSH before being transformed into phenol, which further amplifies the oxidative stress and increases the

https://doi.org/10.1021/acsnano.2c05379
ACS Nano 2022, 16, 13513−13553

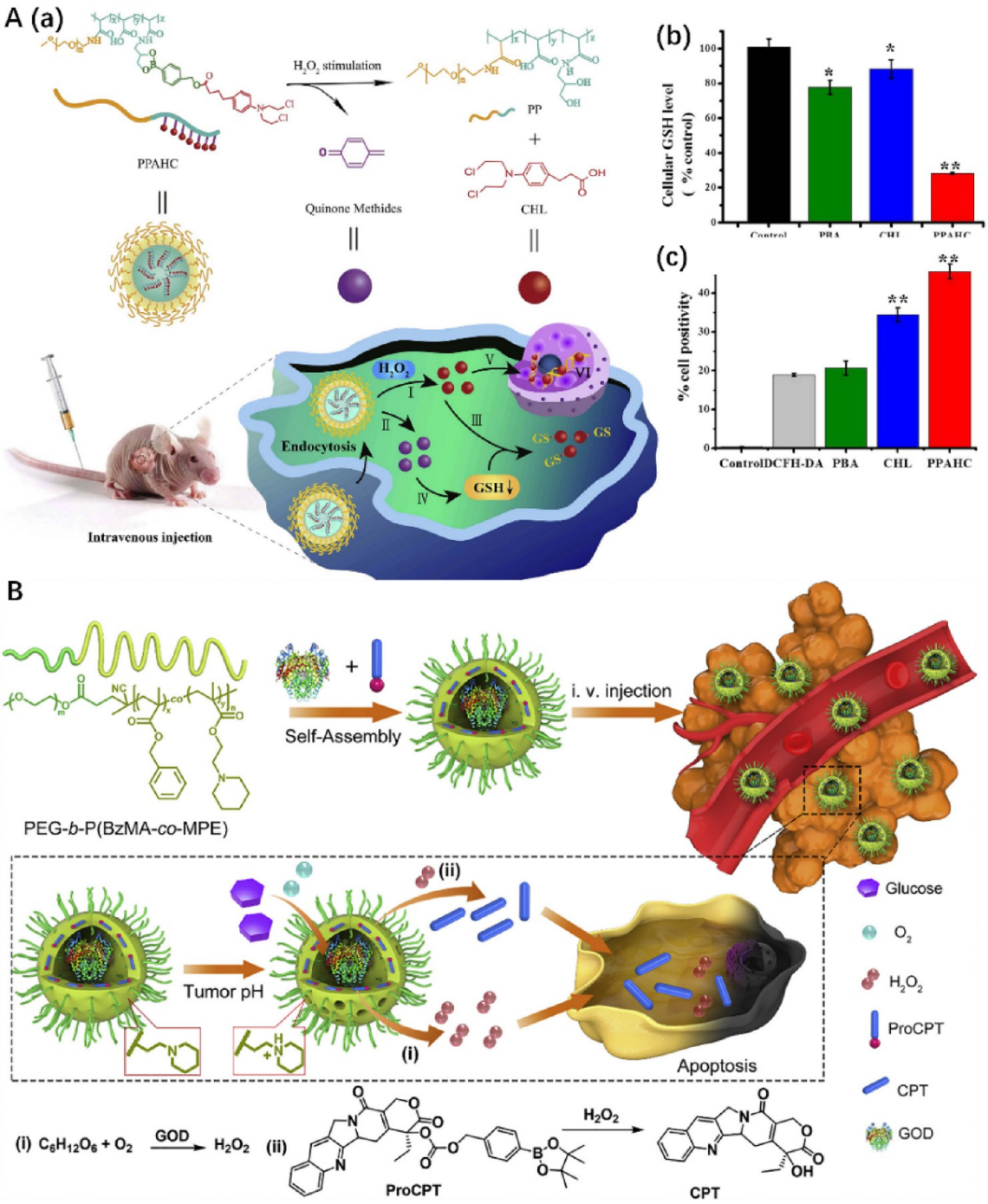

Figure 12. (A) (a) Scheme illustrating that arylboronic acid modified chlorambucil prodrug nanoparticles were activated by H_2O_2. Self-immolative arylboronic acid linker was transformed into GSH depleting agent QM to promote ROS accumulation in cancer cells. (b) Cellular GSH levels and (c) ROS levels after nanoscale prodrug treatment. Reproduced with permission from ref 66. Copyright 2018 Elsevier. (B) Schematic illustration of self-amplifying oxidation-responsive CPT prodrug caged by arylboronic ester. The coloaded GOx inside the nanoreactor generated H_2O_2 during the reaction with glucose, promoting the activation of prodrug in the tumor region. Reproduced with permission from ref 67. Copyright 2019 Elsevier.

antitumor performance.[52] The QM-induced massive production of ROS further activates more prodrug molecules in a positive feedback manner. In recent research, Jiang et al. measured the MCF-7 cellular content of GSH after being treated by arylboronic ester-linked chlorambucil polymer prodrug and found that GSH levels dropped by approximately 70% compared to the control group (Figure 12A).[66] Since the activation of arylboronic ester or acid self-immolative linkers depends mainly on H_2O_2 participation, the combination of GOx and arylboronic ester or arylboronic acid-modified prodrugs can also realize enhanced on-demand drug release effect. Ge et al. constructed a nanoreactor by coencapsulating GOx and arylboronic ester-modified CPT prodrug (Figure 12B).[67] This therapeutic nanoreactor showed a synergistic effect between GOx and CPT prodrug and efficient cancer cell killing effects. In this work, the arylboronic ester modified CPT

https://doi.org/10.1021/acsnano.2c05379
ACS Nano 2022, 16, 13513−13553

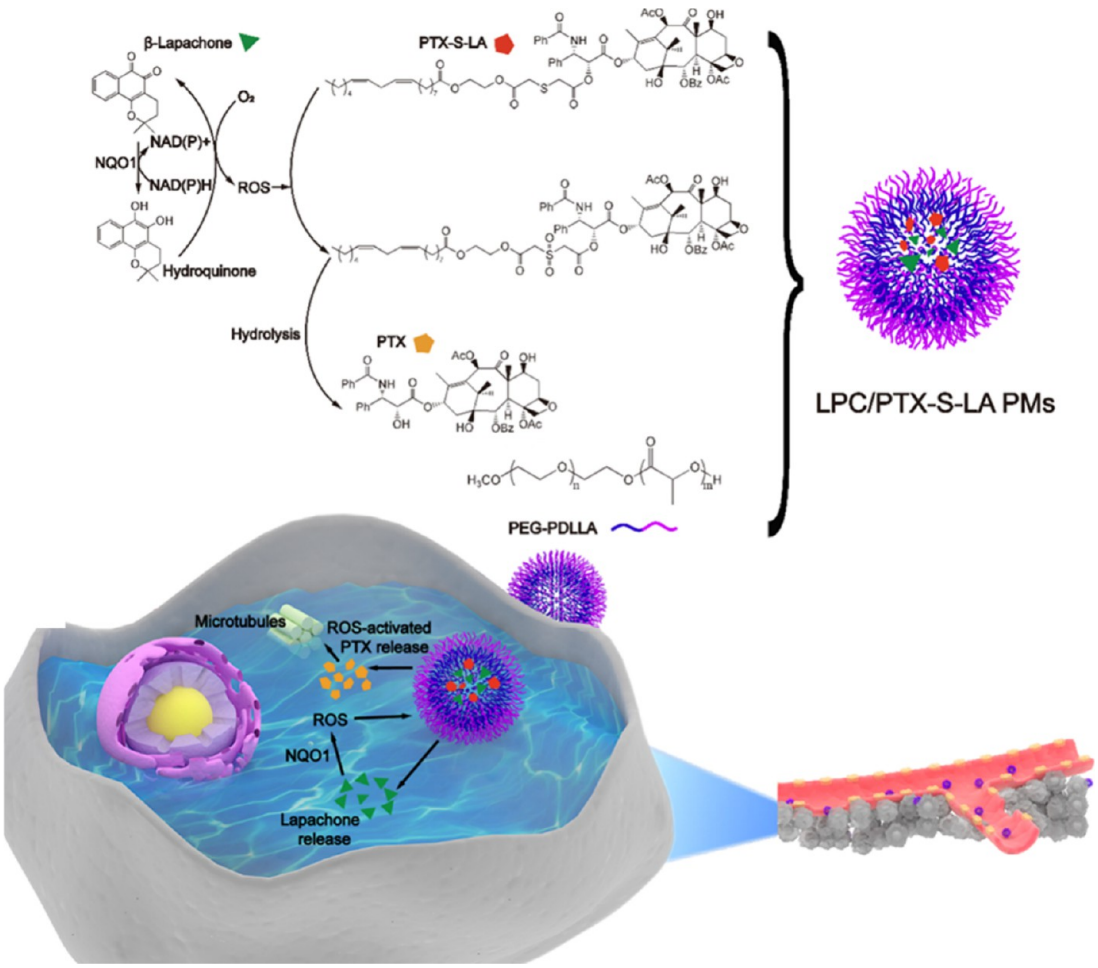

Figure 13. Oxidation-activable prodrug based on thioether linkers: Schematic illustration of thioether modified PTX prodrug, synthetic route, and anticancer mechanism. The coloaded β-lapachone promoted the generation of intracellular ROS, boosting the activation of prodrug. Reproduced with permission from ref 70. Copyright 2019 American Chemical Society.

prodrug was designed as a loaded cargo. The CPT prodrug was rapidly uncaged thanks to the *in situ* generated H_2O_2. The prodrug activation ratio exceeded 80% within 40 h. The prodrug nanosystem showed antitumor effects in H22 tumor-bearing mice with synergistically enhanced oxidative stress. Tumor volume shrank obviously in 22 days of therapy. Chen et al. explored another possibility for arylboronic acid-based prodrug loading by simultaneously modifying 10- and 20-positioned hydroxyl groups of SN38 with arylboronic acid linkers to afford a therapeutic hydrogel. This SN38 prodrug was then used as a cross-linker to construct an injectable hydrogel with biocompatible poly(vinyl alcohol) (PVA) and PEG. With the ROS activation of arylboronic ester linkers, the hydrogel degraded at the tumor site to release preloaded immune checkpoint inhibitor aPDL1. The released SN38 initiated cancer cell immunogenic cell death, and aPDL1 promoted immune response of T cells.[68]

Thioether. A plethora of ROS-activable prodrugs were designed based on thioether linkers. Thioether structures can be converted to hydrophilic sulfoxide or sulfone groups, facilitating the hydrolysis and release of active drug molecules. For example, He et al. compared dithioether- and thioether-linked prodrug conjugates in terms of selective release of PTX.[69] The *in vitro* drug release results indicated that the thioether conjugated PTX prodrug exhibited a more rapid H_2O_2- and GSH-responsive drug release behavior than the dithioether linked prodrug. They supposed that the reason behind this phenomenon is that the thioether linker is closer to 2-hydroxyethyl ester, making the hydrolysis of this ester bond easier once thioether was oxidized to hydrophilic sulfone. In another study, Sun et al. improved the thioether-based prodrug responsiveness by incorporating β-lapachone with thioether-linked linoleic-acid PTX prodrugs (Figure 13).[70] The colloidal stability of the obtained prodrug was further enhanced by being encapsulated into poly(ethylene glycol)-*b*-poly(D,L-lactic acid) polymeric micelles. Through the catalysis of NAD(P)H/quinone oxidoreductase-1 (NQO1), β-lapachone produced ROS and increased the intracellular ROS level, resulting in more sensitive release behavior.

α-Ketoamide. In addition to the above summarized ROS-sensitive linkages, several more structures were recently developed. For instance, Zhang et al. were inspired by a H_2O_2-responsive fluorescent probe based on an α-ketoamide moiety.[71] This linker can be selectively cleaved by H_2O_2 through a similar activation mechanism of oxalate ester: the H_2O_2 anion attacks the carbonyl group of the α-ketoamide linkage with subsequent the Baeyer−Villiger rearrangement; the payload was then released via a 1,6-elimination process, which can be used for designing more oxidation-activable prodrugs.

Redox Signal Manipulation Strategies for Prodrug Activation. Compared with normal cells from healthy tissues,

https://doi.org/10.1021/acsnano.2c05379
ACS Nano 2022, 16, 13513−13553

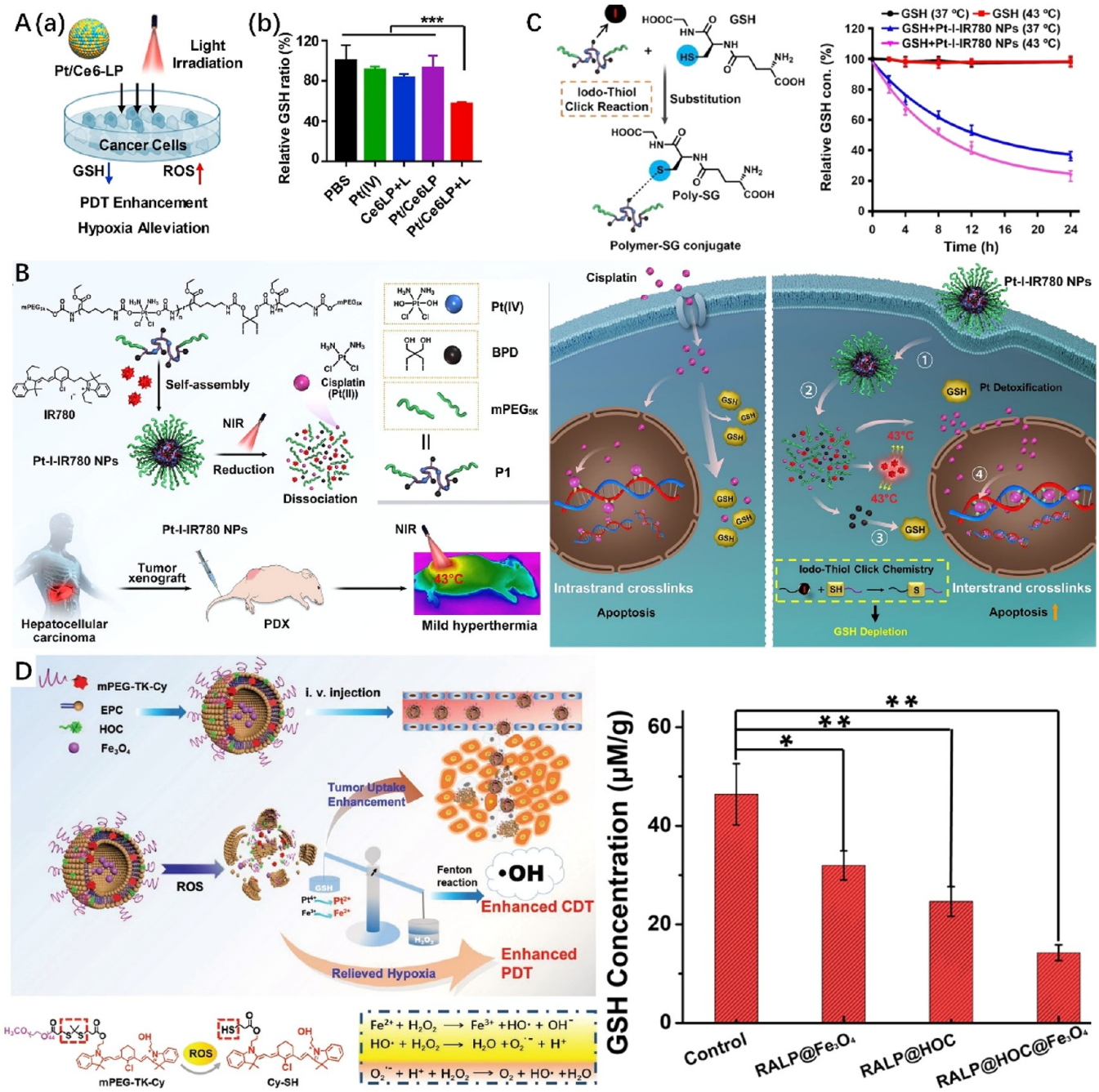

Figure 14. (A) (a) Schematic illustration of Pt(IV)−Ce6 coloaded nanoparticle regulation toward intracellular GSH. (b) Relative intracellular GSH ratio after treated by Pt(IV) prodrugs. Reproduced with permission from ref 73. Copyright 2021 Elsevier. (B) Cisplatin based Pt(IV) prodrug and photothermal agent IR780 coloaded nanomedicine could deplete endogenous GSH by light induced hyperthermia: synthetic route and anticancer mechanism. (C) GSH depletion mechanism based on iodo-thiol based click reaction and GSH level changes after treatment with this nanomedicine. Reproduced with permission from ref 74. Copyright 2020 American Chemical Society. (D) Anticancer mechanism of ROS responsive nanoscale liposome based on Pt(IV) prodrug and Fe_3O_4 nanoparticles and GSH concentrations in CT26 cells co-incubated with nanoscale liposomes. Reproduced with permission from ref 75. Copyright 2019 WILEY-VCH.

the upregulated GSH level in cancer cells can be viewed as a key element in the self-protection mechanism of cancers, which not only shelters the cancer cells from being attacked by ROS but also induces resistance to cancer therapies, including chemotherapy and ROS-based therapies.[72] Therefore, researchers often follow two principles to design effective redox-responsive therapies: depleting GSH and boosting ROS.

GSH-Depletion Strategies for Prodrug Activation. Theoretically speaking, the chemical structures that GSH can activate, such as disulfide bond, diselenide bond, and Pt(IV) prodrugs, also contribute to GSH consumption because GSH also participates in the reaction during the activation process. For instance, Yu et al. found that during the reduction-activation of Pt(IV) prodrugs, the intracellular GSH ratio was indeed decreased (Figure 14A).[73] However, for single Pt(IV)

https://doi.org/10.1021/acsnano.2c05379
ACS Nano 2022, 16, 13513−13553

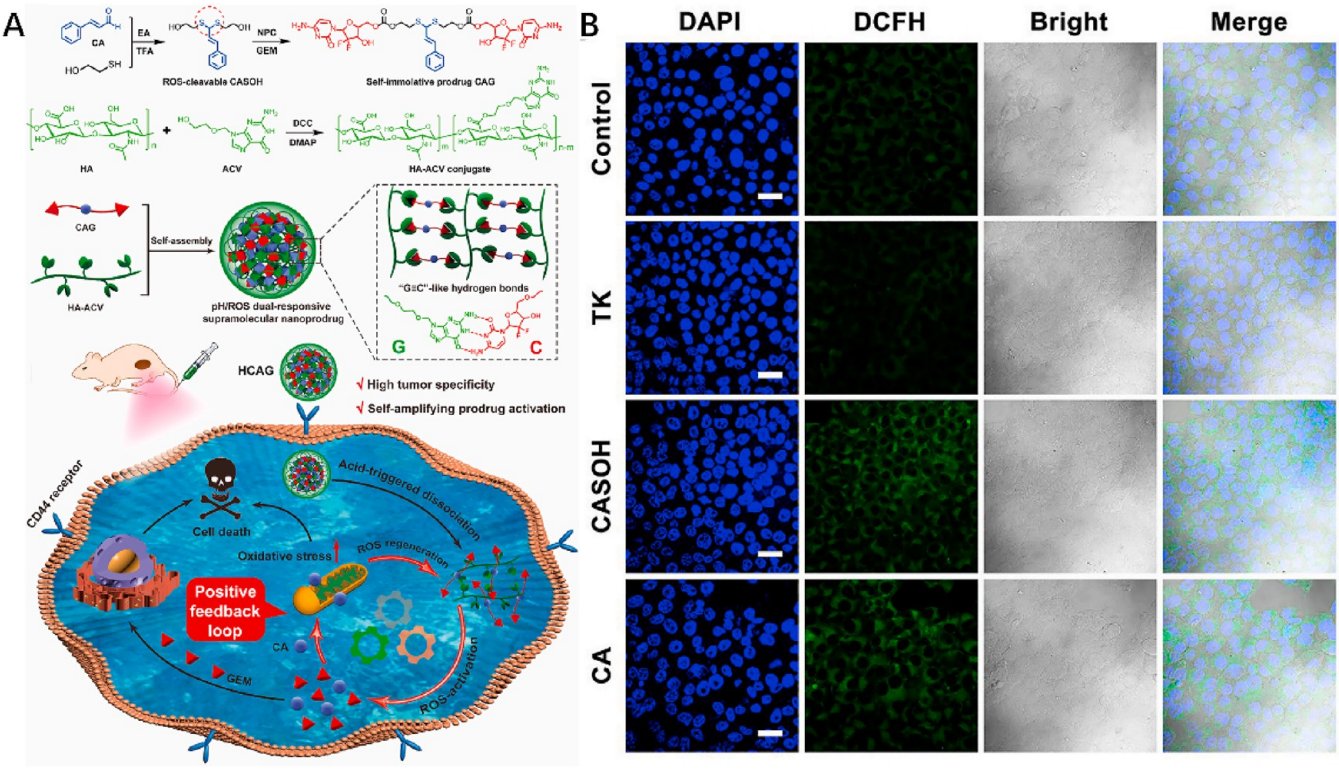

Figure 15. (A) Construction route of cinnamaldehyde−gemcitabine conjugate prodrug, which was then loaded into the guanine modified hyaluronic acid scaffold. The prodrug nanoparticles were disassembled in an acidic microenvironment. Prodrug molecules were released and activated by ROS. Free cinnamaldehyde further promoted ROS generation for self-promoting prodrug activation. (B) Confocal laser scanning microscopy observation of 4T1 cells treated with prodrug nanoparticles, showing enhanced ROS signal after co-incubation. Reproduced with permission from ref 86. Copyright 2021 Elsevier.

treatment, the GSH eliminating effect was inconspicuous, while for the group treated with combined Pt(IV) and chlorin e6 (Ce6) based PDT, the endogenous GSH content decreased to 57% of the original level. Xiao et al. proposed a hyperthermia-induced GSH elimination strategy to develop a more useful method for consuming intracellular GSH (Figure 14B).[74] Through the integration of GSH-activable Pt(IV) and a photothermal agent (IR780), the light-excited hyperthermia could accelerate Pt(IV) activation and promote iodo-thiol substitution click reaction between GSH and iodide on the polymer scaffold. The synergistic mechanisms consumed intracellular GSH rapidly, as confirmed by *in vitro* experiments (Figure 14C).

Nanoscale carrier materials by rational design can also function as adjuvant components for therapeutic purposes. Metallic nanoparticles, such as MnO_2, can also consume GSH during the degradation process, which can be designed for carrier vehicles to deliver redox-activable prodrugs.[75−77] Another metallic nanoparticle, Fe_3O_4, is also used for GSH elimination. Yu et al.[75] constructed a nanoscale liposome integrating Fe_3O_4 nanoparticles and oxaliplatin-based Pt(IV) prodrug (Figure 14D). The intracellular GSH annihilates ROS, which hinders the therapeutic effect of nanomedicine. However, this nanosystem consumes GSH by Pt(IV) activation as well as Fenton reaction induced by Fe_3O_4. It was confirmed that this synergistic effect substantially reduced GSH level when CT26 cells were co-incubated with the nanoscale liposomes. ROS then rapidly accumulated inside cancer cells, breaking the equilibrium between reductive and oxidative species. Both the *in vitro* and *in vivo* experiments verified the tumor inhibition performance of this nanoscale liposome. Apart from those mentioned above, there are many other strategies to deplete GSH within cancer cells, such as intracellular GSH synthesis inhibition by hammerhead ribozymes.[78] More related methods were recently summarized,[79] but their potential co-use with redox-activable prodrugs remains to be explored.

ROS-Boosting Strategies for Prodrug Activation. Although tumor cells accumulate ROS due to vigorous metabolism and mitochondrial dysfunction, their concentration is not high enough to fully activate prodrugs due to a series of factors such as tumor heterogeneity. ROS inside cancer cells have long been considered a weak stimulus.[80] Based on the cases discussed above, it can be concluded that an important design factor for ROS-activated prodrugs to inhibit tumors successfully is the cooperation of a ROS boosting agent. Up to now, GOx,[81] β-lapachone,[82] α-tocopheryl succinate,[83] and lipid hydroperoxide[84] have been used to enhance intracellular oxidative stress and incorporated in ROS-activable prodrug therapy. Due to the lack of modification sites, these ROS-promoting molecules are usually co-delivered with ROS-activable prodrugs through physical encapsulation, leaving a hidden risk of drug leakage during blood circulation. Cinnamaldehyde, derived from the cinnamon tree, exhibited anticancer function by increasing intracellular ROS.[85] With the existence of the aldehyde group, cinnamaldehyde can be covalently conjugated to prodrug nanosystems, which guarantees that the ROS boosting agent and prodrug could be tethered together. For instance, Zhao et al. recently tailored a cinnamaldehyde−gemcitabine conjugate molecule for ROS-responsive self-immolative prodrug activa-

https://doi.org/10.1021/acsnano.2c05379
ACS Nano 2022, 16, 13513−13553

tion (Figure 15A).[86] Anticancer drug GEM was covalently attached to cinnamaldehyde by forming ROS-cleavable thioacetal linkers. Considering the cytosine structure of GEM, a hyaluronic acid scaffold was further modified with guanine moieties to form Watson−Crick nucleobase pairs with cinnamaldehyde−gemcitabine conjugate molecules. The resultant nanoparticles exhibited spherical morphology with a diameter of approximately 100 nm. In the acidic tumor microenvironment, the hydrogen bond between the polymeric carrier and prodrug was disrupted, releasing cinnamaldehyde−gemcitabine conjugate molecules. Intracellular ROS cleaved thioacetal linkers to release GEM and cinnamaldehyde. The free cinnamaldehyde molecules further promoted ROS generation, achieving a "snowballing" effect on ROS accumulation. The ROS-boosting performance of this prodrug was verified by confocal laser scanning microscopy (CLSM) (Figure 15B). The 4T1 cells treated with 2′,7′-dichlorofluorescein diacetate as a ROS probe exhibited intensified green fluorescence after the release of cinnamaldehyde.

Mitochondria damage could also elevate intracellular ROS levels. Xing et al. recently explored the possibility of attacking mitochondria for better activation of ROS-responsive prodrugs.[87] A polymeric CPT prodrug constructed with thioketal linkages was functionalized with tumor cell targeting unit cRGD and mitochondria targeting species triphenylphosphonium. After prodrug nanoparticles reached the tumor cells, they accumulated in mitochondria, releasing CPT to cause mitochondrial damage and inhibit cellular respiration, leading to burst release of mitochondrial ROS and improving cellular oxidation stress.

ROS-generating dynamic therapies (including PDT, CDT, and sonodynamic therapy (SDT)), which also inhibit tumor cell proliferation by enhancing oxidative stress, can also improve the therapeutic index of ROS-activable prodrugs. Among these strategies, PDT, which relies upon a photosensitizer and light irradiation to generate singlet oxygen, has been studied in depth in the aspect of combination treatment with prodrug-based chemotherapy. For example, an aminoacrylate linker can respond to singlet oxygen and be cleaved.[88] Thus, this feature can be exploited to achieve combined ROS-responsive chemotherapy and PDT. In the course of our research, recently, we prepared a co-delivery nanosystem consisting of aminoacrylate linker modified PTX and boron dipyrromethene (BODIPY) based photosensitizer (Figure 16).[89] Both components were decorated with an adamantane moiety to associate with a β-CD modified PEG−poly(L-glutamic acid) (PGA) amphiphilic block polymer backbone. The ratio between these components was finely tuned by adjusting the mixing ratio during the coassembly process. When the ratio between PTX prodrug and the BODIPY based photosensitizer was 3:2, the obtained prodrug nanoparticle exhibited the highest cytotoxicity. The ROS level in HeLa cells was considerably higher in the NIR light irradiated group than in the nonirradiated samples; thus, the PTX prodrug was better activated with NIR light irradiation. By maximizing the synergistic effects of chemotherapy and PDT, this co-delivery nanoplatform efficiently inhibited HeLa tumor growth both *in vitro* and *in vivo*.

HYPOXIA-ACTIVABLE PRODRUGS

Most solid tumors will develop hypoxia after a certain stage of development (Scheme 4) due to the combined effects of rapid tumor proliferation and abnormal vascular. The hypoxic tumor microenvironment hinders multiple therapies because it causes undesirable consequences like tumor metastasis and tolerance to various treatment.[90] Therefore, technical methods to reverse tumor hypoxia have attracted extensive attention in the early research stage. The oxygen supply methods can be roughly divided into two categories: tumor delivery of oxygen and *in situ* oxygen production. Oxygen carrier materials such as hemoglobin and perfluorocarbon, have been explored to improve tumor endogenous oxygen concentration and increase the therapeutic index.[91,92] However, the application of this kind of tumor oxygenation materials only shows limited improvement of oxygen level since one hemoglobin molecule can only bind four oxygen molecules[92] and the carried oxygen is easily released prematurely in the veins and other hypoxic tissues during blood circulation; as for perfluorocarbon, although it has high affinity with oxygen, the O_2 release rate through simple diffusion is also too low to rapidly increase oxygen concentration in tumors. For the *in situ* oxygen generation through catalase[93] and MnO_2 nanomaterials,[94] though these approaches decompose H_2O_2 into oxygen with high efficiency, their reoxygenation effect only alleviates hypoxia to a limited level, due to the low endogenous H_2O_2 concentration (<50 mM).

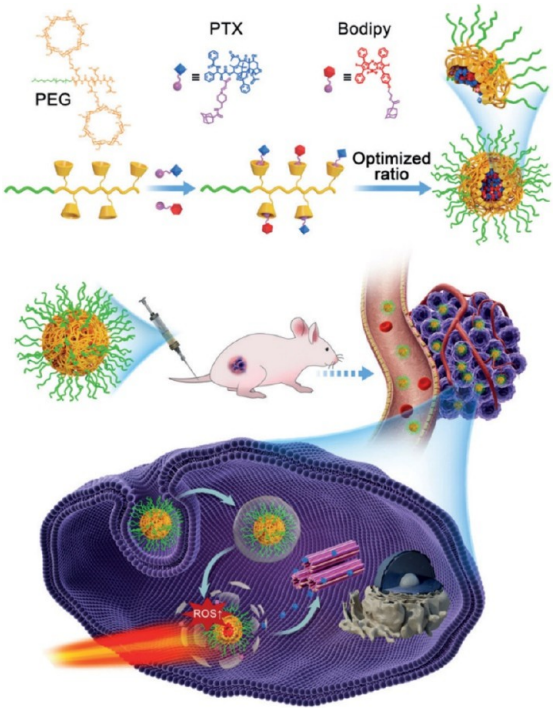

Figure 16. PDT boosted PTX prodrug activation: BODIPY and aminoacrylate modified PTX prodrug were coloaded to polymer scaffold through host−guest supramolecular interaction. BODIPY generated singlet oxygen under NIR irradiation promoted prodrug activation for synergistic PDT-chemotherapy. Reproduced with permission from ref 89. Copyright 2019 Wiley-VCH.

Hypoxia-activated prodrugs (HAPs), on the other hand, represent a different strategy to deal with the hypoxic tumor microenvironment, turning this problem of hypoxia into a therapeutic target.[95] Now, 11 types of HAPs have entered the clinical trial stage.[96] HAPs are also known as bioreductive prodrugs. Under normoxic conditions, their dormant state will not cause toxic side effects to healthy organs, while in hypoxic regions, HAPs are activated by reductive metabolism and

https://doi.org/10.1021/acsnano.2c05379
ACS Nano 2022, 16, 13513−13553

Scheme 4. Schematic Illustration of Hypoxia Responsive Prodrugs Activated in Hypoxic Tumor Regions and Hypoxia-Responsive Structures for Prodrug Design

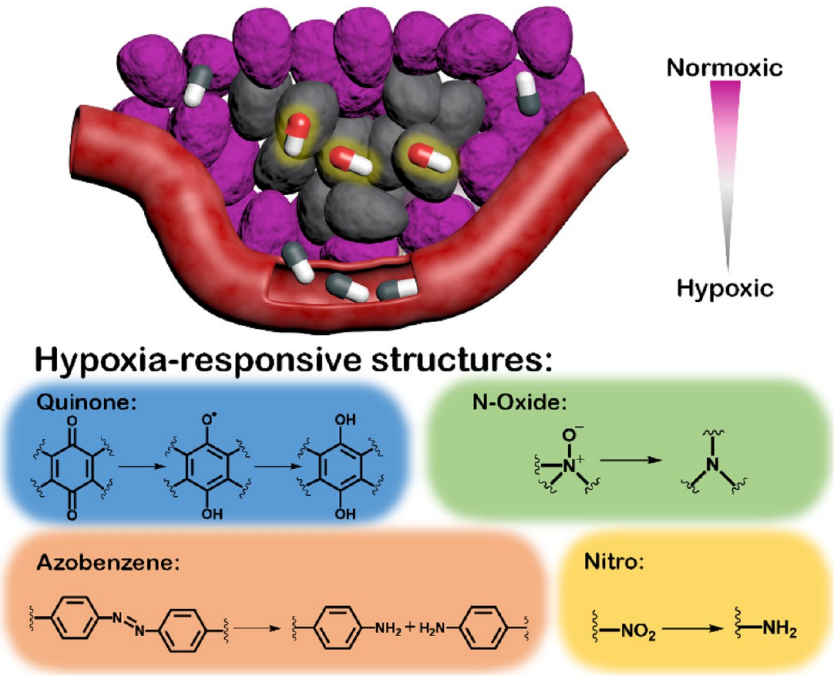

selectively kill hypoxic tumor cells. This is because, in hypoxic tumor cells, the unstable, oxygen-sensitive one-electron reduced HAP intermediates cannot be reversibly oxidized back to parent form as in normoxic conditions. Typical bioreductive drugs include quinones, *N*-oxides, and nitro-compounds. However, the current mainstream HAPs lack modification sites and do not need extra caging modification. Compared with other types of stimulus-activated prodrugs, the category of HAPs is still on a small scale, and many chemotherapy drugs that have been proven effective have not been developed into hypoxia activation mechanisms.

Hypoxia-Responsive Chemical Structures for Developing Prodrugs. *Quinones.* Quinones are involved in the regulation of the redox balance in tumor cells. They undergo one-electron reduction or two-electron reduction under the action of upregulated reductases inside tumor cells to produce toxic radicals. The hypoxic environment prolongs the half-life of the generated radicals for killing cancer cells. Mitomycin represents early quinone-based HAPs, which can be activated by NQO1 in solid tumors and be transformed into hydroquinones by a two-electron reduction process. Mitomycin also inhibits tumor cell proliferation by DNA alkylation.[97] Despite the hypoxia selectivity, quinone-based HAPs did not exhibit satisfactory therapeutic effects in clinical trials due to poor pharmacokinetic performances. Until now, no quinone-based HAPs have been developed as nanoscale formulations or decorated with tumor-targeting moieties. Zhang et al. exploited the NQO1 responsiveness of quinone compounds and developed a self-immolative 5-fluorouracil (5-Fu) prodrug.[98] 5-Fu was conjugated to quinone propionic acid through a self-immolative linker. Triggered by overexpressed NQO1, 5-Fu was released and exhibited *in vivo* anticancer effects in A549-tumor-bearing mice. However, whether the metabolic product of quinone contributed to the tumor suppression was not analyzed.

N-Oxides. *N*-Oxide is one of the most extensively studied hypoxia-responsive structures; until now, more than 30 kinds of *N*-oxide compounds have been developed as HAPs. Among them, the most representative cases are tirapazamine (TPZ)[99] and banoxantrone (AQ4N).[100] To increase their tumor availability, current studies focus on delivering them through specially designed nanovehicles. Koo et al. screened a set of anticancer drugs and found that TPZ showed strong synergism with pheophorbide a (Pba) involving PDT through *in vitro* screening.[101] They then loaded TPZ in Pba-containing gelatin nanoparticles. In this case, the prepared nanoparticles showed good internalization in SCC7 cells. MTT assays showed significant toxicity of the nanoparticles when treated with laser irradiation due to PDT-induced hypoxia intensification and subsequent TPZ activation. In dark conditions, the effect of the TPZ−Pba combination shifted from synergistic to antagonistic. Finally, administration of the prepared nanoparticles in SCC7 tumor-bearing mice with laser irradiation induced the most obvious tumor volume reduction compared with the laser-free and PDT-monotherapy control groups. Despite the hypoxia selectivity of HAPs, further clinical application of these drugs could be limited by tumor heterogeneity since there exist several regions with insufficient hypoxia levels inside the tumor, which may hinder the full activation of HAPs. A chemical motif with a more hypoxia-sensitive feature was designed by Kim et al. to address this problem.[96] Upon optimizing the *N*-oxide, they introduced α,β-unsaturation on the amine *N*-oxide to delocalize the N-lone pair electrons for two-electron irreversible bioreduction, therefore strengthening the hypoxia sensitivity. It was found that after modification of enamine *N*-oxide in the γ-lactam position of staurosporine the cytotoxicity was alleviated. When multiple cancer cell lines were incubated in hypoxic conditions, this prodrug exhibited lower half maximal inhibitory concentration than under normoxic conditions. Replacing the anticancer drug with a

https://doi.org/10.1021/acsnano.2c05379
ACS Nano 2022, 16, 13513−13553

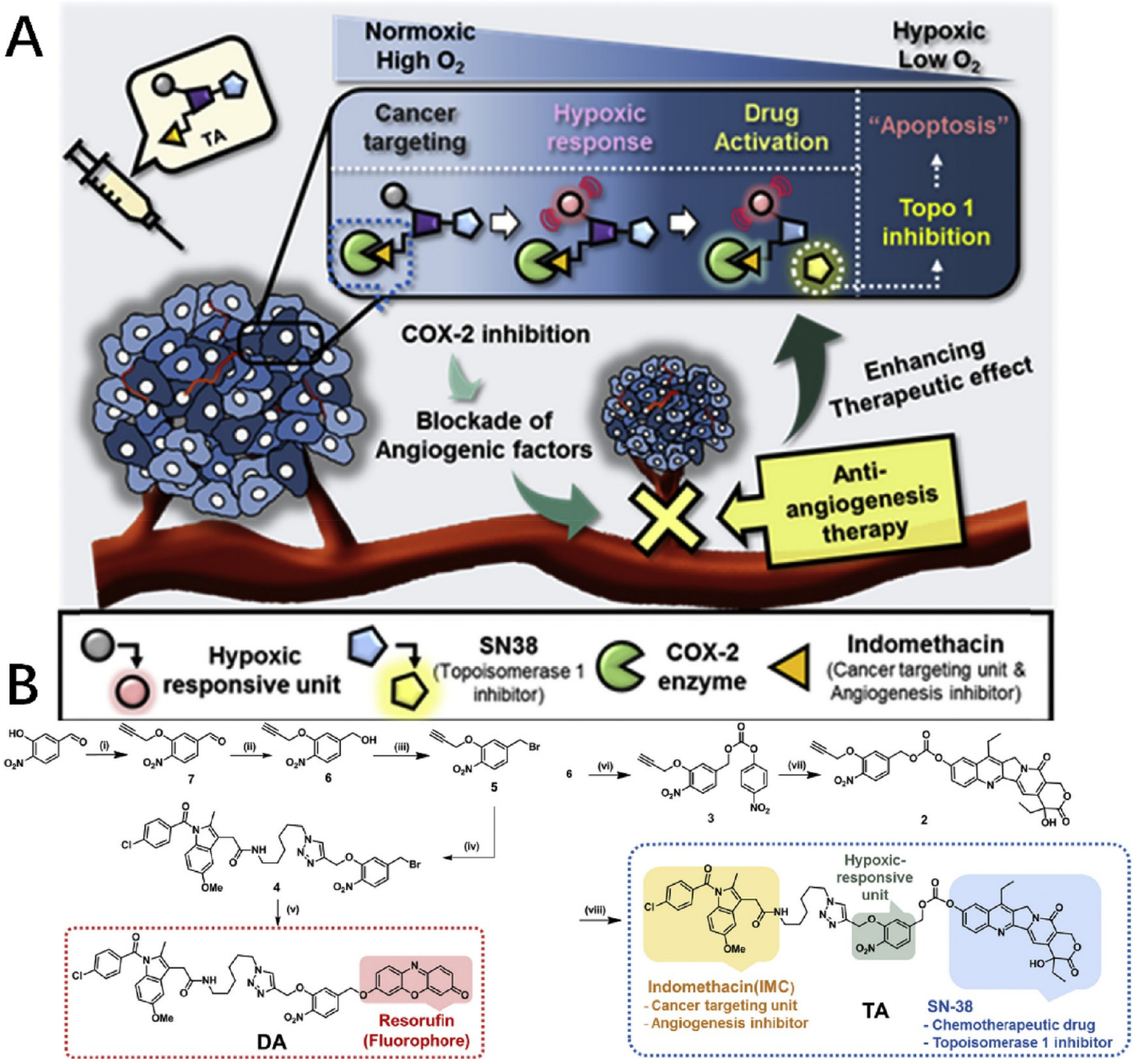

Figure 17. Hypoxia-responsive nitrobenzyl group used for prodrug design: (A) Theranostic prodrug system containing IND as tumor targeting moiety, angiogenesis inhibitor SN-38 as anticancer chemotherapy drug, and resorufin as diagnostic unit was activated in hypoxic tumor microenvironment, which was intensified by suppressing angiogenesis. (B) Synthetic route of nitrobenzyl containing diagnostic unit and therapeutic unit. Reproduced with permission from ref 103. Copyright 2018 Elsevier.

NIR fluorophore, the probe molecule could be utilized as a hypoxia imaging agent with high sensitivity.

Nitro-Compounds. Nitroreductases were found to be upregulated in hypoxic tumors, specifically when oxygen concentrations were below 10%.[102] Nitroaromatic and nitroimidazole compounds were therefore developed into nitroreductase-responsive prodrug cages and hypoxia-imaging units.[103,104] Electron-withdrawing nitro groups were reduced to amines upon nitroreductase exposure, triggering fluorescence restoration or releasing active anticancer drugs. For instance, the effective anticancer therapeutic outcome of the floxuridine oligomer was overshadowed by severe adverse effects, but Okamoto et al. addressed this issue by caging floxuridine monomers with a hypoxia-activable 4-nitrobenzyl group.[105] 4-Azobenzyl and 4-nitroazobenzyl groups were also introduced on the 4-oxygen atom of floxuridine. Compared with the non-biodegradable control group, these three prodrugs could be activated by $Na_2S_2O_4$, confirmed by high-performance liquid chromatography (HPLC). During *in vitro* screening experiments, the 4-nitroazobenzyl group exhibited the most potent cancer cell inhibition, especially under hypoxia conditions. Its hypoxia-activated anticancer effect was also shown in A549 tumor-bearing mice, alleviating systemic side effects of oligonucleotides as well. However, the pharmacokinetic parameters could be improved by optimizing oligomeric floxuridine length or developing this prodrug into nanoscale delivery platforms. In another study, Kim et al. constructed an indomethacin (IND)-containing prodrug system modified with

https://doi.org/10.1021/acsnano.2c05379
ACS Nano 2022, 16, 13513−13553

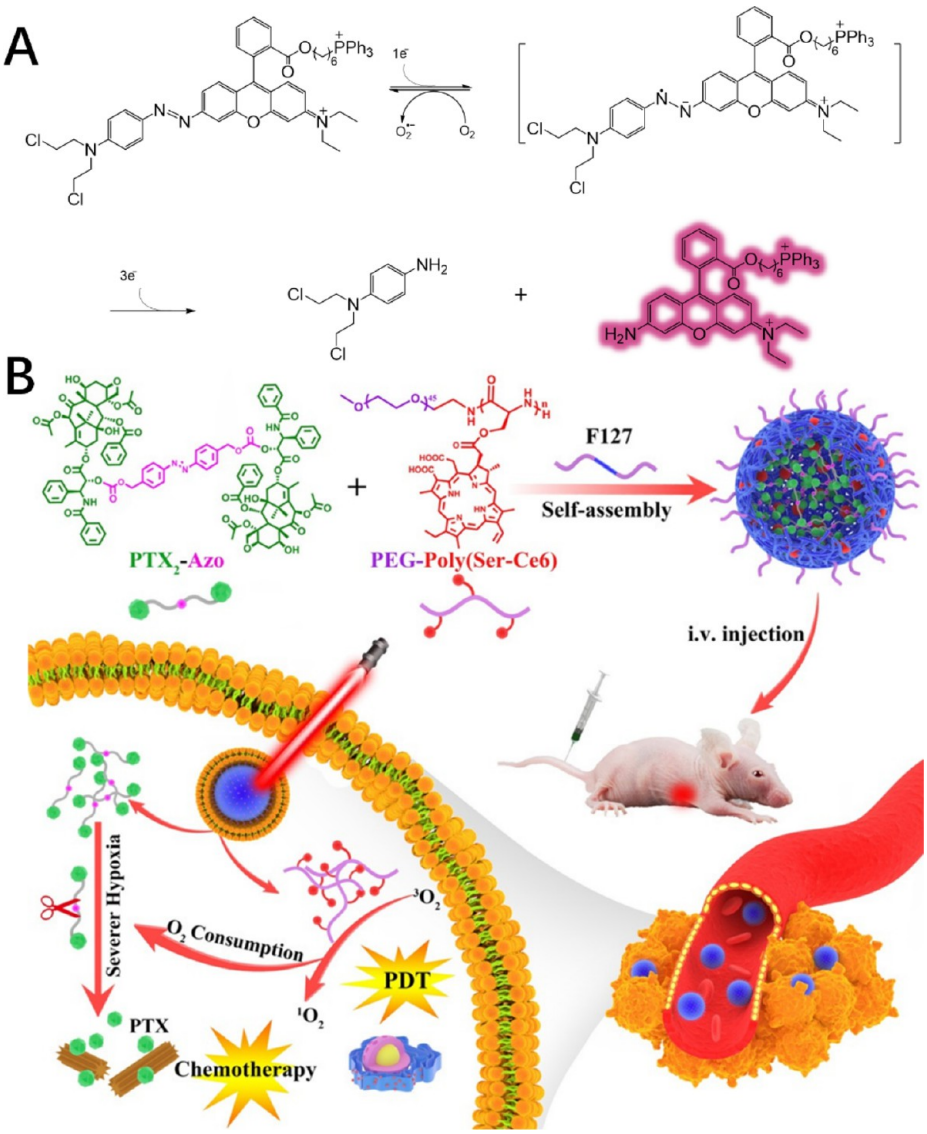

Figure 18. (A) Hypoxia-activation mechanism and *in vivo* anticancer effect of the azobenzene-based theranostic prodrugs. The structures were redrawn according to ref 108. (B) Structure of hypoxia-cleavable azobenzene linker modified PTX dimer prodrug, which was quickly activated in hypoxic tumor microenvironment intensified by co-delivered Ce6 photosensitizers. Reproduced with permission from ref 109. Copyright 2020 Wiley-VCH.

a nitrobenzyl unit to further conjugate with therapeutic SN38 and diagnostic fluorophore molecule resorufin (Figure 17).[103] IND in this platform is the key component as it accomplished two important functions, targeting tumor cells and inhibiting the angiogenesis factor cyclooxygenase 2. The SN-38 prodrug modified with the nitro group was designed to suppress hypoxia-promoted tumor metastasis caused by indomethacin. Through the co-incubation with nitroreductase, the nitroaromatic linker was bioreduced to an amine group, which further triggered the release of SN-38 parent drug molecules. The release of fluorophore resorufin also followed the same mechanism, which was verified by UV−vis absorption and fluorescence emission spectroscopic methods. As a result, IND created an enhanced hypoxia tumor microenvironment for antitumor activity and diagnostic effect.

Azobenzene Compounds. The azobenzene structure was also found to be hypoxia-responsive. The overexpressed azoreductase could cleave azobenzene into two separated amines. This hypoxia-responsive feature was adopted in designing a series of stimuli-responsive degradable drug delivery systems.[106] For example, Jiang et al. reported that an azobenzene containing covalent organic framework (COF) could effectively release payloads in hypoxic conditions because the cleavage of azobenzene linkers induced carrier degradation.[107] Recently, azobenzene was designed as a hypoxia-activable linkage to modify drug molecules into prodrugs. Kim et al. recently evaluated the possibility of using azobenzene to construct hypoxia-activated diagnostic materials (Figure 18A).[108] They coupled the anticancer alkylative drug nitrogen mustards and a rhodamine-like fluorescent molecule together through azobenzene linkers. It was clearly observed that upon treatment with hypoxia-mimicking sodium dithionite, the fluorescence intensity increased dramatically because the quenching effect of azobenzene structure was lifted, which was then developed as the probe mechanism for reporting bioreduction in DU145 tumor spheroids. With the aid of triphenylphosphine as a mitochondria-targeting unit, this diagnostic molecule triggered

https://doi.org/10.1021/acsnano.2c05379
ACS Nano 2022, 16, 13513−13553

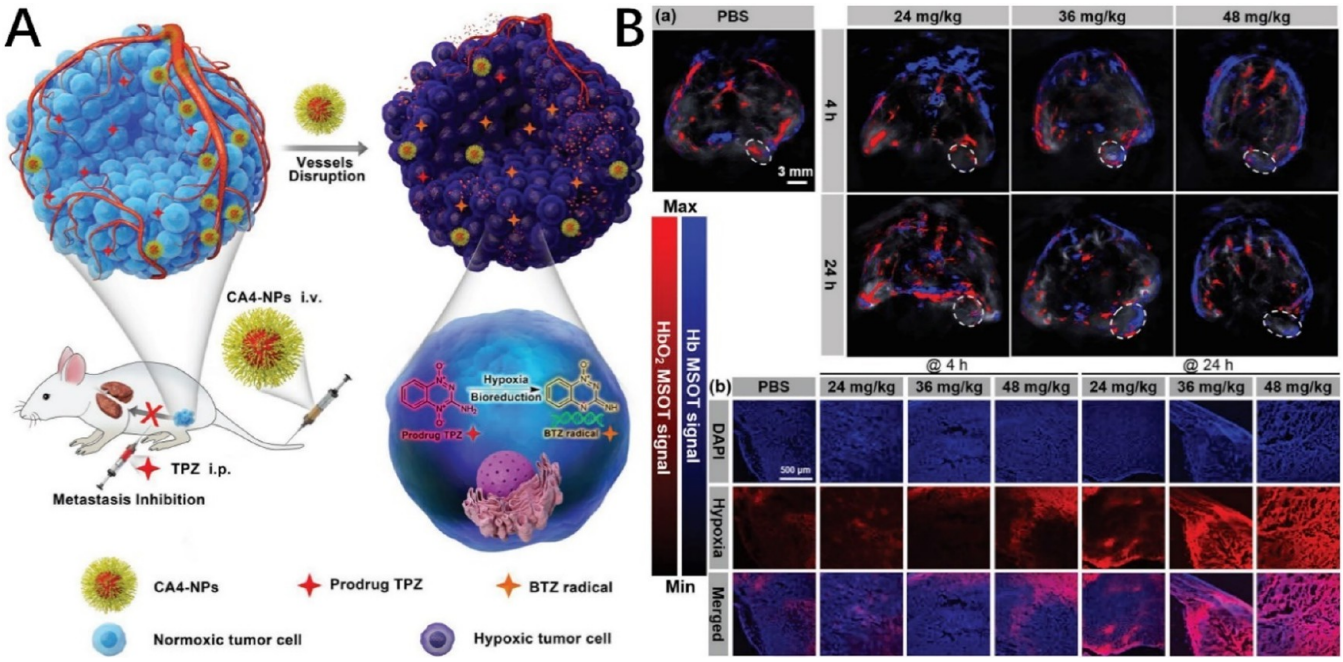

Figure 19. Hypoxia-intensifying strategies for better activation of HAPs. (A) Antitumor mechanism based on co-utilization of vascular-disrupting agent CA4 nanoparticles and HAP TPZ. Tumor-bearing mice were intravenously injected with CA4 nanoparticles to convert tumor into fully hypoxic state. Then, the TPZ prodrug was intraperitoneally injected to further inhibit tumor expansion. (B) Visualization of intensified hypoxic state in tumors by (a) photoacoustic imaging and (b) CLSM. Reproduced with permission from ref 110. Copyright 2019 WILEY-VCH.

mitochondria-mediated apoptosis and exhibited enhanced oxygen-state-related toxicity in multiple cancer cell lines. The *in vivo* antitumor activities of this azobenzene-based prodrug were also prominent in DU145 tumor models. Recently, Xie et al. leveraged this feature of azobenzene linker to obtain an azobenzene bridged PTX dimer prodrug (Figure 18B).[109] In this case, an azobenzene hypoxia-responsive linker was designed as a part of the prodrug activation mechanism. It was revealed by HPLC and mass spectrometer (MS) analysis that with $Na_2S_2O_4$ as a simulator of azoreductase the azobenzene bridged PTX prodrug could be converted to active PTX. After coassembly with Ce6-containing PEG, the two-component nanoparticles exhibited synergistic tumor inhibition effect under NIR irradiation; Ce6 consumed oxygen during the photodynamic process, which intensified hypoxia inside the tumor tissue, and azobenzene functionalized PTX prodrug was rapidly transformed into the active form. After intravenous injection of this prodrug, a considerable tumor inhibition effect was observed in HeLa tumor-bearing mice.

Hypoxia-Intensifying Strategies for Prodrug Activation. In addition to developing hypoxia-sensitive chemical structures, the combination of HAPs and oxygen-depletion agents has been viewed as a promising approach for cancer therapy that makes full use of tumor hypoxia as a trigger to initiate therapies. Several hypoxia-enhancing agents have been proven to induce aggravated hypoxia within tumors, such as vascular disruption agents and photosensitizers. The former represents the oxygen cutoff strategy, while the latter relies on intensified oxygen consumption. Chen et al. reported a vascular disrupting nanodrug based on amphiphilic polymer-coated combretastatin A4 (CA4) and TPZ capable of suppressing large volume tumors (Figure 19A).[110] After intravenous injection of CA4 nanoparticles, the elevated hypoxia level was verified by a photoacoustic imaging technique, a hypoxia detection probe in CLSM (Figure 19B), and upregulated hypoxia-inducible factor 1α (HIF-1α). Subsequently, the intraperitoneally injected TPZ was selectively activated into its cytotoxic radical form, leading to boosted therapeutic effect compared to the monotherapies. Notably, this strategy also exhibited an antimetastasis effect. In 4T1 tumor-bearing mice, metastasis was not evident in the CA4 nanoparticle plus TPZ group, bringing hope for treating advanced tumors prone to metastasis, such as breast cancer. Based on this research, subsequently, the combination of coagulation protease thrombin and TPZ has also been reported. Thrombin was considered a superior vascular disrupting agent since it could directly promote blood coagulation without the participation of other cofactors. Han et al. demonstrated that thrombin and TPZ can be coencapsulated into metal−organic framework (MOF) nanoparticles, possibly saving patients from administering the drugs twice.[111] This delivery system exhibited advantages such as mild synthesis conditions and high loading efficiencies of 92.92% (for thrombin) and 13.82% (for TPZ). The surface of the MOF container was further decorated with folic acid to recognize cancer cells. After these nanoparticles selectively accumulated at tumor sites, the ZIF-8 MOF scaffold was degraded in the acidic microenvironment to quickly release thrombin. It was observed that the released thrombin induced blood clot formation and cut off the oxygen supply, aggravating tumor hypoxia and further promoting the activation of TPZ. After intravenous injection treatment, HepG2 tumor-bearing mice treated with this combination therapy showed obvious tumor shrinkage due to synergistic therapy.

The strategy of co-delivering HAPs with photosensitizers has also been put forward for better activating HAPs by depleting oxygen within tumors. Since most HAPs lack functional groups suitable for covalent conjugation on carrier materials, it is

https://doi.org/10.1021/acsnano.2c05379
ACS Nano 2022, 16, 13513−13553

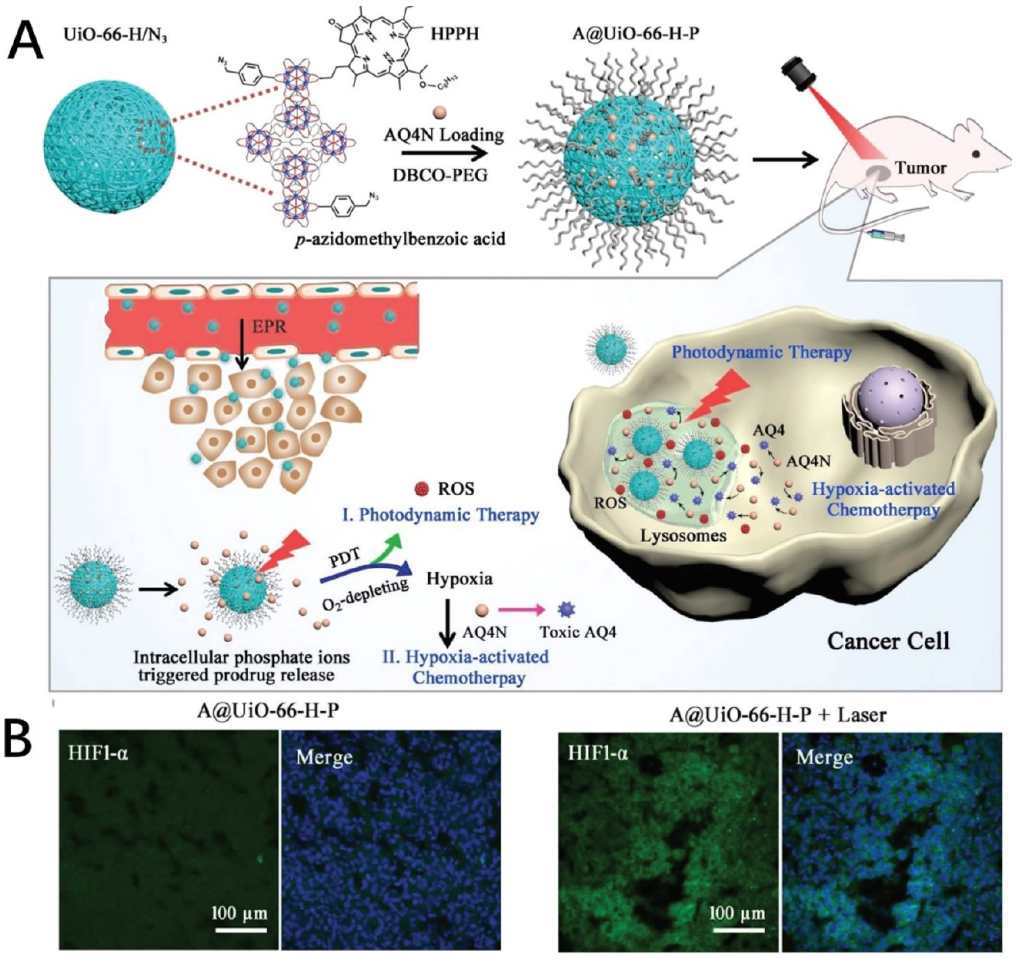

Figure 20. (A) MOF nanosystems utilized for co-delivery of photosensitizer photochlor and HAP AQ4N. Photochlor was covalently attached onto the scaffold of UiO-66 typed MOF carriers, while the AQ4N was physically encapsulated into the pores, waiting to be released by high concentrations of phosphate inside cancer cells. Photodynamic process aggravated the hypoxia degree, promoting the activation of AQ4N. (B) *In vivo* tumor model treated with this nanoplatform plus NIR irradiation exhibiting elevated HIF-1α expression compared with irradiation-free group. Reproduced with permission from ref 112. Copyright 2018 WILEY-VCH.

essential to develop advanced carrier materials for co-delivery of HAPs and photosensitizers and avoid preactivation and prerelease of HAPs during blood circulation. For instance, UiO-66 MOF nanoparticles were reported to simultaneously deliver photosensitizer photochlor and the hydrophilic HAP AQ4N (Figure 20A).[112] By fine-tuning the pore size of MOF nanoparticles, the AQ4N was well-encapsulated within carrier materials. AQ4N remained inside MOF nanoparticles during blood circulation due to low phosphate concentration in plasma. Only after entering cancer cells does a much higher phosphate concentration inside cells trigger the release of AQ4N. The photosensitizer photochlor was integrated on the surface of MOF nanoparticles during one-pot solvothermal synthesis. This hierarchical loading strategy guaranteed the reliable binding of photosensitizers and HAPs. With NIR light exposure, ROS generation intensified the tumor hypoxia. The decreased oxygen concentration was proven by the upregulation of HIF-1α in immunofluorescence staining experiments. Thus, AQ4N activation was facilitated through the photodynamic process. Further experimental results showed that the MOF nanoparticles were promising for effective accumulation of both photochlor and AQ4N in tumors, as the tumor suppression performance is better than the photochlor/AQ4N mixture group. In another study, Fan et al. designed a hybrid nanoplatform to simultaneously deliver AQ4N and a semiconducting polymeric photosensitizer (Figure 20B).[113] Here, the photosensitizer component also contained $NaYF_4$:Yb/Tm@$NaYF_4$ upconversion nanoparticles (UCNPs) to transform tissue penetrable NIR light into UV light for generating singlet oxygen and inducing hypoxic activation stimulus. Also, a pH degradable MnCaP shell was incorporated to encapsulate photosensitizer and AQ4N, increasing the diameter of the obtained delivery system for a longer circulation time. Moreover, the breakdown of this layer allowed both components to penetrate deep into the interior tumor region, resulting in effective synergistic tumor suppression ratio of 83% in HepG2 tumor-bearing mice. However, for more adjustable co-delivery of photosensitizers and HAPs such as precise ratio control, the interaction between the loading component and the carrier materials should be upgraded in the future, for example, developing more sensitive hypoxia-degradable linkers and designing more advanced drug-loading approaches to replace physical encapsulation. On the other hand, the therapeutic potential of other oxygen-consuming therapies, such as SDT and radiotherapy, in combination with HAPs remains to be developed.

https://doi.org/10.1021/acsnano.2c05379
ACS Nano 2022, 16, 13513−13553

ENZYME-ACTIVABLE PRODRUGS

The activation of the above-discussed hypoxia-responsive prodrugs depends on the participation of reductases. As a matter of fact, apart from reductases, some other enzymes are also upregulated in tumor cells due to increased metabolic rate.[114] For example, phospholipase A2 is overexpressed in prostate cancer cells, cyclooxygenase-2 is overexpressed in colorectal cancer, and glucuronidase is overexpressed in bladder cancer. Therefore, these overexpressed enzymes can promote the therapeutic effect of enzyme-responsive drug delivery materials, which are highly selective for tumors and contribute to the development of imaging materials for diagnostic purposes. In this section, we will focus on recent advances in enzyme-activable prodrugs mainly based on cleavable chemical structures (Scheme 5). Although common structures like ester bonds can be degraded by overexpressed esterases in tumors, they can also be slowly hydrolyzed over time. Therefore, it lacks specificity to some extent. Strategies to adjust enzyme levels for precisely activating prodrugs are also discussed.

Scheme 5. Typical Structures Responsive to Enzymes Upregulated in Tumors for Prodrug Design

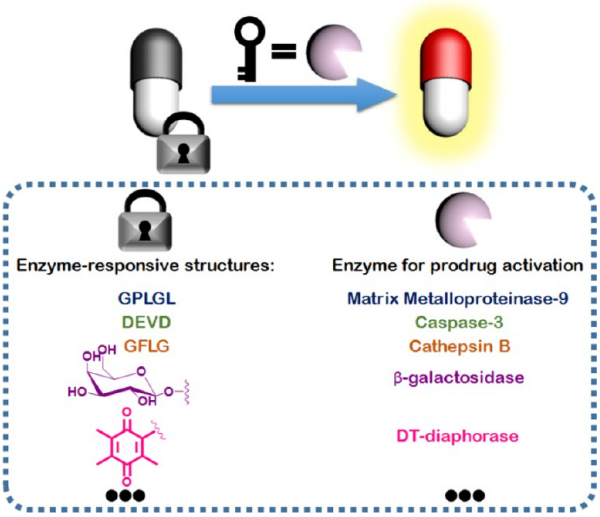

Enzymes as Triggers for Activating Prodrugs. *Matrix Metalloproteinase.* Like the mildly acidic microenvironment, the dysregulation of certain enzymes is also an effective tumor biomarker. Prodrugs can thus be designed to incorporate peptide spacers as the substrate of these enzymes for more specifically triggering the cleavage of a linker moiety. The matrix metalloproteinase (MMP) family participates in the physiological process of extracellular matrix degradation and is also involved in tumor proliferation and metastasis.[115] Due to the upregulated level of MMPs in tumors, Chen et al. designed an MMP9-activable DOX prodrug for tumor-selective drug release (Figure 21).[116] DOX molecules were covalently attached to a MMP9-responsive peptide, Fmoc-GPLGL. They found that after incubation with MMP9, DOX was released in a time-dependent manner. With the MS identification, the cleavage site was confirmed, which was between Gly and Leu. Thus, the released DOX was not in its original form. However, considering the existence of amino-peptidases in tumors, the released Leu-DOX could be finally restored to active DOX intracorporeally. To fully activate this prodrug within tumor cells, they improved MMP9 concentration by developing a cooperative strategy with CA4 nanoparticles. The vascular disrupting agent CA4 destroys tumor blood vessels to induce hypoxia and promotes the expression of MMP9, as evidenced by immunofluorescence staining results. By amplifying the MMP9 activation signal, the CA4 nanoparticles promoted the therapeutic index of this DOX prodrug in both orthotopic and subcutaneous tumor models.

Caspase. Caspases have been the subject of extensive interest in oncology research. Up to now, 14 kinds of caspases, which are involved in regulating various biological processes and are closely related to apoptosis, in addition to cell growth, differentiation, proliferation, and motility, have been identified. Particularly, in dying tumor cells, caspase-3 is activated, increasing the secretion of prostaglandin E2, which leads to resistance to treatment such as radiation therapy. With the discovery of a caspase-responsive cleavable peptide linker, DEVD, caspase-3 was recognized as a trigger for prodrug-based chemotherapy.[117] Byun et al. conjugated cytotoxic DOX and the targeting peptide RGD to DEVD for developing self-triggered apoptosis enzyme prodrug therapy.[118] This kind of prodrug exhibited a distinct advantage: it does not require the involvement of other mediators and could amplify the caspase-3 activation signal when activated. The prodrug was activated upon treatment with caspase-3 to produce an intermediate state. After further metabolism by intracellular carboxylesterases, the parent form of DOX was restored (Figure 22). This process was characterized by a high degree of selectivity and speed. According to HPLC analysis, 80% of the incubated prodrug was activated within 30 min. The released DOX induced apoptosis of targeted cells, which upregulated caspase-3 and increased cellular caspase-3 activity to overcome the obstacle of tumor heterogeneity. Therefore, it effectively inhibited the growth of U-87 MG xenograft tumors and also 4T1-luc2 metastatic tumors.

Cysteine Cathepsin. Cysteine cathepsins are usually located in lysosomes to mediate protein hydrolysis. Among different types of cathepsins, cathepsin B is closely related to various diseases, including arthritis and malignant tumors. It degrades the extracellular matrix to release metastatic cancer cells, facilitating the invasion and metastasis of tumors. Therefore, cathepsin B is considered a biomarker for cancer diagnosis. Also, since it can identify peptide bonds at specific sites of amino acids, prodrugs activated by cathepsin B are developed for the controlled release of cytotoxic payloads. For example, the oligopeptide GFLG can be recognized and degraded by cathepsin B and thus be designed as a cleavable linker. In the early stage, Kopeček et al. explored the capacity of GFLG to introduce functional components into drug delivery polymer *N*-(2-hydroxypropyl)methacrylamide, including the chemotherapy drugs PTX and GEM, isotope labels ^{125}I and ^{111}In, and fluorophores FITC and Cy5.[119] Wang et al. used the GFLG linker to introduce the broad-spectrum chemotherapy drug docetaxel (DTX) into a pH degradable polymer drug carrier to maximize DTX accumulation in tumors through size switch and controlled drug release (Figure 23).[120] The C7A moieties were protonated and transformed into a hydrophilic state. Then the nanoparticles were dissociated into small fragments with diameters of 5 nm. In lysosomes, the cathepsin B cleaved the GFLG linker and released DTX, which induced apoptosis of multiple cancer cell lines, 4T1, B16OVA, and MCF-7. The DTX also aroused immune responses in tumors.

https://doi.org/10.1021/acsnano.2c05379
ACS Nano 2022, 16, 13513−13553

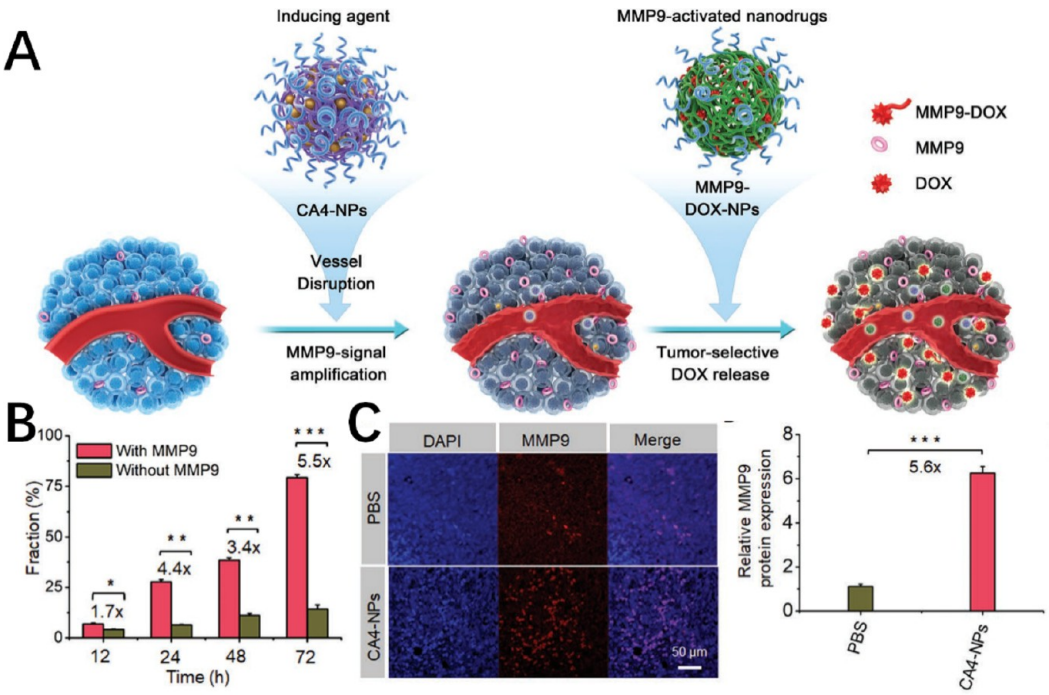

Figure 21. MMP9 activated DOX prodrug. (A) Vascular disrupting agent CA4 nanoparticles improved the intratumoral MMP9 level to better activate DOX prodrug. (B) Prodrug activation ratio with or without the presence of MMP9. (C) MMP9 amplification effect induced by CA4 nanoparticles. Reproduced with permission from ref 116. Copyright 2019 WILEY-VCH.

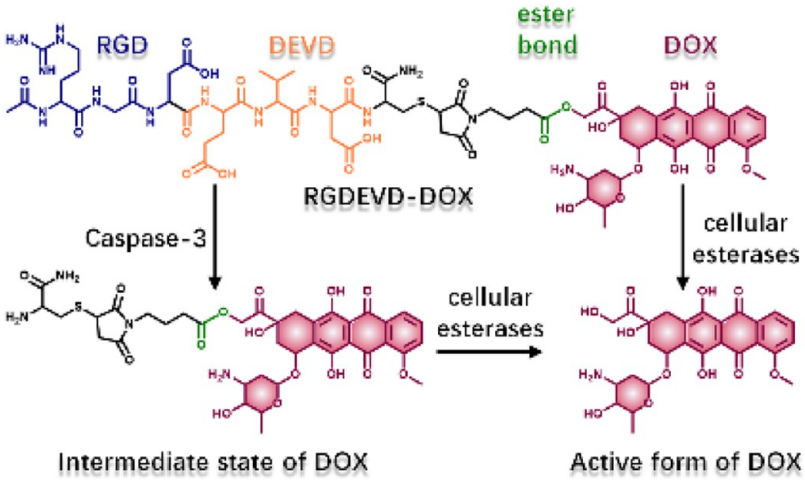

Figure 22. Activation mechanism of caspase-3-responsive prodrugs. The structures were redrawn according to ref 118.

With synergistic chemotherapy and immunotherapy, the tumor inhibition rate against 4T1 tumors was detected to be up to 73% after intravenous injection. Moreover, the relapse rate in B16OVA-bearing mice was as low as 43%.

β-Galactosidase. β-Galactosidase (β-gal) is located inside lysosomes and catalyzes glycosidic bond breakdown to generate monosaccharides.[121] β-gal responsiveness is one of the most frequently used strategies for drug delivery. Moreover, this enzyme is upregulated in various cancer types, including lung, colon, liver, and ovarian cancers. A recent example of β-gal responsive prodrug therapy involved an enzyme-activable platform containing a chemiluminescent agent (phenoxy dioxetane), the cytotoxic drug monomethyl auristatin E (MMAE), and a substrate for β-gal (Figure 24).[122] The β-galactose group was cleaved by β-gal to trigger a 1,6-elimination reaction within the molecules, followed by the release of MMAE and quinone methide. Then a water molecule was involved in generating an oxyanion intermediate. Through intramolecular electron transfer, 2-adamantanone was ejected, accompanied by chemiluminescence of the remaining benzoate. Therefore, the researchers established a correlation between diagnostic and therapeutic effects. Chemiluminescence signal was observed with the activation of prodrug by β-gal. In the control sample, which did not contain the β-galactose group, or in the absence of β-gal, no light was emitted. Although this prodrug molecule was not developed into a nanoscale formulation, direct injection of this prodrug also resulted in measurable emission in CT26-LacZ tumor-bearing mice. In contrast, the emission intensity was much weaker for the CT26-wt tumor model, which exhibited low β-gal levels. Compared to conventional fluorescence probes, this chemiluminescence diagnosis presented a higher signal-to-

https://doi.org/10.1021/acsnano.2c05379
ACS Nano 2022, 16, 13513−13553

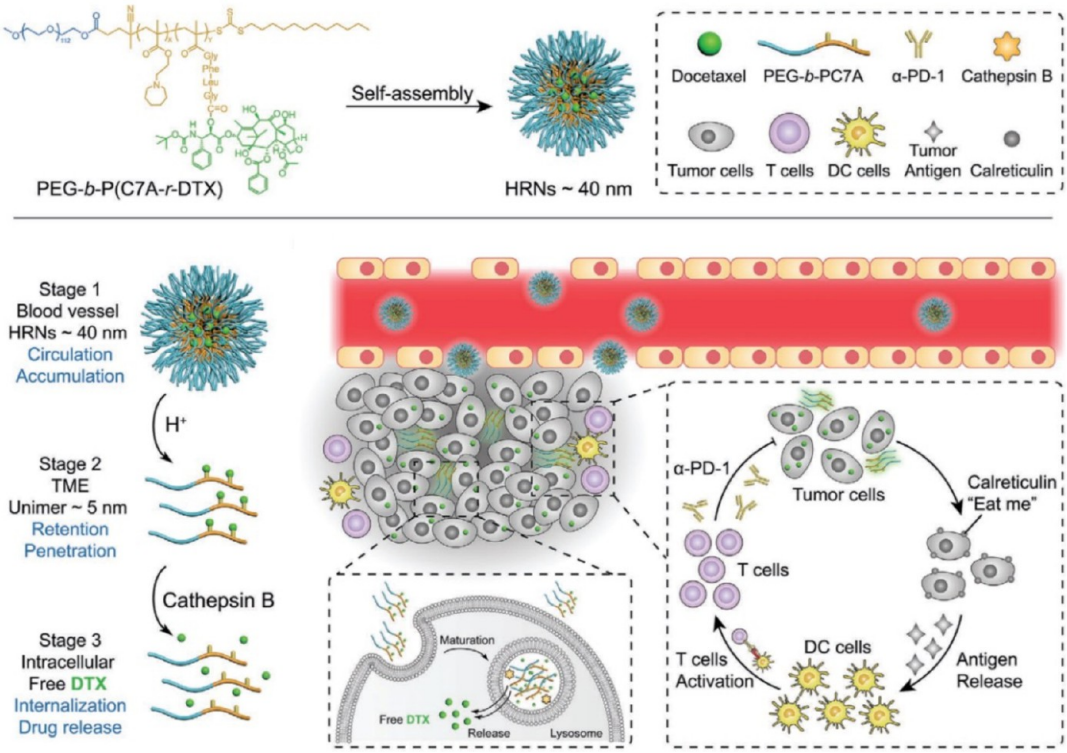

Figure 23. Docetaxel prodrug constructed based on GFLG cleavable linkers: the polymer carrier was degraded by the acidic tumor microenvironment to promote deep penetration; then in lysosomes, the DTX was released by cathepsin B to directly kill cancer cells while invoking immune response at the same time. Reproduced with permission from ref 120. Copyright 2020 WILEY-VCH.

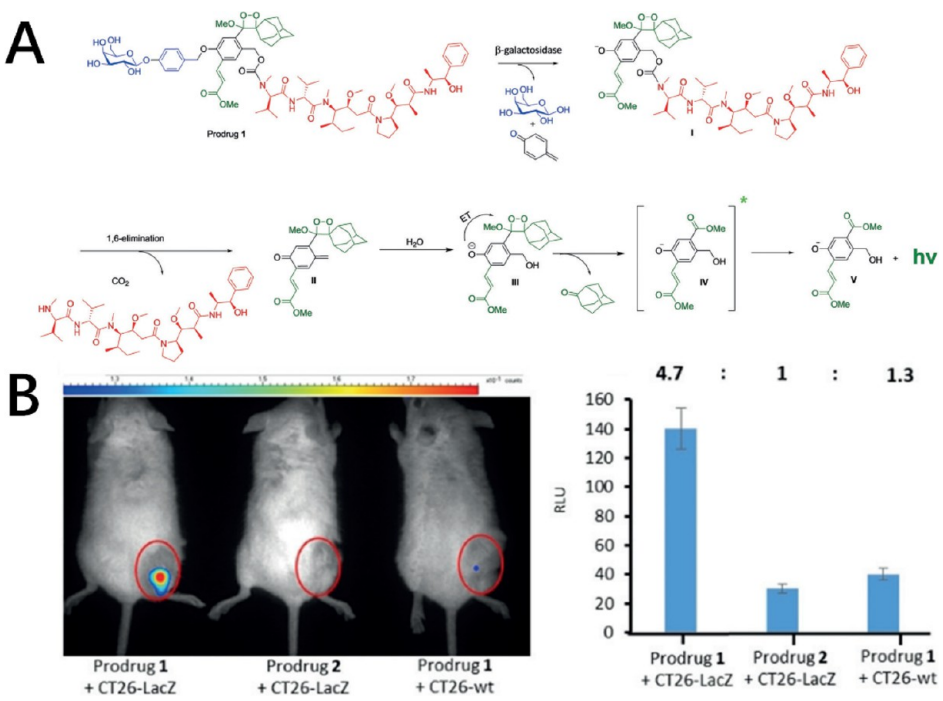

Figure 24. β-Galactosidase-responsive prodrug activation and synchronously generated chemiluminescence for diagnostic of tumors. (A) Activation mechanism and (B) *in vivo* imaging of prodrug activation. Reproduced with permission from ref 122. Copyright 2018 Wiley-VCH.

noise ratio, whereby *in vivo* β-galactosidase activity could be monitored.

DT-Diaphorase. DT-diaphorase belongs to the family of quinone reductases, which biocatalyze conversion of quinone species into the corresponding hydroquinones through a two-electron reduction process. These enzymes are overexpressed in breast cancer, non-small-cell lung cancer, colorectal cancer, and cervical cancer. Wu et al. developed a series of DT-diaphorase-responsive prodrugs by covalently attaching cytotoxic drug molecules to quinone through self-immolative

https://doi.org/10.1021/acsnano.2c05379
ACS Nano 2022, 16, 13513−13553

Scheme 6. Schematic Illustration of Activation Process and Typical Structure of Light-Activable Prodrugs

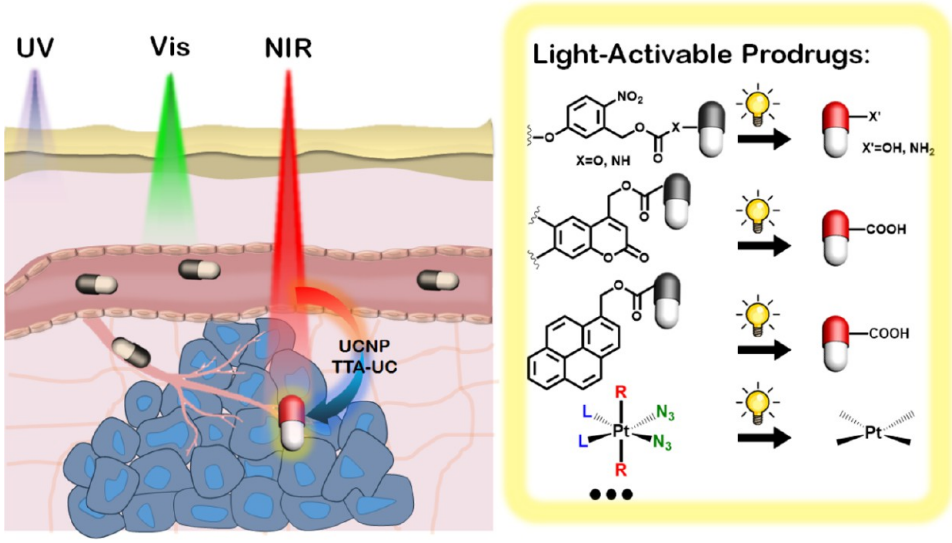

linkers.[123,124] For example, they recently reported an MTX-based prodrug containing quinone propionic acid as caging moiety.[125] Without the DT-diaphorase, the quinone moiety, as an electron-withdrawing group, quenched the fluorescence of the coumarin due to photoinduced electron transfer. However, in the presence of DT-diaphorase, quinone was reduced and then cut off from the prodrug molecules, restoring the fluorescence of coumarin. With extra one-photon or two-photon irradiation, coumarin was also removed to release free MTX. The dual-locking mechanism integrated both endogenous and exogenous activation triggers, which improved the biosafety of the obtained prodrug, also endowing the prodrug with the capability of discriminating cancer cells from normal cells. Flow cytometry experiments confirmed that this prodrug induced pro-apoptotic effect on multiple DT-diaphorase overexpressing cancer cell lines with light irradiation.

Enzyme Boosting Strategies for Prodrug Activation. Even though the enzymatic stimulus for prodrug activation is widely viewed as highly selective, there are still several obstacles for such an activation mechanism to overcome. Making such therapies not limited by the heterogeneity of tumors is urgently needed. Therefore, to ensure the success of enzyme-activable prodrugs, designing amplification strategies to improve the target enzyme level is crucial. Other therapy methods can control the dysregulation of endogenous enzyme levels. One of the studies on combination therapy was reported by Byun et al.[126] They designed a chemo-radiotherapy strategy that can precisely define the site of prodrug activation; after exposure to radiotherapy, the caspase-3 expression level was elevated to metabolize benign prodrug into cytotoxic MMAE to treat the tumor by cleavage of DEVD linkers. This kind of therapy is beneficial for solid tumors such as triple negative breast cancer that lack a valid molecular target.

However, there are concerns about improving the concentration of such enzymes through artificial methods. For example, the elevated cathepsin enzyme in tumors may result in the invasion and metastasis of cancer cells. The results obtained from animal experiments do not offer safety assurances for patients in real life. Considering this, researchers looked to exogenous enzymes. Enzymes native to non-human species, such as bacteria, can also catalyze prodrug activation, making them another choice for enzyme-activable prodrugs. It has been found that better prodrug affinity, higher enzymatic stability, and decreased side effects can be realized in the presence of these enzymes, although inappropriate exogenous enzymes might be immunogenic. Bhujwalla et al. decorated bacterial cytosine deaminase with multimodal imaging agents (rhodamine and Gd^{3+}-DOTA) for determining the best prodrug administration time window.[127] One of the highly influential factors to be considered for non-human native enzyme prodrug therapy is how to deliver the enzyme to the desired sites. To date, the therapeutic enzymes have been designed to be delivered either directly or indirectly. In most cases, the direct delivery method involves the conjugation of the enzyme with a polymer chain, an antibody, a MOF, and inorganic nanoparticles. Mendes and Zelikin used PVA-based biocatalytic hydrogels to directly deliver β-glucuronidase in order to overcome the low delivery efficiency obstacle.[128] The implanted hydrogel model converted SN-38, 5-fluorouracil, and curcumin prodrugs with the same kind of enzyme and accomplished a more flexible drug administration style in which multiple therapeutic agents can be used individually, in sequence, or in combination. Yuan et al. encapsulated exogenous enzyme myrosinase in honeycomb gold nanoparticles to catalyze nontoxic glucoraphanin transformation into the active form of sulforaphene.[129] With NIR irradiation, myrosinase was rapidly released out of carriers in a spatiotemporally controlled manner. Hyperthermia was also aroused due to the photothermal effect from the Au-based carrier materials. The generated sulforaphene exhibited a synergistic therapeutic effect with hyperthermia since sulforaphene disrupted the function of heat shock protein 90. The *in vivo* treatment effect was verified in mice bearing 4T1 subcutaneous xenograft tumors, and apparent tumor regression was observed in the chemotherapy and PTT synergy group.

Indirect delivery of activator enzymes refers to gene-directed enzyme prodrug therapy. The related approaches are highly preferred because this technique can afford prolonged expression and adequate intratumoral distribution of the therapeutic enzyme at the target site.[130] Tumor tropic cells are the optimal choice for gene transfer engineering since they possess the intrinsic ability to target tumor locations. The

https://doi.org/10.1021/acsnano.2c05379
ACS Nano 2022, 16, 13513−13553

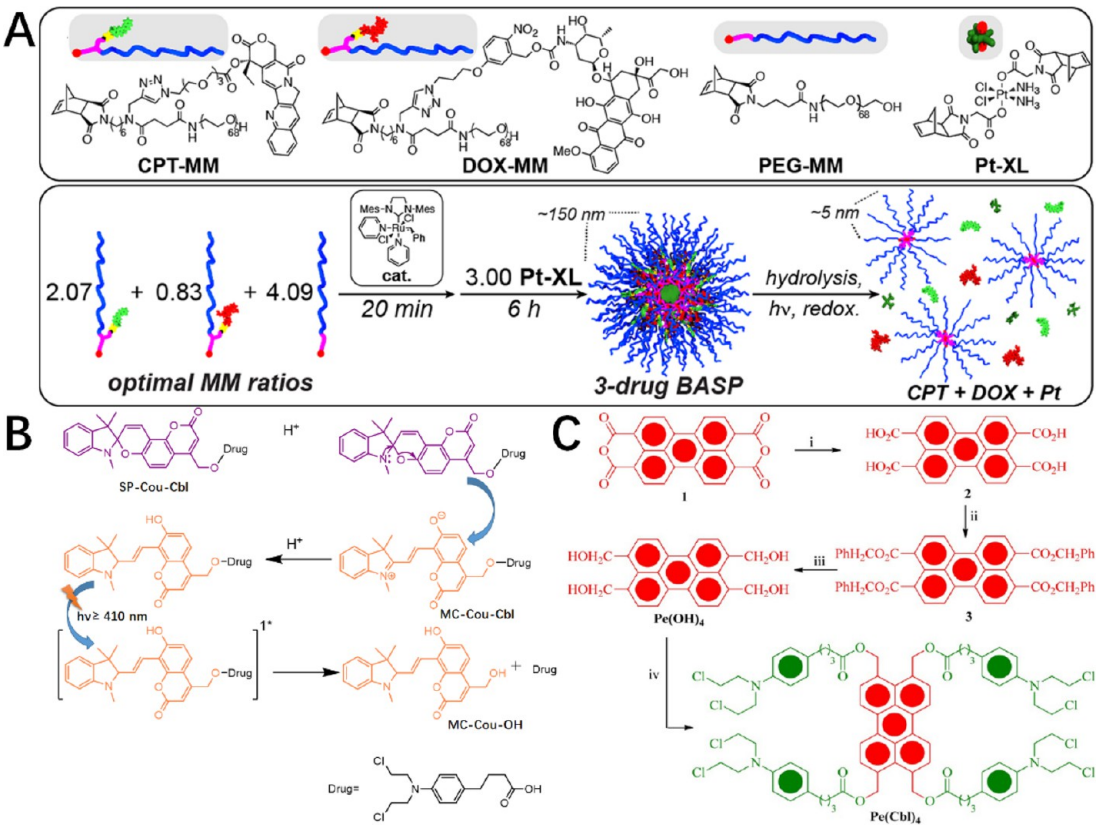

Figure 25. (A) Ternary prodrug loaded polymer nanoparticles for synergistic tumor therapy, in which light-activation was achieved through the UV light induced cleavage of the *O*-nitrobenzyl linker. Reprinted with permission from ref 132. Copyright 2014 American Chemical Society. (B) Activation mechanism of coumarin based chlorambucil prodrug: The spiropyran was protonated to unlock the coumarin moiety within the molecule. Then, the ester bond between coumarin and chlorambucil was cleaved in response to visible light. The structures were redrawn according to ref 133. (C) Perylene as cage for construction of photoactivable chlorambucil prodrug: the ester bond between perylene and chlorambucil was cleaved with visible light irradiation, releasing chlorambucil to kill tumor cells. Reproduced with permission from ref 134. Copyright 2014 American Chemical Society.

summary of current gene transfer methods is beyond the scope of this review; thus, we do not discuss them in detail.

LIGHT-ACTIVABLE PRODRUGS

Unlike the aforementioned stimuli, which naturally exist in tumors, light is gaining popularity in designing prodrugs and drug delivery materials since adjusting such stimulus does not need complicated design. Benefiting from the upgraded fiber-optic light-guiding equipment and NIR laser techniques, light-activable prodrugs offer promising clinical application opportunities since they have exhibited convenient spatiotemporal manipulation and the degree of photochemical reaction can be precisely controlled via adjustment of the irradiation dosage (Scheme 6). In addition, the triggering incident light is exerted *ex vivo*; it is not a pathological feature of a certain disease. Therefore, such a drug release mechanism can be applied in a variety of disease models or used to control bioactivities inside the human body. For example, Kohane et al. synthesized a macromolecular prodrug with anesthetic tetracaine as payload linked by photolabile coumarin to realize precise local anesthesia by irradiation with 400 nm light.[131]

Light-Responsive Chemical Structures for Developing Prodrugs. *Photolabile Linkages.* Photolabile linkers such as coumarin, 2-nitrobenzyl, 7-nitroindoline, and pyrene have been extensively studied to construct various biomedical materials, including photodegradable hydrogels and drug delivery nanocontainers. The studies on these structures contribute to the development of light-activable prodrugs through a light-activated cleavage strategy. For example, Johnson et al. constructed ternary prodrug-based polymer nanoparticles for combination therapy against ovarian cancer (Figure 25A).[132] DOX, CPT, and cisplatin-based Pt(IV) prodrugs were covalently modified for ring-opening metathesis polymerization on macromonomers. An *O*-nitrobenzyl linker was chosen to connect DOX and a norbornene monomer. Pt(IV) was modified with two norbornene moieties in the axial positions acting as a cross-linker during nanoparticle formation. An ester bond was designed to link CPT and norbornene. The loading ratio of these prodrugs can be precisely controlled by changing their feeding ratio before polymerization. The ternary prodrug loaded nanoparticles plus light irradiation (365 nm) outperformed one- and two-drug-loaded control groups, exhibiting the lowest IC_{50} value against OVCAR3 cells.

Coumarin is one of the most studied photocleavable groups, responding to light in the UV−vis region and then uncaging anticancer drugs. Barman and co-workers fused coumarin with acid-chromic compound spiropyran to obtain a light-activable chlorambucil prodrug, which allowed monitoring of the light-activation of this prodrug in the acidic tumor environment (Figure 25B).[133] The spiropyran component was transformed into a ring-opened state in an acidic milieu, exhibiting changed color and recovering the fluorescence of coumarin. With

https://doi.org/10.1021/acsnano.2c05379
ACS Nano 2022, 16, 13513−13553

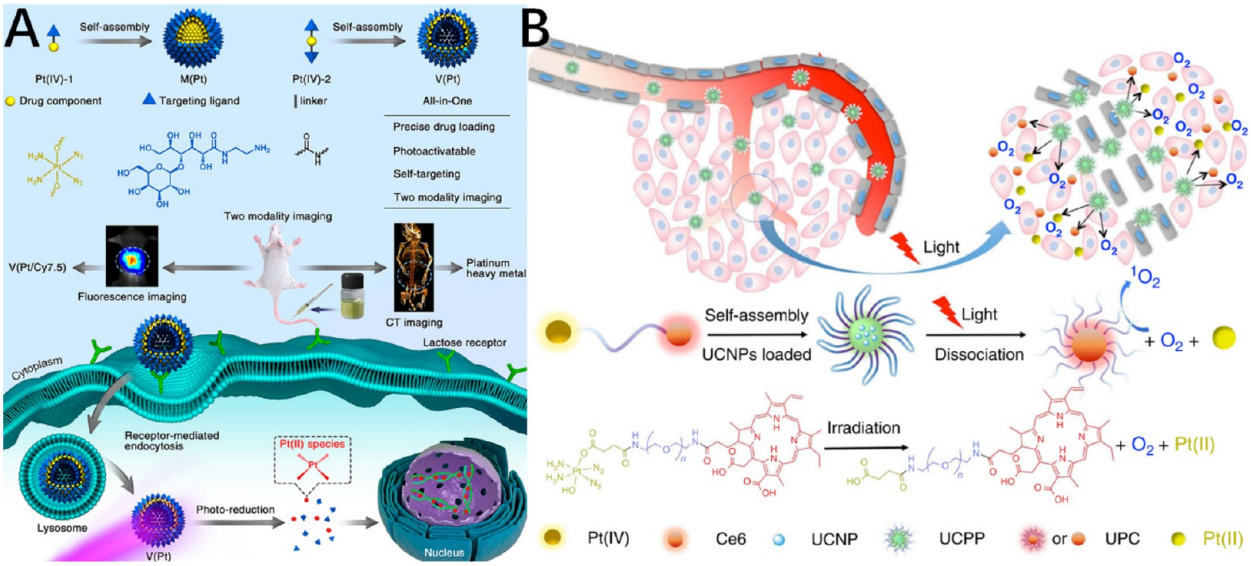

Figure 26. (A) Azido-Pt(IV) prodrug was modified with lactose in the axial positions to obtain amphiphilic molecules that can be assembled into nanoparticles with fixed Pt content. With UV light activation, the Pt(IV) prodrug was activated to kill tumor cells and also worked as a diagnostic agent providing fluorescence and CT dual imaging signals. Reproduced with permission from ref 139. Copyright 2018 American Chemical Society. (B) Azido-Pt(IV) coloaded with Ce6 in UCNPs can be synergistically activated through NIR irradiation. The azido-Pt(IV) moieties released oxygen during activation process thus promoting Ce6 involved PDT. Reprinted with permission under a Creative Commons Attribution 4.0 International License from ref 140. Copyright 2018 The Authors.

further irradiation with visible light, uncaging of coumarin released chlorambucil molecules, which inhibited the proliferation of MDA-MB-231 cells. Our group reported a perylene-derived photoactivable prodrug (Figure 25C).[134] Anticancer drug chlorambucil was photocaged by perylene-3,4,9,10-tetrayltetramethanol, and the photorelease of the active drug was executed by irradiation with visible light (≥410 nm), which photolyzed the ester bonds between the chlorambucil moiety and the perylene core. Fluorescence signals changed along with the cleavage process, acting as the indicator of drug release and evolution of our therapy. Despite the rapid and clean photoactivation features, the major obstacles that restrict their clinical application are the non-biocompatible irradiation light and the limited penetration depth: photoinduced bond cleavage such as the photolysis of ester or carbonate bonds conjugating the light-sensitive moieties requires relatively high energy input; thus, the activation lights are typically located in the deep blue light or UV region, which will result in inevitable cytotoxicity. On the other hand, due to the strong scattering and absorption effect of the intracorporeal hemoglobin and water, the tissue penetration capacity of UV light is weak, and its micrometer-scale penetration depth cannot completely activate prodrug materials *in vivo*. Thus, the anticancer effect of these prodrug systems is mainly validated by *in vitro* experiments, and it was difficult to get satisfying results from *in vivo* tumor models.

Photo-Activable Metal-Prodrug Therapeutics. Therapeutic metal complexes have consistently been recognized as an important branch of anticancer agents. Compared with pure organic antitumor drugs, metallodrugs exhibit more diverse physicochemical properties: their pharmacological activity can be precisely regulated by appropriate adjustment of coordination center atom or configuration or functionalized ligands. In addition to the above-mentioned reduction-activable properties, they also respond to exogenous light activators, exhibiting anticancer effects through recovering to original cytotoxic forms or releasing therapeutic agents or bioactive ligands. Photoactivable Pt(IV) prodrugs are inert against bioreducing reagents and hydrolysis in the dark; thus, they might be more stable during blood circulation. Pt(IV) with iodo or azido ligands can respond to UV or blue light stimuli, generating Pt(II) species to form Pt−DNA adducts, interfering with the normal cell cycle, and killing cancer cells. Azido-Pt(IV) prodrugs outperform the iodo-Pt(IV) ones due to better stability; therefore, we will not discuss the iodo-Pt(IV) in detail; a related summary can be found in an earlier review article by Zia-ur-Rehman et al.[135]

Generally, transition metal−azido complexes are photosensitive (including photosubstitution, photoisomerization, and photoreduction), regardless of the oxidation state of the central metal atom. Sadler et al. highlighted the photochemistry of a series of azido-Pt(IV) molecules, reporting detailed photodecomposition mechanisms and structure−activity relationships.[136,137] Their in-depth studies also revealed that through careful choice of ligand, the photochemical properties of azido-Pt(IV) species could be finely tuned; for instance, when the non-leaving groups are *trans*-pyridine ligands, the photoexcitation of azido-Pt(IV) can be realized using visible blue or green light, thus avoiding the potential UV phototoxicity during the activation of the congener with NH_3 as ligand.[138] In addition, unlike the NH_3 ligand in *trans,trans,trans*-$[Pt(N_3)_2(OH)_2(NH_3)(Py)]$ and *trans,trans,trans*-$[Pt(N_3)_2(OH)_2(NH_3)_2]$, the liberation of relatively bulkier pyridine ligands in *trans,trans,trans*-$[Pt(N_3)_2(OH)_2(Py)_2]$ is not likely to happen; therefore, the Pt−DNA adduct remains stable during the photoactivation process. The axial hydroxyl ligands can also be modified by acid anhydrides, isocyanates, etc., to promote endocytosis and further enhance therapeutic effects.

The modification of azido-Pt(IV) prodrugs through click reactions on azido ligands has been explored, hoping to further expand the therapeutic functionality of azido-Pt(IV). Zhou et

https://doi.org/10.1021/acsnano.2c05379
ACS Nano 2022, 16, 13513−13553

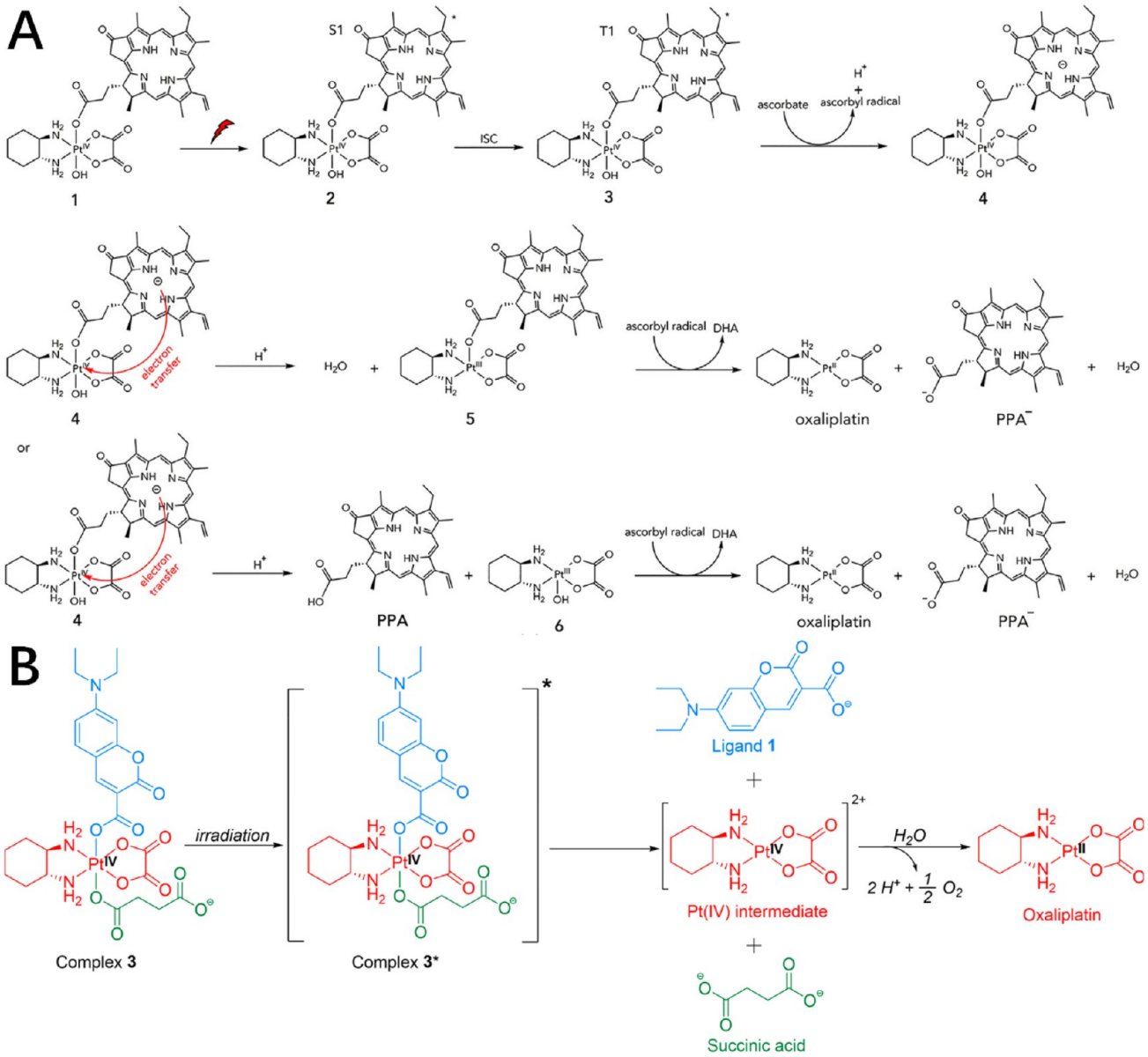

Figure 27. (A) Light-activation mechanisms of phorbiplatin. Reproduced with permission from ref 142. Copyright 2019 Elsevier. (B) Coumaplatin activation mechanism by blue light. Reproduced with permission from ref 143. Copyright 2020 American Chemical Society.

al. endowed photoactivable azido-Pt(IV) prodrugs with imaging and targeted delivery functions considering the real clinical needs.[139] Targeting ligand lactose was covalently conjugated with $Pt(NH_3)_2(N_3)_2(OH)_2$ molecules to afford an amphiphilic prodrug with high, fixed Pt contents, thus avoiding batch-to-batch variation (Figure 26A). Compared with the pristine azido-Pt(IV) group without lactose modification, this kind of nanomedicine exhibited selective inhibition effect and Pt accumulation toward *in vitro* HepG2 cancer cells and *in vivo* H22 tumor model in response to 365 nm light irradiation. The heavy metal property of platinum made this prodrug work as a computed tomography (CT) contrast agent, which facilitated tracking its intracorporeal fate. Yan et al. utilized UCNPs to convert 980 nm NIR light to 365 and 660 nm light for synchronously activating light-sensitive Pt(IV)-azido prodrug and Ce6 photosensitizer (Figure 26B).[140] This nanoplatform was constructed by coassembly between $NaYbF_4$:Tm@CaF_2 UCNPs and amphiphilic Ce6−PEG−Pt(IV) moieties. This system features improved photodynamic efficacy in treating hypoxic cancer since the Pt(IV)-azido prodrug can generate oxygen to overcome the hypoxic tumor microenvironment and promote ROS production. Along with the released Pt(II), the synergistic PDT−chemotherapy exhibited enhanced cancer cell killing performance. Experimental mice bearing four different kinds of tumors, HeLa, HCT116, MDA-MB-231, and B16, were intravenously injected with this prodrug nanosystem and irradiated with 980 nm NIR light. All the tumors disappeared at the end of treatment due to the synergic effect of photoactivated chemotherapy and PDT. In the future, the azido-Pt(IV) prodrugs will show high potential for use as multimodal therapeutic agents, just like their reduction-activated Pt(IV) congeners.

For light-activable Pt(IV) prodrugs to obtain further progress toward real clinical application, several factors still need further optimization: The explosive and unstable

https://doi.org/10.1021/acsnano.2c05379
ACS Nano 2022, 16, 13513−13553

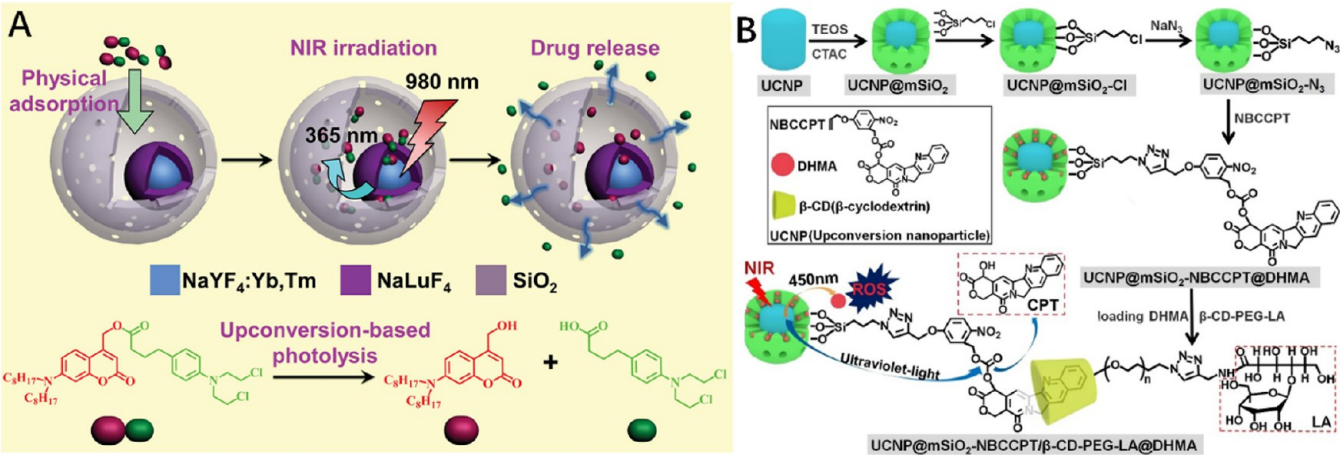

Figure 28. UCNPs as light adjusters in prodrug activation. (A) $NaYF_4$:Yb,Tm@$NaLuF_4$ inside mesoporous silica shell converted 980 nm NIR light into UV emission (365 nm), which cleaved the light-sensitive ester bond in coumarin caged chlorambucil prodrug to inhibit tumor progression. Reproduced with permission from ref 149. Copyright 2013 WILEY-VCH. (B) 2-Nitrobenzyl modified CPT activated by UV light using $NaYF_4$:Yb,Tm@β-$NaYF_4$ UCNPs, generating visible light of 450 nm after NIR irradiation to activate photosensitizers for synergistic PDT. Reproduced with permission ref 150. Copyright 2020 Elsevier.

character of metal−azido complexes requires very careful handling during the preparation process, thus limiting large-scale preparation. On the other hand, the excitation wavelengths of most azido-Pt(IV) prodrugs are in the UV range. Although the excitation wavelength can be shifted to the blue light range by replacing amine ligands with pyridine as a non-leaving group, considering further clinical development, more efforts are needed considering the tissue penetration issue. Zhu et al. have recently made some progress toward solving this technical problem. They proposed the idea of covalently linking photosensitizer molecules and Pt(IV) prodrugs, whose parental forms are clinical approved platinum drugs, such as oxaliplatin and carboplatin.[141] In their design, a red light (650 nm) activated Pt(IV) prodrug was obtained through introducing photosensitizer Ppa on the axial position appended to an oxaliplatin core, which was named as phorbiplatin (Figure 27A).[142] The energy of red light could be absorbed by the Ppa moiety to facilitate the electron transfer during the reduction process with sodium ascorbate as an intermediate electron transfer agent. The stability of phorbiplatin in the dark was verified through HPLC. Even in the presence of sodium ascorbate, phorbiplatin was not easily reduced. Phorbiplatin exhibited substantially improved cellular accumulation performance and cytotoxicity upon light irradiation as the released oxaliplatin effectively bound to genomic DNA even in platinum-resistant cancer cells. Similarly, coumarin-modified oxaliplatin Pt(IV) exhibited photoactivable properties;[143] this prodrug was named coumaplatin and was responsive to blue light (450 nm). However, no extra electron transfer intermediate was needed since the solvent water played the role of an electron donor during the activation process, generating oxygen as a byproduct (Figure 27B). Oxaliplatin is known to induce immunogenic cell death (ICD) and provoke antitumor immunity. Therefore, after irradiation treatment, increased calreticulin level on the cell membrane, high-mobility group box 1 protein release, and adenosine triphosphate (ATP) secretion were all detected as major hallmarks of ICD. The participation of the immune system also enhances the lethality of this prodrug on drug-resistant tumors.

The therapeutic potential of metal complexes is coming into view, including those with ruthenium (Ru), rhenium (Re), rhodium (Rh), and iridium (Ir) as a center atom. Among them, Ru complexes possess multiple attractive photorelated properties such as photosensitization, photoactivation, and photorelease of bioactive molecules. Due to these advantages, Ru complexes, especially Ru(II) species, have been integrated into many nanoplatforms for improving therapeutic effects. When functioning as an anticancer agent, Ru(II) species work by a similar mechanism to platinum drugs; both of them disrupt the normal structure of DNA to induce apoptosis of cancer cells.[144] Recently, the co-use of Pt(IV) and Ru(II) species was reported for overcoming multidrug resistance.[145] In this research, the reduction-activable Pt(IV) and light-sensitive Ru(II) were designed as monomers to construct an ABA-type metallic polymer (PolyPt/Ru) since their ligands can be integrated on the polymer chain. Under red light (671 nm) irradiation, the Ru(II) moieties were photoactivated and released, generating singlet oxygen and degrading polymer assemblies simultaneously. The photocytotoxicity of Ru(II) here derives from the generated $^1O_2$ and released Ru(II) monomer, causing damage to cancer cells in a different way than cisplatin, which can also overcome DNA repair caused drug resistance. *In vivo* experimental results confirmed the therapeutic performance of the bimetallic polymer nanoparticles on cisplatin-resistant tumor models. The antitumor outcome of PolyPt/Ru nanoparticles plus red-light irradiation was the most prominent compared with the group treated by only cisplatin in the same dosage.

Light Manipulation Strategies for Prodrug Activation. Effectively exploiting more tissue-penetrable and biocompatible near-infrared light for prodrug activation has gained considerable interest. In order to achieve long-wavelength light-induced covalent bond cleavage, a photon upconversion process is necessary. Relevant strategies are divided into four categories: (i) two-photon absorption, (ii) UCNP-based drug delivery materials, (iii) triplet−triplet annihilation, and (iv) developing X-ray responsive structures for precise prodrug activation.

Compared with the one-photon absorption-based photoactivation mechanism, the two-photon technique utilizes tissue penetrable NIR light, which shows better *in vivo* application opportunities. Coumarin, as a typical photoresponsive

https://doi.org/10.1021/acsnano.2c05379
ACS Nano 2022, 16, 13513−13553

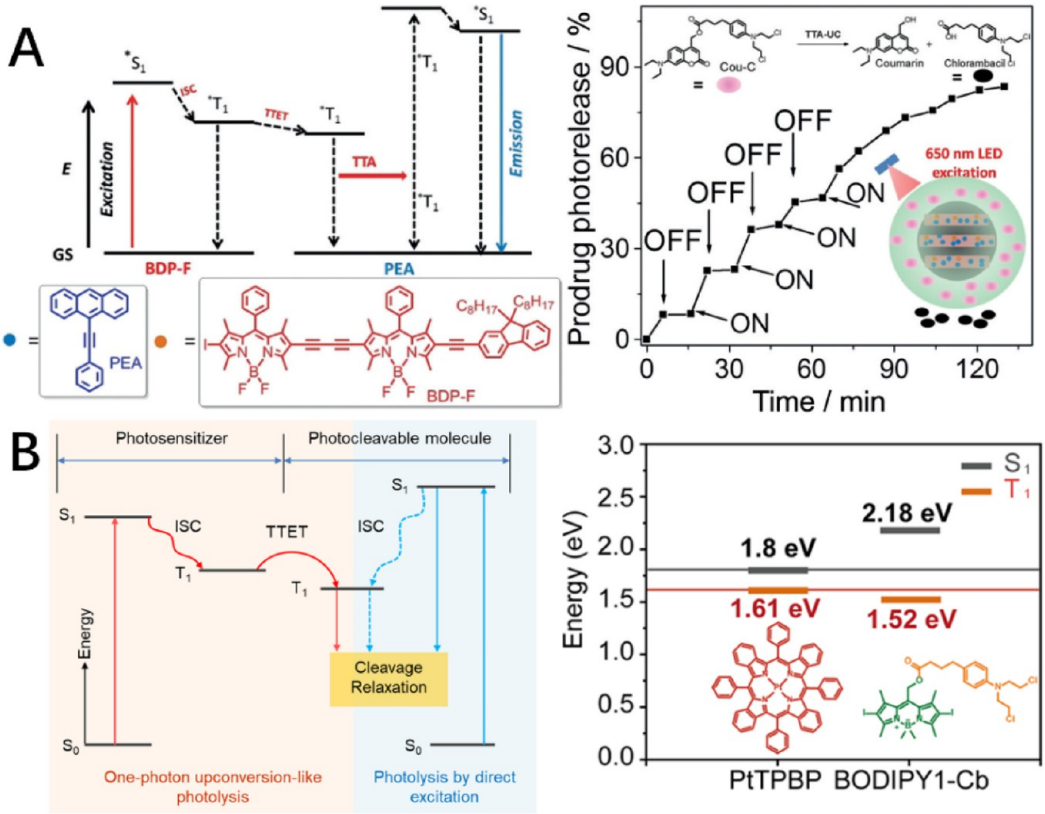

Figure 29. (A) TTA-UC system for activating light-responsive prodrug: 650 nm light was upconverted by BDP-F/PEA TTA-UC pair to blue light for activation of co-delivered chlorambucil prodrug through cleavage of the coumarin based ester bonds. Jablonski diagram of TTA-UC photophysical process (left) and chlorambucil release kinetics (right). Reproduced with permission from ref 152. Copyright 2017 Wiley-VCH. (B) Prodrug activation through triplet−triplet energy transfer: chlorambucil was released from BODIPY1-Cb by irradiation with 530 nm light. The energy of excitation light was transferred to the BODIPY1-Cb via the PtTPBP. Jablonski diagram (left), energy levels of PtTPBP and BODIPY1-Cb (right). Reproduced with permission from ref 153. Copyright 2019 American Chemical Society.

molecule, exhibits usable two-photon absorption efficiency for being applied in drug delivery.[146] Beyond its photocaging function, the coumarin moiety also serves as a drug activation indicator for monitoring *in vitro* or *in vivo* drug release. A 2-amino-1,3-phenylenedimethanol cored prodrug was recently developed to realize the above idea, integrating dual functions of two-photon-absorption activated drug release and luminescence.[147] The photoremovable coumarin motif was conjugated on the 2-amino position through a carbamate linkage, and the anticancer drug CPT along with the NIR fluorophore dicyanomethylene-4*H*-pyran (DCM) was tethered to the hydroxyl groups. Before two-photon irradiation, the fluorescence of coumarin was blocked by the fluorescence resonance energy transfer (FRET) interaction with the DCM group. After the release of CPT, the concomitantly cleaved coumarin recovered its fluorescence. Recently, a 2-nitrobenzyl linker was also found to exhibit two-photon-absorption-induced activation behavior.[148] Singh et al. reported the two-photon-absorption triggered photocleavage of 2-nitrobenzyl, which released Cu-chelating ligand pyrithione from the prodrug molecules. The subsequently formed copper−pyrithione complex decreased the viability of the HeLa cells. It is noticeable that, for this kind of two-photon-activated prodrug system, due to the low two-photon absorption cross-section, a femtosecond laser source with high power is needed, which limits its practical application.

UCNPs are also consistently used as intermediate energy donors to avoid side effects caused by UV exposure. During the process of converting NIR excitation light to anti-Stokes UV or vis emission, the UCNP-based scaffold activated prodrugs, worked as an imaging agent, and triggered synergistic combination therapy. Li et al. reported UCNP-based prodrug delivery examples in living animals. The $NaYF_4$:Yb,Tm@$NaLuF_4$ nanocrystal activated the encapsulated coumarin caged chlorambucil by converting NIR light into UV emission (Figure 28A).[149] In this prodrug system, coumarin caged chlorambucil was encapsulated inside the hollow inner cavity and could be converted to the parental form with external NIR light stimulus. Luo et al. recently designed a synergistic PDT−chemotherapy nanoplatform based on mesoporous silica-coated β-$NaYF_4$:Yb,Tm@β-$NaYF_4$ UCNPs (Figure 28B).[150] The CPT was conjugated on the silica shell through 2-nitrobenzyl linkers, while the photosensitizer molecules 1,8-dihydroxy-3-methylanthraquinone were encapsulated into the mesopores. To further improve the biocompatibility of the delivery material and prevent leakage of photosensitizers, lactobionic acid-modified PEGylated β-CD was capped on the CPT moieties due to supramolecular host−guest interaction between β-CD and CPT, which also prevented CPT from being hydrolyzed at the lactone position. The UCNP cores converted 980 nm NIR illumination to UV and vis dual emission to activate the prodrug and photosensitizer molecules, respectively. When the systme was used for cell-killing, the generated ROS facilitated the escape of the nanocarriers from the lysosome, increasing the bioavailability index of the whole system. The *in vivo* therapeutic efficacy was

https://doi.org/10.1021/acsnano.2c05379
ACS Nano 2022, 16, 13513−13553

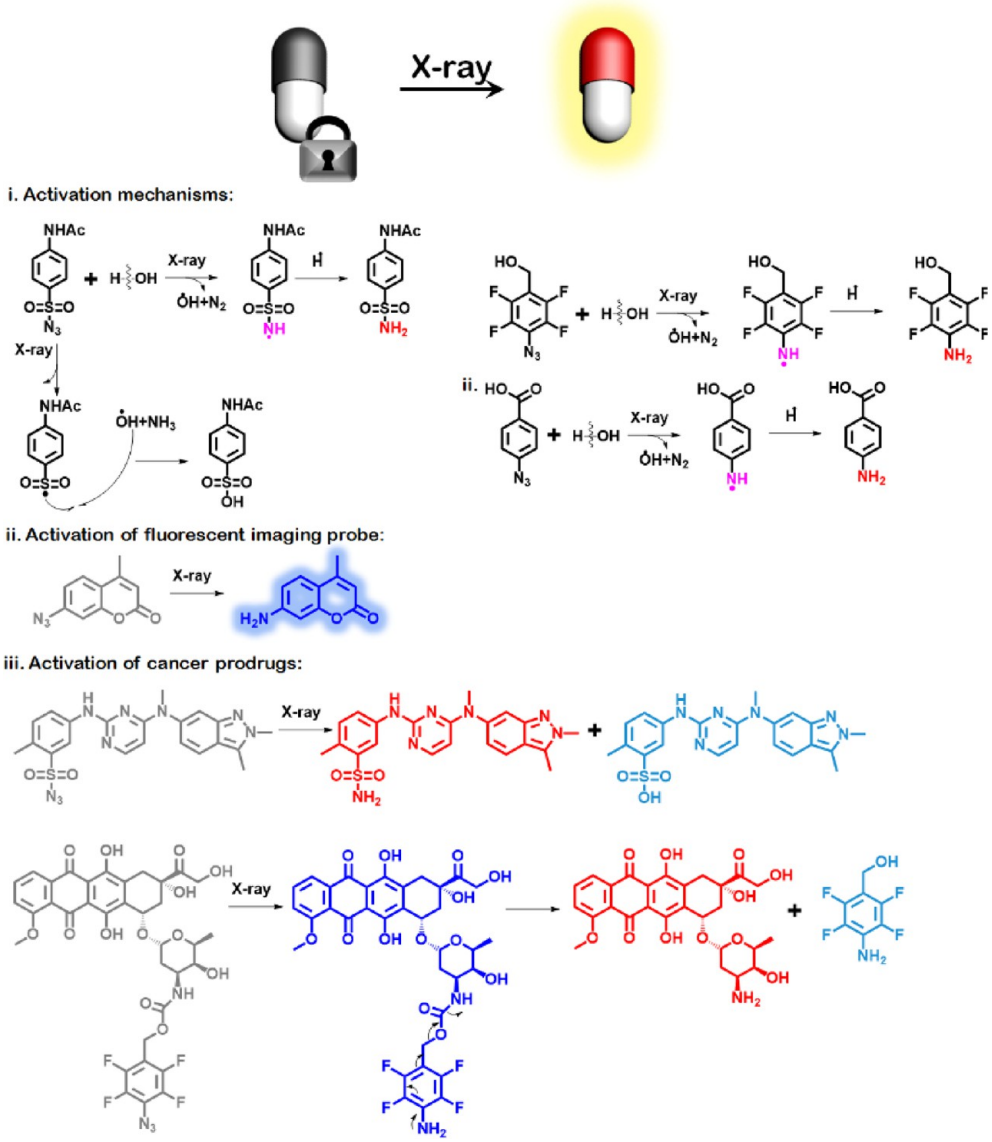

Figure 30. X-ray-responsive structures for developing prodrugs: activation mechanisms and their application in constructing fluorescent imaging probes and anticancer prodrugs.

verified using HepG2 tumor-bearing mice. After 21 days of treatment, tumor progression was inhibited by injection of UCNP@mSiO$_2$-NBCCPT/β-CD-PEG-LA@DHMA plus NIR irradiation.

Despite the advances and intensive research in two-photon absorption and UCNP-based therapy strategies, several key issues like small two-photon absorption cross sections, high instrument demands on laser source, and low upconversion quantum yield have impeded transforming such light-responsive prodrug-based oncotherapy from bench to bedside. Triplet−triplet annihilation upconversion (TTA-UC) nanoparticles, which relied on choosing suitable photosensitizer and emitter pairs, emerged as another method to confront these drawbacks.[151] To realize efficient tumor inhibition, the TTA-UC system must meet a series of prerequisites, including sufficiently tissue-penetrable incident light, a long triplet−triplet lifetime of photosensitizers, and high fluorescence quantum yield of the emitter. For example, a metal-free iodized boron-dipyrromethene dimer (BDP-F) and 9-phenylacetylene anthracene (PEA) were synthesized as photosensitizer and deep-blue emitter, respectively.[152] The light absorption efficiency of BDP-F in the far-red region was high, with an ideal triplet state lifetime; PEA exhibited outstanding fluorescence quantum yield in the deep-blue region. These characteristics could be used for rapid cleavage of light-sensitive linkages such as coumarin. As shown in Figure 29A, the photosensitizer and emitter were loaded into mesoporous silica nanoparticles; then, coumarin-caged chlorambucil prodrugs were encapsulated by the amphiphilic polymer F-127. Such a combination improved the anti-Stokes shift from far-red to deep blue regions. The ratio of photosensitizer and emitter was optimized as 20 mM BDP-F and 200 mM PEA to maximize quantum yield. They also dispersed photosensitizer and emitter in methyl oleate oil to prevent oxygen quenching. The photoinduced chlorambucil release was observed through irradiation with 650 nm light, and the release pattern showed on−off mode dependent on excitation light. With controllable chlorambucil release, the designed TTA-UC nanocomposite displayed excellent anticancer cell effect, suppressing 4T1 tumor growth in mice. In another recent report by Wang et al.,

https://doi.org/10.1021/acsnano.2c05379
ACS Nano 2022, 16, 13513−13553

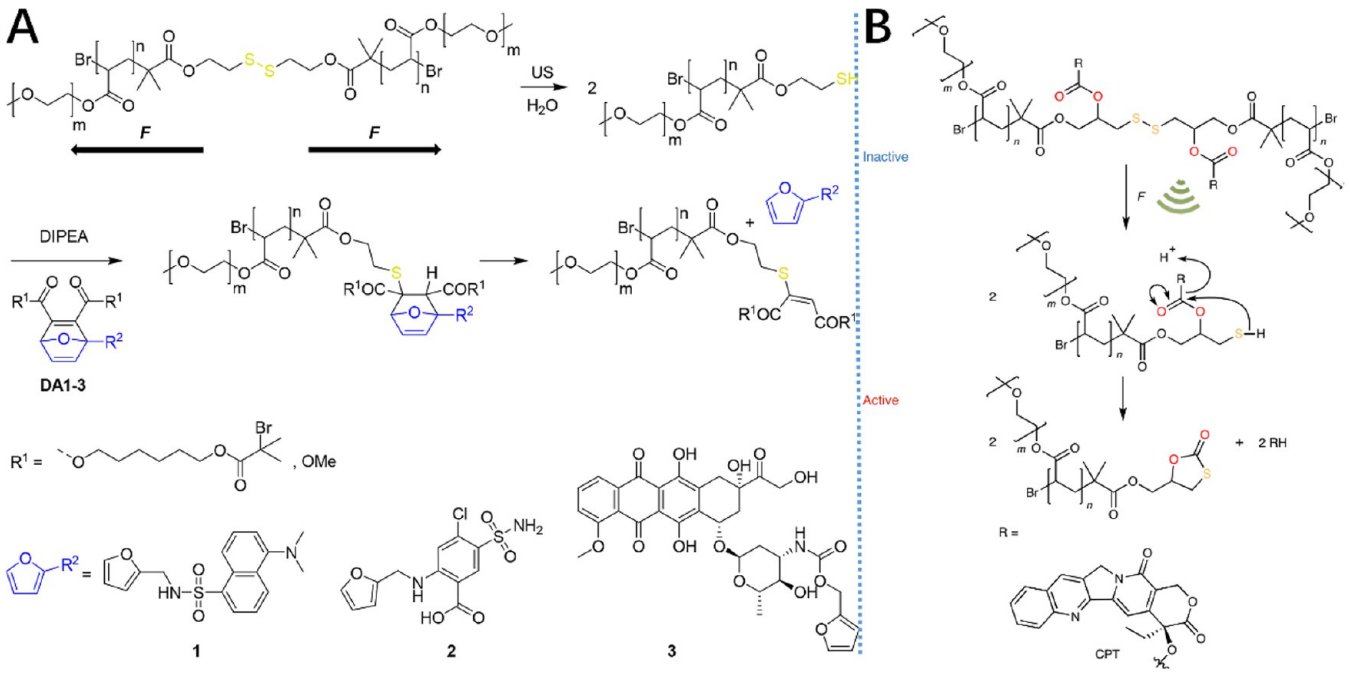

Figure 31. (A) Ultrasound induced disulfide cleavage for activation of furylated DOX through thiol-triggered retro-DA reaction. Reproduced with permission from ref 157. Copyright 2020 American Chemical Society. (B) Mechanism of disulfide caged CPT prodrug activation through ultrasound induced 5-exo−trig cyclization. Reproduced with permission from ref 158. Copyright 2021 Springer Nature.

the authors verified that during the triplet−triplet energy transfer process, photo-uncaging of prodrug molecules could be achieved from the first excited triplet state (T1) directly; therefore, this one-photon upconversion-like strategy does not need the participation of emitter molecules, simplifying the multistep energy transfer process and improving upconversion quantum yield (Figure 29B).[153] The key factor for photolysis is that the photosensitizer should have a higher T1 energy level and a lower first excited singlet state (S1) energy level than photocleavable prodrugs. According to calculation, the T1 energy levels of Pt(II) tetraphenyltetrabenzoporphyrin (PtTPBP) as a photosensitizer and BODIPY-based chlorambucil prodrug (BODIPY1-Cb) were 1.61 eV and 1.52 eV, respectively, and their corresponding S1 energy levels were 1.8 eV and 2.18 eV, which perfectly matched the prerequisite for upconversion-like photolysis to happen. The quantum yield of photolysis was 2.8% with 625 nm red light irradiation. This principle can be extended to find other suitable photosensitizer−photocleavable molecule pairs and exhibits promising potential for further application in photoactivated tumor therapy.

In radiotherapy, radiation sources such as X-rays are essentially electromagnetic waves with extremely high frequency, ultrashort wavelength, and high energy. In broad terms, such an activation signal could be counted as a special light-activation mechanism. Compared with visible light and NIR light, the tissue penetration depth of X-ray is much higher, which provides distinct advantages in treating deep-seated solid tumors. In addition to being directly used to ablate tumors, X-ray irradiation can be transferred to light emission for triggering other types of therapeutics. Bu et al. developed a scintillator−Pt(IV) hybrid nanodevice. Upon X-ray irradiation, the scintillator absorbed the energy of the X-ray, generating fluorescence and producing hydroxyl radicals.[154] In the meantime, the cisplatin-based Pt(IV) prodrug worked as a sacrificial electron acceptor to improve the photosensitizer and could be restored to the original cisplatin form, further assisting DNA damage caused by X-ray induced photodynamic therapy. In this case, X-ray irradiation indirectly activated Pt(IV) prodrugs and induced the generation of cytotoxic hydroxyl radicals. In extension of this work by their research group, X-ray was also used to trigger the release of reactive nitrogen species from zeolitic imidazole framework based nanoparticles.[155] However, little research has been conducted to directly activate prodrugs. Bradley et al. explored the possibility of using radiation as a trigger to activate prodrugs in their pioneering work (Figure 30).[156] In their research, through extensive screening of different kinds of chemical groups, they found that certain types of azide compounds can be transformed into amine compounds by clinically relevant doses of gamma or X-ray. They proposed the following activation theory for photolysis of sulfonyl azides: The irradiation induced the generation of hydroxyl radicals that react with the azide compounds, then the intermediate amido radical was formed. The azide group was finally reduced to an amine by further reacting with hydrogen radical. The conversion from azide to amine was used for realizing the activation of the coumarin fluorescent probe and anticancer prodrugs of pazopanib and doxorubicin. The use of high-energy irradiation as an activation source offers advantages such as treatment position accuracy and real-time uncaging.

ULTRASOUND-ACTIVABLE PRODRUGS

Ultrasound is also commonly applied in clinical applications. Ultrasound technology is not only used for safe and accurate imaging to diagnose diseases but also was developed as a therapeutic modality. For example, it can be used in tissue ablation and SDT, which utilizes tissue-penetrable ultrasound to induce ROS generation by cooperation with sonosensitizers. With the help of ultrasound, drug release behavior can also be precisely controlled via the disintegration of carrier materials, including vesicles, micelles, and polymeric nanocapsules.

https://doi.org/10.1021/acsnano.2c05379
ACS Nano 2022, 16, 13513−13553

Table 2. Summary of Prodrugs That Have Been Developed for Stimuli-Responsive Activation

stimuli	activation mechanism	parent drug	morphology	application	ref
acid	imine hydrolysis	MTX	self-assembled nanoparticles (~90 nm)	targeted delivery of anticancer drugs in HeLa tumor-bearing nude mice	16
	hydrazone hydrolysis	MTX/DOX	self-assembled nanoparticles (~57 nm)	multiple drug synergistic anticancer therapy	19
	cis-aconityl hydrolysis	DOX	dendrimer nanoparticles (~17 nm)	active targeting and controlled drug release based anticancer therapy	22
	silyl ether hydrolysis	GEM	antibody−drug conjugates	acid dependent prodrug activation	31
	ortho-ester hydrolysis	IND	self-assembled nanoparticles (~160 nm)	combination therapy for drug-resistant breast cancer	32
redox	disulfide cleavage-induced self-immolation	LND NLG919	micelles (~100 nm)	synergistic tumor glycolysis interruption and immunosuppression alleviation	44
	diselenide cleavage-accelerated hydrolysis	PTX	self-assembled nanoparticles (~160 nm)	redox-responsive prodrug therapy for 4T1 tumor-bearing BALB/c mice	45
	GSH-induced Pt(IV) activation to Pt(II) species	cisplatin	nanofibers (~332 nm)	reversing cisplatin drug resistance through *in situ* supramolecular assembly	51
	GSH-triggered NO release from precursors	NO	nanoparticles (~200 nm)	synergistic NO and CDT for treating liver cancer	55
	dinitrophenyl-cleavage triggered self-immolation	CPT	liposomes (~100 nm)	GSH-dependent theranostic prodrug nanosystems for HeLa tumor-bearing nude mice	59
	GSH nucleophilic attack induced trisulfide cleavage	DOX	self-assembled nanoparticles (~150 nm)	GSH-responsive prodrug therapy for B16-F10 tumor-bearing mice with alleviated systemic toxicity	60
	thioketal-cleavage induced self-immolation	CPT	filomicelles (~180 nm)	ROS-responsive prodrug therapy with enhanced drug delivery efficiency	61
	H_2O_2-induced oxalate ester linker degradation	CPT	vesicular nanoparticles (~105 nm)	synergistic oxidation/chemotherapy for suppressing tumor growth in A549 tumor-bearing mice	64
	H_2O_2-induced arylboronic ester linker hydrolysis	chlorambucil	self-assembled nanoparticles (~169 nm)	synergistic ROS-responsive chemotherapy and GSH-depletion therapy	66
	thioether cleavage accelerated hydrolysis	PTX	self-assembled nanoparticles (~100 nm)	redox dual-responsive chemotherapy against KB-3-1 xenograft tumors	69
hypoxia	quinone reduction induced self-immolation	5-FU		hypoxia-responsive prodrug chemotherapy with improved biosafety	69,98
	reductase induced *N*-oxide activation through yielding cytotoxic radicals	TPZ	self-assembled nanoparticles (~139 nm)	synergistic hypoxia-activated chemotherapy and PDT against SCC7 tumor	101
	hypoxia-induced nitro group reduction	5-FU		hypoxia-activated chemotherapy against A549 xenograft tumors	105
	azobenzene cleavage induced self-immolation	PTX	self-assembled nanoparticles (~35 nm)	synergistic hypoxia-activated chemotherapy and PDT in HeLa tumor-bearing nude mice	109
enzyme	MMP9-responsive GPLGL linker cleavage	DOX	self-assembled nanoparticles (~80 nm)	MMP9-activated prodrug therapy against 4T1 tumor	116
	caspase-responsive DEVD linker cleavage accelerated hydrolysis	DOX		caspase-activated prodrug therapy against U-87 MG xenografted tumor	116,118
	cathepsin B-responsive GFLG linker cleavage	DTX	self-assembled nanoparticles (~40 nm)	pH/enzyme dual-responsive chemo-immunotherapy against 4T1 tumor	120
	β-galactosidase induced self-immolation	MMAE		β-galactosidase responsive prodrug therapy with chemiluminescence diagnostic function	122
	DT-diaphorase induced self-immolation	CPT		DT-diaphorase responsive theranostic prodrug	124
light	UV light induced *O*-nitrobenzyl linker cleavage	DOX	polymer nanoparticles (~180 nm)	multiple-stimuli-responsive prodrug activation and antiproliferative effect	132
	UV light induced Pt(IV) activation	Pt(II)	micelles (~183 nm)	light-responsive prodrug therapy with diagnostic function	139
ultrasound	ultrasound-responsive disulfide cleavage induced self-immolation	CPT		ultrasound-responsive prodrug activation with *in vitro* anticancer effect	158

Recently, the possibility of using ultrasound technology to directly break chemical bonds and activate prodrugs has been verified. Herrmann et al. found that disulfide moieties can be designed for ultrasound-activable prodrugs since they are mechanochemically labile bonds cleavable in response to mechanical force derived from controllable ultrasound. They constructed a disulfide-centered PEG polymer chain and treated it with ultrasound at a frequency of 20 kHz (Figure 31A).[157] The embedded disulfide bonds underwent homolytic cleavage to generate thiyl radicals and were finally converted to thiol groups by reaction with surrounding water molecules. Finally, the anticancer prodrug, furylated DOX, was released because the thiol-ended polymer chains underwent a Michael addition to Diels−Alder (DA) adducts of furylated DOX prodrugs and acetylene dicarboxylate derivatives, triggering the retro-DA reaction to liberate furylated DOX. As a result, the ultrasound-treated samples exhibited higher toxicity toward HeLa cells than ultrasound-free groups. Recently, they managed to find a more direct way to activate prodrug molecules through ultrasound activation (Figure 31B).[158] The anticancer drug CPT was covalently conjugated to polymer chains through a carbonate linker in the β-position to a disulfide moiety. After disulfide cleavage generated thiol groups, the CPT was immediately released through 5-exo-trig cyclization. With this approach, the active structure of the anticancer drug is completely restored.

CONCLUSIONS AND OUTLOOK

It can be seen from the experience of previous research that a successful prodrug nanoplatform is like a rationally designed

https://doi.org/10.1021/acsnano.2c05379
ACS Nano 2022, 16, 13513−13553

integrated circuit board, to some extent. The most important component is the "switch" that controls the prodrug to turn from an "off" state to an "on" state to restore the bioavailability of drugs and reduce the damage of chemotherapy drugs to normal tissues and organs. After decades of development, the prodrug activation process has become more refined to adapt to the complex tumor pathological environment. In addition, with the advancement of nanomaterial preparation technology, this "circuit board" can be made into nanoscale structures to improve the uptake by tumors (refer to Table 2 for a summary).

However, as the degree of complexity and refinement increases, this also means that the difficulty of scale-up preparation and industrial production creeps up. There is also a long way to evaluate the nanocarrier materials due to the lack of pharmacological and toxicological data. Considering this, artificial intelligence methods provide a range of tools for prodrug development, and a wealth of high-quality data are derived from computer algorithms based on machine learning approaches.[159−161] In addition, molecular dynamics simulation technology can also assist the design of prodrug formulations, which would shorten the research cycle and lower the cost. Wu et al. used a computing aided design strategy to screen a Pt(IV) prodrug that could form stable complexes with human serum albumin for *in vivo* drug delivery.[162] Despite prodrug research making some progress, the design of prodrugs is still extremely challenging. Through the analysis of the above cases with our own research experience, we believe that the following points should be considered in the future.

Expanding the Categories of Prodrugs. Not all drugs can be developed into prodrugs. We often think that there must be modifiable groups in drug molecules, such as hydroxyl, carboxyl, and amino groups. Recently, the concept of orthogonal prodrugs has attracted considerable attention since they expand the categories of prodrugs. Researchers redefined the way prodrugs are activated and the activation stimuli. For example, prodrugs can be activated in a "stitch" way.[163] Zhang et al. synthesized a CA4-like drug *in situ* by delivering two fragments of drug molecules and catalyst Cu nanoparticles. The fragments of molecules were modified with azide and alkynyl groups. Through copper-catalyzed azide−alkyne 1,3-cycloaddition reactions, they were stitched together to generate active drug molecule with cytotoxicity. Not only the way prodrugs are activated, but the activation signals can also be customized. Miller et al. developed a strategy to colocalize prodrug and palladium compound to catalyze the uncaging reaction for activation, which effectively inhibited tumor growth.[164] Due to this kind of prodrug involving a relatively more complicated activation reaction, it is vital to design dependable carrier materials to deliver the reactants and catalysts.

Introducing Reasonable Logic in the Prodrug Activation Process. In the early stage, prodrugs only respond to a single type of activation signal. As more and more stimuli-responsive variable chemical structures are developed, prodrugs can now simultaneously respond to multiple activation signals. Due to the complexity of the tumor microenvironment, the introduction of a multistimuli-responsive activation mechanism has become an important research direction.[165,166] Multistimuli responsiveness can generally be categorized as "and" and "or" logic gates based on different design logics. Traditional stimuli-responsive materials could only recognize simple single input. Sophisticated Boolean logic computations have now begun to play a critical role in constructing smart prodrug nanomaterials. For example, Yu et al. developed a smart prodrug that exhibited a reasonable biocomputation function in response to overexpressed MMP, GSH, and mild acidity in the tumor microenvironment. After precise logic operations, this prodrug nanosystem enabled tumor-specific retention and ultimately promoted accurate release of an immune modulator.[167] Therefore, introducing reasonable logic to prodrug design and integrating endogenous and exogenous stimuli factors are of practical importance.

Developing Effective Monitoring Mechanisms to Evaluate the Activation Process *in Vivo*. The human body after prodrug administration is a black box to researchers. Although we can evaluate the activation behavior of prodrugs in cell experiments, once the prodrugs enter the human body, their fate is difficult to directly observe, leaving many unsolved puzzles, including when, where, and how they are actually activated. Reporting agents that give a signal as soon as the activation occurs should be incorporated to answer these questions. Up to now, NIR emission, photoacoustic signal, and heat generation have been developed as reporting mechanisms. In the next stage, we must consider improving the reporting precision and developing other strategies to reflect the activation process.

In summary, with an advance in the studies of stimuli-responsive nanoscale prodrugs, the prodrugs have shown growing success in both fundamental research and the market (including irinotecan, cyclophosphamide, capecitabine, and melflufen). We hope that through analyzing recent progress in this field, more and better prodrug therapeutics will be developed for the precision treatment of tumors.

AUTHOR INFORMATION

Corresponding Authors

Hongzhong Chen − *Institute of Pharmaceutics, School of Pharmaceutical Sciences (Shenzhen), Sun Yat-sen University, Guangzhou 510275, China; School of Chemistry, Chemical Engineering and Biotechnology, Nanyang Technological University, Singapore 637371, Singapore*; Email: chenhzh58@mail.sysu.edu.cn

Yanli Zhao − *School of Chemistry, Chemical Engineering and Biotechnology, Nanyang Technological University, Singapore 637371, Singapore*; orcid.org/0000-0002-9231-8360; Email: zhaoyanli@ntu.edu.sg

Authors

Chendi Ding − *Clinical Research Center, Maoming People's Hospital, Maoming 525000, China; School of Medicine, Jinan University, Guangzhou 510632, China; School of Chemistry, Chemical Engineering and Biotechnology, Nanyang Technological University, Singapore 637371, Singapore*

Chunbo Chen − *Clinical Research Center, Maoming People's Hospital, Maoming 525000, China*; orcid.org/0000-0001-5662-497X

Xiaowei Zeng − *Institute of Pharmaceutics, School of Pharmaceutical Sciences (Shenzhen), Sun Yat-sen University, Guangzhou 510275, China; School of Chemistry, Chemical Engineering and Biotechnology, Nanyang Technological University, Singapore 637371, Singapore*; orcid.org/0000-0002-2804-2689

Complete contact information is available at: https://pubs.acs.org/10.1021/acsnano.2c05379

https://doi.org/10.1021/acsnano.2c05379
ACS Nano 2022, 16, 13513−13553

Author Contributions

[Δ]C.D. and C.C. contributed equally.

Notes

The authors declare no competing financial interest.

ACKNOWLEDGMENTS

This work was supported by the start-up fund (BS2021001) from Maoming People's Hospital, the Guangdong Medical Science and Technology Research Fund (A2021213), the Programs Supported by Tianjin Key Laboratory of Biomedical Materials, the National Natural Science Foundation of China (32101065), and the Singapore National Research Foundation Investigatorship (NRF-NRFI2018-03).

VOCABULARY

endogenous stimuli, the differences in physicochemical properties between tumor tissues and normal healthy tissues; **exogenous stimuli**, the artificially introduced energy form outside the tumor microenvironment for initiating therapies; **self-immolative reaction**, the cascade of disassembling reactions triggered by stimulation to result in the sequential release of smaller components; **theranostic prodrugs**, multifunctional prodrugs that integrate both diagnostic and therapeutic functions; **tumor heterogeneity**, the differences that exist among tumor cells within the same tumor tissue

REFERENCES

(1) Rautio, J.; Meanwell, N. A.; Di, L.; Hageman, M. J. The Expanding Role of Prodrugs in Contemporary Drug Design and Development. *Nat. Rev. Drug Discovery* **2018**, *17*, 559−587.

(2) Gong, F.; Yang, N.; Wang, X.; Zhao, Q.; Chen, Q.; Liu, Z.; Cheng, L. Tumor Microenvironment-Responsive Intelligent Nanoplatforms for Cancer Theranostics. *Nano Today* **2020**, *32*, 100851.

(3) Imberti, C.; Zhang, P.; Huang, H.; Sadler, P. J. New Designs for Phototherapeutic Transition Metal Complexes. *Angew. Chem., Int. Ed.* **2020**, *59*, 61−73.

(4) Shi, Z.; Song, Q.; Göstl, R.; Herrmann, A. Mechanochemical Activation of Disulfide-Based Multifunctional Polymers for Theranostic Drug Release. *Chem. Sci.* **2021**, *12*, 1668−1674.

(5) Ekdawi, S. N.; Jaffray, D. A.; Allen, C. Nanomedicine and Tumor Heterogeneity: Concept and Complex Reality. *Nano Today* **2016**, *11*, 402−414.

(6) Skorepova, E.; Čerňa, I.; Vlasáková, R.; Zvoníček, V.; Tkadlecová, M.; Dušek, M. Spirocyclic Character of Ixazomib Citrate Revealed by Comprehensive XRD, NMR and DFT Study. *J. Mol. Struct.* **2017**, *1148*, 22−27.

(7) Lu, K.; Lin, S.; Wang, Y.; Hao, R.; Fang, L.; Zhu, J.; Zhao, D.; Yu, J.; Tong, S.; Wu, Y.; Si, Y.; Ye, T.; Yang, Q.; Wang, Y. Pharmacokinetics and Safety of Fosaprepitant Dimeglumine in Healthy Chinese Volunteers: Bioequivalence Study. *Clin. Pharmacol. Drug Dev.* **2021**, *10*, 748−755.

(8) Leung, M.; Rogers, J. E.; Shureiqi, I. Use of Uridine Triacetate to Reverse Severe Persistent Myelosuppression Following 5-Fluorouracil Exposure in a Patient with a c.557A>G Heterozygous DPYD Variant. *Clin. Colorectal Cancer* **2021**, *20*, 273−278.

(9) Gong, J.; Yan, J.; Forscher, C.; Hendifar, A. Aldoxorubicin: A Tumor-Targeted Doxorubicin Conjugate for Relapsed or Refractory Soft Tissue Sarcomas. *Drug Des., Dev. Ther.* **2018**, *12*, 777−786.

(10) Li, Y.; Zhao, L.; Li, X.-F. The Hypoxia-Activated Prodrug TH-302: Exploiting Hypoxia in Cancer Therapy. *Front. Pharmacol.* **2021**, *12*, 636892.

(11) Zhang, Y.; Qin, S.; Chao, J.; Luo, Y.; Sun, Y.; Duan, J. The *In-Vitro* Antitumor Effects of AST-3424 Monotherapy and Combination Therapy with Oxaliplatin or 5-Fluorouracil in Primary Liver Cancer. *Front. Oncol.* **2022**, *12*, 885139.

(12) Peppicelli, S.; Bianchini, F.; Calorini, L. Extracellular Acidity, a "Reappreciated" Trait of Tumor Environment Driving Malignancy: Perspectives in Diagnosis and Therapy. *Cancer Metastasis Rev.* **2014**, *33*, 823−832.

(13) Zhou, S.; Zhong, Q.; Wang, Y.; Hu, P.; Zhong, W.; Huang, C.-B.; Yu, Z.-Q.; Ding, C.-D.; Liu, H.; Fu, J. Chemically Engineered Mesoporous Silica Nanoparticles-Based Intelligent Delivery Systems for Theranostic Applications in Multiple Cancerous/Non-Cancerous Diseases. *Coord. Chem. Rev.* **2022**, *452*, 214309.

(14) Wang, C.; Zhao, T.; Li, Y.; Huang, G.; White, M. A.; Gao, J. Investigation of Endosome and Lysosome Biology by Ultra pH-Sensitive Nanoprobes. *Adv. Drug Delivery Rev.* **2017**, *113*, 87−96.

(15) Huang, P.; Wang, D.; Su, Y.; Huang, W.; Zhou, Y.; Cui, D.; Zhu, X.; Yan, D. Combination of Small Molecule Prodrug and Nanodrug Delivery: Amphiphilic Drug−Drug Conjugate for Cancer Therapy. *J. Am. Chem. Soc.* **2014**, *136*, 11748−11756.

(16) Li, Y.; Song, L.; Lin, J.; Ma, J.; Pan, Z.; Zhang, Y.; Su, G.; Ye, S.; Luo, F.-h.; Zhu, X.; Hou, Z. Programmed Nanococktail Based on pH-Responsive Function Switch for Self-Synergistic Tumor-Targeting Therapy. *ACS Appl. Mater. Interfaces* **2017**, *9*, 39127−39142.

(17) Song, C.; Li, Y.; Li, T.; Yang, Y.; Huang, Z.; de la Fuente, J. M.; Ni, J.; Cui, D. Long-Circulating Drug-Dye-Based Micelles with Ultrahigh pH-Sensitivity for Deep Tumor Penetration and Superior Chemo-Photothermal Therapy. *Adv. Funct. Mater.* **2020**, *30*, 1906309.

(18) Mou, Q.; Ma, Y.; Zhu, X.; Yan, D. A Small Molecule Nanodrug Consisting of Amphiphilic Targeting Ligand−Chemotherapy Drug Conjugate for Targeted Cancer Therapy. *J. Controlled Release* **2016**, *230*, 34−44.

(19) Hou, M.; Gao, Y.-E.; Shi, X.; Bai, S.; Ma, X.; Li, B.; Xiao, B.; Xue, P.; Kang, Y.; Xu, Z. Methotrexate-Based Amphiphilic Prodrug Nanoaggregates for Co-Administration of Multiple Therapeutics and Synergistic Cancer Therapy. *Acta Biomater.* **2018**, *77*, 228−239.

(20) Tao, R.; Gao, M.; Liu, F.; Guo, X.; Fan, A.; Ding, D.; Kong, D.; Wang, Z.; Zhao, Y. Alleviating the Liver Toxicity of Chemotherapy *via* pH-Responsive Hepatoprotective Prodrug Micelles. *ACS Appl. Mater. Interfaces* **2018**, *10*, 21836−21846.

(21) Wan, X.-L.; Lu, Y.-F.; Xu, S.-F.; Wu, Q.; Liu, J. Oeanolic Acid Protects against the Hepatotoxicity of D-Galactosame Plus Endotoxin in Mice. *Biomed. Pharmacother.* **2017**, *93*, 1040−1046.

(22) Zhu, S.; Qian, L.; Hong, M.; Zhang, L.; Pei, Y.; Jiang, Y. RGD-Modified PEG-PAMAM-DOX Conjugate: *In Vitro* and *In Vivo* Targeting to Both Tumor Neovascular Endothelial Cells and Tumor Cells. *Adv. Mater.* **2011**, *23*, H84−H89.

(23) Huang, P.; Wang, W.; Zhou, J.; Zhao, F.; Zhang, Y.; Liu, J.; Liu, J.; Dong, A.; Kong, D.; Zhang, J. Amphiphilic Polyelectrolyte/Prodrug Nanoparticles Constructed by Synergetic Electrostatic and Hydrophobic Interactions with Cooperative pH-Sensitivity for Controlled Doxorubicin Delivery. *ACS Appl. Mater. Interfaces* **2015**, *7*, 6340−6350.

(24) Gillies, E. R.; Goodwin, A. P.; Frechet, J. M. J. Acetals as pH-Sensitive Linkages for Drug Delivery. *Bioconjugate Chem.* **2004**, *15*, 1254−1263.

(25) Mu, J.; Zhong, H.; Zou, H.; Liu, T.; Yu, N.; Zhang, X.; Xu, Z.; Chen, Z.; Guo, S. Acid-Sensitive PEGylated Paclitaxel Prodrug Nanoparticles for Cancer Therapy: Effect of PEG Length on Antitumor Efficacy. *J. Controlled Release* **2020**, *326*, 265−275.

(26) Jain, R.; Standley, S. M.; Frechet, J. M. J. Synthesis and Degradation of pH-Sensitive Linear Poly(Amidoamine)s. *Macromolecules* **2007**, *40*, 452−457.

(27) Paramonov, S. E.; Bachelder, E. M.; Beaudette, T. T.; Standley, S. M.; Lee, C. C.; Dashe, J.; Frechet, J. M. J. Fully Acid-Degradable Biocompatible Polyacetal Microparticles for Drug Delivery. *Bioconjugate Chem.* **2008**, *19*, 911−919.

(28) Yu, N.; Liu, T.; Zhang, X.; Gong, N.; Ji, T.; Chen, J.; Liang, X.-J.; Kohane, D. S.; Guo, S. Dually Enzyme- and Acid-Triggered Self-Immolative Ketal Glycoside Nanoparticles for Effective Cancer Prodrug Monotherapy. *Nano Lett.* **2020**, *20*, 5465−5472.

(29) Zhong, H.; Mu, J.; Du, Y.; Xu, Z.; Xu, Y.; Yu, N.; Zhang, S.; Guo, S. Acid-Triggered Release of Native Gemcitabine Conjugated in

Polyketal Nanoparticles for Enhanced Anticancer Therapy. *Biomarcomolecules* **2020**, *21*, 803−814.
(30) Parrott, M. C.; Finniss, M.; Luft, J. C.; Pandya, A.; Gullapalli, A.; Napier, M. E.; DeSimone, J. M. Incorporation and Controlled Release of Silyl Ether Prodrugs from PRINT Nanoparticles. *J. Am. Chem. Soc.* **2012**, *134*, 7978−7982.
(31) Finniss, M. C.; Chu, K. S.; Bowerman, C. J.; Luft, J. C.; Haroon, Z. A.; DeSimone, J. M. A Versatile Acid-Labile Linker for Antibody-Drug Conjugates. *MedChemComm* **2014**, *5*, 1355−1358.
(32) Wang, X.; Cheng, X.; He, L.; Zeng, X.; Zheng, Y.; Tang, R. Self-Assembled Indomethacin Dimer Nanoparticles Loaded with Doxorubicin for Combination Therapy in Resistant Breast Cancer. *ACS Appl. Mater. Interfaces* **2019**, *11*, 28597−28609.
(33) Nagamani, C.; Liu, H.; Moore, J. S. Mechanogeneration of Acid from Oxime Sulfonates. *J. Am. Chem. Soc.* **2016**, *138*, 2540−2543.
(34) Song, R.; Li, T.; Ye, J.; Sun, F.; Hou, B.; Saeed, M.; Gao, J.; Wang, Y.; Zhu, Q.; Xu, Z.; Yu, H. Acidity-Activatable Dynamic Nanoparticles Boosting Ferroptotic Cell Death for Immunotherapy of Cancer. *Adv. Mater.* **2021**, *33*, 2101155.
(35) Pe'er, D.; Ogawa, S.; Elhanani, O.; Keren, L.; Oliver, T. G.; Wedge, D. Tumor Heterogeneity. *Cancer Cell* **2021**, *39*, 1015−1017.
(36) Zhang, Y.; Wan, Y.; Liao, Y.; Hu, Y.; Jiang, T.; He, T.; Bi, W.; Lin, J.; Gong, P.; Tang, L.; Huang, P. Janus γ-Fe_2O_3/SiO_2-Based Nanotheranostics for Dual-Modal Imaging and Enhanced Synergistic Cancer Starvation/Chemodynamic Therapy. *Sci. Bull.* **2020**, *65*, 564−572.
(37) Zheng, H.; Wang, S.; Zhou, L.; He, X.; Cheng, Z.; Cheng, F.; Liu, Z.; Wang, X.; Chen, Y.; Zhang, Q. Injectable Multi-Responsive Micelle/Nanocomposite Hybrid Hydrogel for Bioenzyme and Photothermal Augmented Chemodynamic Therapy of Skin Cancer and Bacterial Infection. *Chem. Eng. J.* **2021**, *404*, 126439.
(38) Saikolappan, S.; Kumar, B.; Shishodia, G.; Koul, S.; Koul, H. K. Reactive Oxygen Species and Cancer: A Complex Interaction. *Cancer Lett.* **2019**, *452*, 132−143.
(39) Catalano, V.; Turdo, A.; Di Franco, S.; Dieli, F.; Todaro, M.; Stassi, G. Tumor and Its Microenvironment: A Synergistic Interplay. *Semin. Cancer Biol.* **2013**, *23*, 522−532.
(40) Deng, Z.; Hu, J.; Liu, S. Disulfide-Based Self-Immolative Linkers and Functional Bioconjugates for Biological Applications. *Macromol. Rapid Commun.* **2020**, *41*, 1900531.
(41) Sun, F.; Zhu, Q.; Li, T.; Saeed, M.; Xu, Z.; Zhong, F.; Song, R.; Huai, M.; Zheng, M.; Xie, C.; Xu, L.; Yu, H. Regulating Glucose Metabolism with Prodrug Nanoparticles for Promoting Photoimmunotherapy of Pancreatic Cancer. *Adv. Sci.* **2021**, *8*, 2002746.
(42) Ye, J.; Hou, B.; Chen, F.; Zhang, S.; Xiong, M.; Li, T.; Xu, Y.; Xu, Z.; Yu, H. Bispecific Prodrug Nanoparticles Circumventing Multiple Immune Resistance Mechanisms for Promoting Cancer Immunotherapy. *Acta Pharm. Sin. B* **2022**, *12*, 2695−2709.
(43) Zhou, F.; Gao, J.; Tang, Y.; Zou, Z.; Jiao, S.; Zhou, Z.; Xu, H.; Xu, Z. P.; Yu, H.; Xu, Z. Engineering Chameleon Prodrug Nanovesicles to Increase Antigen Presentation and Inhibit PD-L1 Expression for Circumventing Immune Resistance of Cancer. *Adv. Mater.* **2021**, *33*, 2102668.
(44) Liu, X.; Li, Y.; Wang, K.; Chen, Y.; Shi, M.; Zhang, X.; Pan, W.; Li, N.; Tang, B. GSH-Responsive Nanoprodrug to Inhibit Glycolysis and Alleviate Immunosuppression for Cancer Therapy. *Nano Lett.* **2021**, *21*, 7862−7869.
(45) Sun, B.; Luo, C.; Zhang, X.; Guo, M.; Sun, M.; Yu, H.; Chen, Q.; Yang, W.; Wang, M.; Zuo, S.; Chen, P.; Kan, Q.; Zhang, H.; Wang, Y.; He, Z.; Sun, J. Probing the Impact of Sulfur/Selenium/Carbon Linkages on Prodrug Nanoassemblies for Cancer Therapy. *Nat. Commun.* **2019**, *10*, 3211.
(46) Zuo, S.; Sun, B.; Yang, Y.; Zhou, S.; Zhang, Y.; Guo, M.; Sun, M.; Luo, C.; He, Z.; Sun, J. Probing the Superiority of Diselenium Bond on Docetaxel Dimeric Prodrug Nanoassemblies: Small Roles Taking Big Responsibilities. *Small* **2020**, *16*, 2005039.
(47) Ma, L.; Wang, N.; Ma, R.; Li, C.; Xu, Z.; Tse, M.-K.; Zhu, G. Monochalcoplatin: An Actively Transported, Quickly Reducible, and Highly Potent PtIV Anticancer Prodrug. *Angew. Chem., Int. Ed.* **2018**, *57*, 9098−9102.
(48) Feng, T.; Ai, X.; Ong, H.; Zhao, Y. Dual-Responsive Carbon Dots for Tumor Extracellular Microenvironment Triggered Targeting and Enhanced Anticancer Drug Delivery. *ACS Appl. Mater. Interfaces* **2016**, *8*, 18732−18740.
(49) Feng, T.; Ai, X.; An, G.; Yang, P.; Zhao, Y. Charge-Convertible Carbon Dots for Imaging-Guided Drug Delivery with Enhanced *in Vivo* Cancer Therapeutic Efficiency. *ACS Nano* **2016**, *10*, 4410−4420.
(50) Feng, B.; Hou, B.; Xu, Z.; Saeed, M.; Yu, H.; Li, Y. Self-Amplified Drug Delivery with Light-Inducible Nanocargoes to Enhance Cancer Immunotherapy. *Adv. Mater.* **2019**, *31*, 1902960.
(51) Wang, Q.; Xiao, M.; Wang, D.; Hou, X.; Gao, J.; Liu, J.; Liu, J. *In Situ* Supramolecular Self-Assembly of Pt(IV) Prodrug to Conquer Cisplatin Resistance. *Adv. Funct. Mater.* **2021**, *31*, 2101826.
(52) Feng, B.; Zhou, F.; Hou, B.; Wang, D.; Wang, T.; Fu, Y.; Ma, Y.; Yu, H.; Li, Y. Binary Cooperative Prodrug Nanoparticles Improve Immunotherapy by Synergistically Modulating Immune Tumor Microenvironment. *Adv. Mater.* **2018**, *30*, 1803001.
(53) Zhang, J.; Song, H.; Ji, S.; Wang, X.; Huang, P.; Zhang, C.; Wang, W.; Kong, D. NO Prodrug-Conjugated, Self-Assembled, pH-Responsive and Galactose Receptor Targeted Nanoparticles for Co-Delivery of Nitric Oxide and Doxorubicin. *Nanoscale* **2018**, *10*, 4179−4188.
(54) Hou, Z.; Wu, Y.; Xu, C.; Reghu, S.; Shang, Z.; Chen, J.; Pranantyo, D.; Marimuth, K.; De, P. P.; Ng, O. T.; Pethe, K.; Kang, E.-T.; Li, P.; Chan-Park, M. B. Precisely Structured Nitric-Oxide-Releasing Copolymer Brush Defeats Broad-Spectrum Catheter-Associated Biofilm Infections In Vivo. *ACS Cent. Sci.* **2020**, *6*, 2031−2045.
(55) Hu, Y.; Lv, T.; Ma, Y.; Xu, J.; Zhang, Y.; Hou, Y.; Huang, Z.; Ding, Y. Nanoscale Coordination Polymers for Synergistic NO and Chemodynamic Therapy of Liver Cancer. *Nano Lett.* **2019**, *19*, 2731−2738.
(56) Cao, X.; Lin, W.; Zheng, K.; He, L. A Near-Infrared Fluorescent Turn-On Probe for Fluorescence Imaging of Hydrogen Sulfide in Living Cells Based on Thiolysis of Dinitrophenyl Ether. *Chem. Commun.* **2012**, *48*, 10529−10531.
(57) Huang, Z.; Ding, S.; Yu, D.; Huang, F.; Feng, G. Aldehyde Group Assisted Thiolysis of Dinitrophenyl Ether: A New Promising Approach for Efficient Hydrogen Sulfide Probes. *Chem. Commun.* **2014**, *50*, 9185−9187.
(58) Wang, G.; Zhu, D.; Zhou, Z.; Piao, Y.; Tang, J.; Shen, Y. Glutathione-Specific and Intracellularly Labile Polymeric Nanocarrier for Efficient and Safe Cancer Gene Delivery. *ACS Appl. Mater. Interfaces* **2020**, *12*, 14825−14838.
(59) Wang, Z.; Wu, H.; Liu, P.; Zeng, F.; Wu, S. A Self-Immolative Prodrug Nanosystem Capable of Releasing a Drug and a NIR Reporter for *in Vivo* Imaging and Therapy. *Biomaterials* **2017**, *139*, 139−150.
(60) Yang, Y.; Sun, B.; Zuo, S.; Li, X.; Zhou, S.; Li, L.; Luo, C.; Liu, H.; Cheng, M.; Wang, Y.; Wang, S.; He, Z.; Sun, J. Trisulfide Bond-Mediated Doxorubicin Dimeric Prodrug Nanoassemblies with High Drug Loading, High Self-Assembly Stability, and High Tumor Selectivity. *Sci. Adv.* **2020**, *6*, eabc1725.
(61) Ke, W.; Lu, N.; Japir, A. A.-W. M. M.; Zhou, Q.; Xi, L.; Wang, Y.; Dutta, D.; Zhou, M.; Pan, Y.; Ge, Z. Length Effect of Stimuli-Responsive Block Copolymer Prodrug Filomicelles on Drug Delivery Efficiency. *J. Controlled Release* **2020**, *318*, 67−77.
(62) Xia, X.; Yang, X.; Huang, P.; Yan, D. ROS-Responsive Nanoparticles Formed from RGD−Epothilone B Conjugate for Targeted Cancer Therapy. *ACS Appl. Mater. Interfaces* **2020**, *12*, 18301−18308.
(63) Xu, X.; Saw, P. E.; Tao, W.; Li, Y.; Ji, X.; Bhasin, S.; Liu, Y.; Ayyash, D.; Rasmussen, J.; Huo, M.; Shi, J.; Farokhzad, O. C. ROS-Responsive Polyprodrug Nanoparticles for Triggered Drug Delivery and Effective Cancer Therapy. *Adv. Mater.* **2017**, *29*, 1700141.
(64) Li, J.; Li, Y.; Wang, Y.; Ke, W.; Chen, W.; Wang, W.; Ge, Z. Polymer Prodrug-Based Nanoreactors Activated by Tumor Acidity for

Orchestrated Oxidation/Chemotherapy. *Nano Lett.* **2017**, *17*, 6983−6990.
(65) Shen, S.; Xu, X.; Lin, S.; Zhang, Y.; Liu, H.; Zhang, C.; Mo, R. A Nanotherapeutic Strategy to Overcome Chemotherapeutic Resistance of Cancer Stem-Like Cells. *Nat. Nanotechnol.* **2021**, *16*, 104−113.
(66) Luo, C.-Q.; Zhou, Y.-X.; Zhou, T.-J.; Xing, L.; Cui, P.-F.; Sun, M.; Jin, L.; Lu, N.; Jiang, H.-L. Reactive Oxygen Species-Responsive Nanoprodrug with Quinone Methides-Mediated GSH Depletion for Improved Chlorambucil Breast Cancers Therapy. *J. Controlled Release* **2018**, *274*, 56−68.
(67) Mukerabigwi, J. F.; Yin, W.; Zha, Z.; Ke, W.; Wang, Y.; Chen, W.; Japir, A. A.-W. M. M.; Wang, Y.; Ge, Z. Polymersome Nanoreactors with Tumor pH-Triggered Selective Membrane Permeability for Prodrug Delivery, Activation, and Combined Oxidation-Chemotherapy. *J. Controlled Release* **2019**, *303*, 209−222.
(68) Gong, Y.; Chen, M.; Tan, Y.; Shen, J.; Jin, Q.; Deng, W.; Sun, J.; Wang, C.; Liu, Z.; Chen, Q. Injectable Reactive Oxygen Species-Responsive SN38 Prodrug Scaffold with Checkpoint Inhibitors for Combined Chemoimmunotherapy. *ACS Appl. Mater. Interfaces* **2020**, *12*, 50248−50259.
(69) Luo, C.; Sun, J.; Liu, D.; Sun, B.; Miao, L.; Musetti, S.; Li, J.; Han, X.; Du, Y.; Li, L.; Huang, L.; He, Z. Self-Assembled Redox Dual-Responsive Prodrug-Nanosystem Formed by Single Thioether-Bridged Paclitaxel-Fatty Acid Conjugate for Cancer Chemotherapy. *Nano Lett.* **2016**, *16*, 5401−5408.
(70) Wang, K.; Yang, B.; Ye, H.; Zhang, X.; Song, H.; Wang, X.; Li, N.; Wei, L.; Wang, Y.; Zhang, H.; Kan, Q.; He, Z.; Wang, D.; Sun, J. Self-Strengthened Oxidation-Responsive Bioactivating Prodrug Nanosystem with Sequential and Synergistically Facilitated Drug Release for Treatment of Breast Cancer. *ACS Appl. Mater. Interfaces* **2019**, *11*, 18914−18922.
(71) Gao, C.; Tian, Y.; Zhang, R.; Jing, J.; Zhang, X. Endoplasmic Reticulum-Directed Ratiometric Fluorescent Probe for Quantitive Detection of Basal H_2O_2. *Anal. Chem.* **2017**, *89*, 12945−12950.
(72) Noh, J.; Kwon, B.; Han, E.; Park, M.; Yang, W.; Cho, W.; Yoo, W.; Khang, G.; Lee, D. Amplification of Oxidative Stress by a Dual Stimuli-Responsive Hybrid Drug Enhances Cancer Cell Death. *Nat. Commun.* **2015**, *6*, 6907.
(73) Yang, Y.; Liu, X.; Ma, W.; Xu, Q.; Chen, G.; Wang, Y.; Xiao, H.; Li, N.; Liang, X.-J.; Yu, M.; Yu, Z. Light-Activatable Liposomes for Repetitive On-Demand Drug Release and Immunopotentiation in Hypoxic Tumor Therapy. *Biomaterials* **2021**, *265*, 120456.
(74) Zhang, J.; Zhao, B.; Chen, S.; Wang, Y.; Zhang, Y.; Wang, Y.; Wei, D.; Zhang, L.; Rong, G.; Weng, Y.; Hao, J.; Li, B.; Hou, X.-Q.; Kang, X.; Zhao, Y.; Wang, F.; Zhao, Y.; Yu, Y.; Wu, Q.-P.; Liang, X.-J.; Xiao, H. Near-Infrared Light Irradiation Induced Mild Hyperthermia Enhances Glutathione Depletion and DNA Interstrand Cross-Link Formation for Efficient Chemotherapy. *ACS Nano* **2020**, *14*, 14831−14845.
(75) Zhao, Z.; Wang, W.; Li, C.; Zhang, Y.; Yu, T.; Wu, R.; Zhao, J.; Liu, Z.; Liu, J.; Yu, H. Reactive Oxygen Species−Activatable Liposomes Regulating Hypoxic Tumor Microenvironment for Synergistic Photo/Chemodynamic Therapies. *Adv. Funct. Mater.* **2019**, *29*, 1905013.
(76) Zhu, J.; Xiao, T.; Zhang, J.; Che, H.; Shi, Y.; Shi, X.; van Hest, J. C. M. Surface-Charge-Switchable Nanoclusters for Magnetic Resonance Imaging-Guided and Glutathione Depletion-Enhanced Photodynamic Therapy. *ACS Nano* **2020**, *14*, 11225−11237.
(77) Gao, F.; Yang, X.; Luo, X.; Xue, X.; Qian, C.; Sun, M. Photoactivated Nanosheets Accelerate Nucleus Access of Cisplatin for Drug-Resistant Cancer Therapy. *Adv. Funct. Mater.* **2020**, *30*, 2001546.
(78) Iida, T.; Kijima, H.; Urata, Y.; Goto, S.; Ihara, Y.; Oka, M.; Kohno, S.; Scanlon, K. J.; Kondo, T. Hammerhead Ribozyme against γ-Glutamylcysteine Synthetase Sensitizes Human Colonic Cancer Cells to Cisplatin by Down-Regulating Both the Glutathione Synthesis and the Expression of Multidrug Resistance Proteins. *Cancer Gene Ther.* **2001**, *8*, 803−814.
(79) Cheng, X.; Xu, H.-D.; Ran, H.-H.; Liang, G.; Wu, F.-G. Glutathione-Depleting Nanomedicines for Synergistic Cancer Therapy. *ACS Nano* **2021**, *15*, 8039−8068.
(80) Saravanakumar, G.; Kim, J.; Kim, W. J. Reactive-Oxygen-Species-Responsive Drug Delivery Systems: Promises and Challenges. *Adv. Sci.* **2017**, *4*, 1600124.
(81) Sun, M.; Wang, C.; Lv, M.; Fan, Z.; Du, J. Mitochondrial-Targeting Nanoprodrugs to Mutually Reinforce Metabolic Inhibition and Autophagy for Combating Resistant Cancer. *Biomaterials* **2021**, *278*, 121168.
(82) Li, Y.; Chen, M.; Yao, B.; Lu, X.; Song, B.; Vasilatos, S. N.; Zhang, X.; Ren, X.; Yao, C.; Bian, W.; Sun, L. Dual pH/ROS-Responsive Nanoplatform with Deep Tumor Penetration and Self-Amplified Drug Release for Enhancing Tumor Chemotherapeutic Efficacy. *Small* **2020**, *16*, 2002188.
(83) Hu, J.-J.; Lei, Q.; Peng, M.-Y.; Zheng, D.-W.; Chen, Y.-X.; Zhang, X.-Z. A Positive Feedback Strategy for Enhanced Chemotherapy Based on ROS-Triggered Self-Accelerating Drug Release Nanosystem. *Biomaterials* **2017**, *128*, 136−146.
(84) Song, J.; Lin, L.; Yang, Z.; Zhu, R.; Zhou, Z.; Li, Z.-W.; Wang, F.; Chen, J.; Yang, H.; Chen, X. Self-Assembled Responsive Bilayered Vesicles with Adjustable Oxidative Stress for Enhanced Cancer Imaging and Therapy. *J. Am. Chem. Soc.* **2019**, *141*, 8158−8170.
(85) Ka, H.; Park, H.-J.; Jung, H.-J.; Choi, J.-W.; Cho, K.-S.; Ha, J.; Lee, K.-T. Cinnamaldehyde Induces Apoptosis by ROS-Mediated Mitochondrial Permeability Transition in Human Promyelocytic Leukemia HL-60 Cells. *Cancer Lett.* **2003**, *196*, 143−152.
(86) Xu, X.; Zeng, Z.; Ding, X.; Shan, T.; Liu, Q.; Chen, M.; Chen, J.; Xia, M.; He, Y.; Huang, Z.; Huang, Y.; Zhao, C. Reactive Oxygen Species-Activatable Self-Amplifying Watson-Crick Base Pairing-Inspired Supramolecular Nanoprodrug for Tumor-Specific Therapy. *Biomaterials* **2021**, *277*, 121128.
(87) Zhang, W.; Hu, X.; Shen, Q.; Xing, D. Mitochondria-Specific Drug Release and Reactive Oxygen Species Burst Induced by Polyprodrug Nanoreactors Can Enhance Chemotherapy. *Nat. Commun.* **2019**, *10*, 1704.
(88) Yuan, Y.; Zhang, C.-J.; Liu, B. A Photoactivatable AIE Polymer for Light-Controlled Gene Delivery: Concurrent Endo/Lysosomal Escape and DNA Unpacking. *Angew. Chem., Int. Ed.* **2015**, *54*, 11419−11423.
(89) Chen, H.; Zeng, X.; Tham, H. P.; Phua, S. Z. F.; Cheng, W.; Zeng, W.; Shi, H.; Mei, L.; Zhao, Y. NIR-Light-Activated Combination Therapy with a Precise Ratio of Photosensitizer and Prodrug Using a Host−Guest Strategy. *Angew. Chem., Int. Ed.* **2019**, *58*, 7641−7646.
(90) Wan, Y.; Fu, L.-H.; Li, C.; Lin, J.; Huang, P. Conquering the Hypoxia Limitation for Photodynamic Therapy. *Adv. Mater.* **2021**, *33*, 2103978.
(91) Jiang, L.; Bai, H.; Liu, L.; Lv, F.; Ren, X.; Wang, S. Luminescent, Oxygen-Supplying, Hemoglobin-Linked Conjugated Polymer Nanoparticles for Photodynamic Therapy. *Angew. Chem., Int. Ed.* **2019**, *58*, 10660−10665.
(92) Song, G.; Ji, C.; Liang, C.; Song, X.; Yi, X.; Dong, Z.; Yang, K.; Liu, Z. TaO_x Decorated Perfluorocarbon Nanodroplets as Oxygen Reservoirs to Overcome Tumor Hypoxia and Enhance Cancer Radiotherapy. *Biomaterials* **2017**, *112*, 257−263.
(93) Phua, S. Z. F.; Yang, G.; Lim, W. Q.; Verma, A.; Chen, H.; Thanabalu, T.; Zhao, Y. Catalase-Integrated Hyaluronic Acid as Nanocarriers for Enhanced Photodynamic Therapy in Solid Tumor. *ACS Nano* **2019**, *13*, 4742−4751.
(94) Zhang, W.; Li, S.; Liu, X.; Yang, C.; Hu, N.; Dou, L.; Zhao, B.; Zhang, Q.; Suo, Y.; Wang, J. Oxygen-Generating MnO_2 Nanodots-Anchored Versatile Nanoplatform for Combined Chemo-Photodynamic Therapy in Hypoxic Cancer. *Adv. Funct. Mater.* **2018**, *28*, 1706375.
(95) Sharma, A.; Arambula, J. F.; Koo, S.; Kumar, R.; Singh, H.; Sessler, J. L.; Kim, J. S. Hypoxia-Targeted Drug Delivery. *Chem. Soc. Rev.* **2019**, *48*, 771−813.

(96) Kang, D.; Cheung, S. T.; Wong-Rolle, A.; Kim, J. Enamine N-Oxides: Synthesis and Application to Hypoxia-Responsive Prodrugs and Imaging Agents. *ACS Cent. Sci.* **2021**, *7*, 631−640.
(97) Tomasz, M.; Palom, Y. The Mitomycin Bioreductive Antitumor Agents: Cross-Linking and Alkylation of DNA as the Molecular Basis of Their Activity. *Pharmacol. Ther.* **1997**, *76*, 73−87.
(98) Zhang, X.; Li, X.; Li, Z.; Wu, X.; Wu, Y.; You, Q.; Zhang, X. An NAD(P)H:Quinone Oxidoreductase 1 Responsive and Self-Immolative Prodrug of 5-Fluorouracil for Safe and Effective Cancer Therapy. *Org. Lett.* **2018**, *20*, 3635−3638.
(99) Xin, F.; Wu, M.; Cai, Z.; Zhang, X.; Wei, Z.; Liu, X.; Liu, J. Tumor Microenvironment Triggered Cascade-Activation Nanoplatform for Synergistic and Precise Treatment of Hepatocellular Carcinoma. *Adv. Healthcare Mater.* **2021**, *10*, 2002036.
(100) Zhang, D.; Cai, Z.; Liao, N.; Lan, S.; Wu, M.; Sun, H.; Wei, Z.; Li, J.; Liu, X. pH/Hypoxia Programmable Triggered Cancer Photo-Chemotherapy Based on a Semiconducting Polymer Dot Hybridized Mesoporous Silica Framework. *Chem. Sci.* **2018**, *9*, 7390−7399.
(101) Lee, D.; Jang, S.-Y.; Kwon, S.; Lee, Y.; Park, E.; Koo, H. Optimized Combination of Photodynamic Therapy and Chemotherapy Using Gelatin Nanoparticles Containing Tirapazamine and Pheophorbide A. *ACS Appl. Mater. Interfaces* **2021**, *13*, 10812−10821.
(102) Li, Y.; Sun, Y.; Li, J.; Su, Q.; Yuan, W.; Dai, Y.; Han, C.; Wang, Q.; Feng, W.; Li, F. Ultrasensitive Near-Infrared Fluorescence-Enhanced Probe for *in Vivo* Nitroreductase Imaging. *J. Am. Chem. Soc.* **2015**, *137*, 6407−6416.
(103) Kim, H. S.; Sharma, A.; Ren, W. X.; Han, J.; Kim, J. S. COX-2 Inhibition Mediated Anti-Angiogenic Activatable Prodrug Potentiates Cancer Therapy in Preclinical Models. *Biomaterials* **2018**, *185*, 63−72.
(104) Hu, B.; Song, N.; Cao, Y.; Li, M.; Liu, X.; Zhou, Z.; Shi, L.; Yu, Z. Noncanonical Amino Acids for Hypoxia-Responsive Peptide Self-Assembly and Fluorescence. *J. Am. Chem. Soc.* **2021**, *143*, 13854−13864.
(105) Morihiro, K.; Ishinabe, T.; Takatsu, M.; Osumi, H.; Osawa, T.; Okamoto, A. Floxuridine Oligomers Activated under Hypoxic Environment. *J. Am. Chem. Soc.* **2021**, *143*, 3340−3347.
(106) Yang, G.; Phua, S. Z. F.; Lim, W. Q.; Zhang, R.; Feng, L.; Liu, G.; Wu, H.; Bindra, A. K.; Jana, D.; Liu, Z.; Zhao, Y. A Hypoxia-Responsive Albumin-Based Nanosystem for Deep Tumor Penetration and Excellent Therapeutic Efficacy. *Adv. Mater.* **2019**, *31*, 1901513.
(107) Ge, L.; Qiao, C.; Tang, Y.; Zhang, X.; Jiang, X. Light-Activated Hypoxia-Sensitive Covalent Organic Framework for Tandem-Responsive Drug Delivery. *Nano Lett.* **2021**, *21*, 3218−3224.
(108) Verwilst, P.; Han, J.; Lee, J.; Mun, S.; Kang, H.-G.; Kim, J. S. Reconsidering Azobenzene as a Component of Small-Molecule Hypoxia-Mediated Cancer Drugs: A Theranostic Case Study. *Biomaterials* **2017**, *115*, 104−114.
(109) Zhou, S.; Hu, X.; Xia, R.; Liu, S.; Pei, Q.; Chen, G.; Xie, Z.; Jing, X. A Paclitaxel Prodrug Activatable by Irradiation in a Hypoxic Microenvironment. *Angew. Chem., Int. Ed.* **2020**, *59*, 23198−23205.
(110) Yang, S.; Tang, Z.; Hu, C.; Zhang, D.; Shen, N.; Yu, H.; Chen, X. Selectively Potentiating Hypoxia Levels by Combretastatin A4 Nanomedicine: Toward Highly Enhanced Hypoxia-Activated Prodrug Tirapazamine Therapy for Metastatic Tumors. *Adv. Mater.* **2019**, *31*, 1805955.
(111) Ma, Z.; Zhang, Y.; Dai, X.; Zhang, W.; Foda, M. F.; Zhang, J.; Zhao, Y.; Han, H. Selective Thrombosis of Tumor for Enhanced Hypoxia-Activated Prodrug Therapy. *Adv. Mater.* **2021**, *33*, 2104504.
(112) He, Z.; Dai, Y.; Li, X.; Guo, D.; Liu, Y.; Huang, X.; Jiang, J.; Wang, S.; Zhu, G.; Zhang, F.; Lin, L.; Zhu, J.-J.; Yu, G.; Chen, X. Hybrid Nanomedicine Fabricated from Photosensitizer-Terminated Metal−Organic Framework Nanoparticles for Photodynamic Therapy and Hypoxia-Activated Cascade Chemotherapy. *Small* **2019**, *15*, 1804131.
(113) Ji, Y.; Lu, F.; Hu, W.; Zhao, H.; Tang, Y.; Li, B.; Hu, X.; Li, X.; Lu, X.; Fan, Q.; Huang, W. Tandem Activated Photodynamic and Chemotherapy: Using pH-Sensitive Nanosystems to Realize Different Tumour Distributions of Photosensitizer/Prodrug for Amplified Combination Therapy. *Biomaterials* **2019**, *219*, 119393.
(114) Olson, O. C.; Joyce, J. A. Cysteine Cathepsin Proteases: Regulators of Cancer Progression and Therapeutic Response. *Nat. Rev. Cancer* **2015**, *15*, 712−729.
(115) Anderson, C. F.; Cui, H. Protease-Sensitive Nanomaterials for Cancer Therapeutics and Imaging. *Ind. Eng. Chem. Res.* **2017**, *56*, 5761−5777.
(116) Jiang, J.; Shen, N.; Ci, T.; Tang, Z.; Gu, Z.; Li, G.; Chen, X. Combretastatin A4 Nanodrug-Induced MMP9 Amplification Boosts Tumor-Selective Release of Doxorubicin Prodrug. *Adv. Mater.* **2019**, *31*, 1904278.
(117) Wang, Y.; Du, W.; Zhang, T.; Zhu, Y.; Ni, Y.; Wang, C.; Sierra Raya, F. M.; Zou, L.; Wang, L.; Liang, G. A Self-Evaluating Photothermal Therapeutic Nanoparticle. *ACS Nano* **2020**, *14*, 9585−9593.
(118) Chung, S. W.; Choi, J. U.; Cho, Y. S.; Kim, H. R.; Won, T. H.; Dimitrion, P.; Jeon, O.-C.; Kim, S. W.; Kim, I.-S.; Kim, S. Y.; Byun, Y. Self-Triggered Apoptosis Enzyme Prodrug Therapy (STAEPT): Enhancing Targeted Therapies via Recurrent Bystander Killing Effect by Exploiting Caspase-Cleavable Linker. *Adv. Sci.* **2018**, *5*, 1800368.
(119) Zhang, R.; Yang, J. Y.; Sima, M.; Zhou, Y.; Kopecek, J. Sequential Combination Therapy of Ovarian Cancer with Degradable N-(2-Hydroxypropyl)Methacrylamide Copolymer Paclitaxel and Gemcitabine Conjugates. *Proc. Natl. Acad. Sci. U. S. A.* **2014**, *111*, 12181−12186.
(120) Du, H.; Zhao, S.; Wang, Y.; Wang, Z.; Chen, B.; Yan, Y.; Yin, Q.; Liu, D.; Wan, F.; Zhang, Q.; Wang, Y. pH/Cathepsin B Hierarchical-Responsive Nanoconjugates for Enhanced Tumor Penetration and Chemo-Immunotherapy. *Adv. Funct. Mater.* **2020**, *30*, 2003757.
(121) Lu, L.; Guo, L.; Wang, K.; Liu, Y.; Xiao, M. β-Galactosidases: A Great Tool for Synthesizing Galactose-Containing Carbohydrates. *Biotechnol. Adv.* **2020**, *39*, 107465.
(122) Gnaim, S.; Scomparin, A.; Das, S.; Blau, R.; Satchi-Fainaro, R.; Shabat, D. Direct Real-Time Monitoring of Prodrug Activation by Chemiluminescence. *Angew. Chem., Int. Ed.* **2018**, *57*, 9033−9037.
(123) Liu, P.; Xu, J.; Yan, D.; Zhang, P.; Zeng, F.; Li, B.; Wu, S. A DT-Diaphorase Responsive Theranostic Prodrug for Diagnosis, Drug Release Monitoring and Therapy. *Chem. Commun.* **2015**, *51*, 9567−9570.
(124) Li, B.; Liu, P.; Yan, D.; Zeng, F.; Wu, S. A Self-Immolative and DT-Diaphorase-Activatable Prodrug for Drug-Release Tracking and Therapy. *J. Mater. Chem. B* **2017**, *5*, 2635−2643.
(125) Chen, Z.; Li, B.; Xie, X.; Zeng, F.; Wu, S. A Sequential Enzyme-Activated and Light-Triggered Pro-Prodrug Nanosystem for Cancer Detection and Therapy. *J. Mater. Chem. B* **2018**, *6*, 2547−2556.
(126) Chung, S. W.; Cho, Y. S.; Choi, J. U.; Kim, H. R.; Won, T. H.; Kim, S. Y.; Byun, Y. Highly Potent Monomethyl Auristatin E Prodrug Activated by Caspase-3 for the Chemoradiotherapy of Triple-Negative Breast Cancer. *Biomaterials* **2019**, *192*, 109−117.
(127) Li, C.; Winnard, P. T.; Takagi, T.; Artemov, D.; Bhujwalla, Z. M. Multimodal Image-Guided Enzyme/Prodrug Cancer Therapy. *J. Am. Chem. Soc.* **2006**, *128*, 15072−15073.
(128) Mendes, A. C.; Zelikin, A. N. Enzyme Prodrug Therapy Engineered into Biomaterials. *Adv. Funct. Mater.* **2014**, *24*, 5202−5210.
(129) Cheng, L.; Zhang, F.; Wang, S.; Pan, X.; Han, S.; Liu, S.; Ma, J.; Wang, H.; Shen, H.; Liu, H.; Yuan, Q. Activation of Prodrugs by NIR-Triggered Release of Exogenous Enzymes for Locoregional Chemo-Photothermal Therapy. *Angew. Chem., Int. Ed.* **2019**, *58*, 7728−7732.
(130) Mooney, R.; Abdul Majid, A.; Batalla, J.; Annala, A. J.; Aboody, K. S. Cell-Mediated Enzyme Prodrug Cancer Therapies. *Adv. Drug Delivery Rev.* **2017**, *118*, 35−51.
(131) Zhang, W.; Ji, T.; Li, Y.; Zheng, Y.; Mehta, M.; Zhao, C.; Liu, A.; Kohane, D. S. Light-Triggered Release of Conventional Local

Anesthetics from a Macromolecular Prodrug for On-Demand Local Anesthesia. *Nat. Commun.* **2020**, *11*, 2323.
(132) Liao, L.; Liu, J.; Dreaden, E. C.; Morton, S. W.; Shopsowitz, K. E.; Hammond, P. T.; Johnson, J. A. A Convergent Synthetic Platform for Single-Nanoparticle Combination Cancer Therapy: Ratiometric Loading and Controlled Release of Cisplatin, Doxorubicin, and Camptothecin. *J. Am. Chem. Soc.* **2014**, *136*, 5896−5899.
(133) Barman, S.; Das, J.; Biswas, S.; Maiti, T. K.; Pradeep Singh, N. D. A Spiropyran−Coumarin Platform: An Environment Sensitive Photoresponsive Drug Delivery System for Efficient Cancer Therapy. *J. Mater. Chem. B* **2017**, *5*, 3940−3944.
(134) Jana, A.; Nguyen, K. T.; Li, X.; Zhu, P.; Tan, N. S.; Ågren, H.; Zhao, Y. Perylene-Derived Single-Component Organic Nanoparticles with Tunable Emission: Efficient Anticancer Drug Carriers with Real-Time Monitoring of Drug Release. *ACS Nano* **2014**, *8*, 5939−5952.
(135) Imran, M.; Ayub, W.; Butler, I. S.; Zia-ur-Rehman. Photoactivated Platinum-Based Anticancer Drugs. *Coord. Chem. Rev.* **2018**, *376*, 405−429.
(136) Phillips, H. I. A.; Ronconi, L.; Sadler, P. J. Photoinduced Reactions of *cis,trans,cis*-$[PtIV(N_3)_2(OH)_2(NH_3)_2]$ with 1-Methylimidazole. *Chem.—Eur. J.* **2009**, *15*, 1588−1596.
(137) Vallotto, C.; Shaili, E.; Shi, H.; Butler, J. S.; Wedge, C. J.; Newton, M. E.; Sadler, P. J. Photoactivatable Platinum Anticancer Complex Can Generate Tryptophan Radicals. *Chem. Commun.* **2018**, *54*, 13845−13848.
(138) Farrer, N. J.; Woods, J. A.; Salassa, L.; Zhao, Y.; Robinson, K. S.; Clarkson, G.; Mackay, F. S.; Sadler, P. J. A Potent Trans-Diimine Platinum Anticancer Complex Photoactivated by Visible Light. *Angew. Chem., Int. Ed.* **2010**, *49*, 8905−8908.
(139) He, S.; Li, C.; Zhang, Q.; Ding, J.; Liang, X.-J.; Chen, X.; Xiao, H.; Chen, X.; Zhou, D.; Huang, Y. Tailoring Platinum(IV) Amphiphiles for Self-Targeting All-in-One Assemblies as Precise Multimodal Theranostic Nanomedicine. *ACS Nano* **2018**, *12*, 7272−7281.
(140) Xu, S.; Zhu, X.; Zhang, C.; Huang, W.; Zhou, Y.; Yan, D. Oxygen and Pt(II) Self-Generating Conjugate for Synergistic Photo-Chemo Therapy of Hypoxic Tumor. *Nat. Commun.* **2018**, *9*, 2053.
(141) Yao, H.; Chen, S.; Deng, Z.; Tse, M.-K.; Matsuda, Y.; Zhu, G. BODI-Pt, a Green-Light-Activatable and Carboplatin-Based Platinum(IV) Anticancer Prodrug with Enhanced Activation and Cytotoxicity. *Inorg. Chem.* **2020**, *59*, 11823−11833.
(142) Wang, Z.; Wang, N.; Cheng, S.-C.; Xu, K.; Deng, Z.; Chen, S.; Xu, Z.; Xie, K.; Tse, M.-K.; Shi, P.; Hirao, H.; Ko, C.-C.; Zhu, G. Phorbiplatin, a Highly Potent Pt(IV) Antitumor Prodrug That Can Be Controllably Activated by Red Light. *Chem* **2019**, *5*, 3151−3165.
(143) Deng, Z.; Wang, N.; Liu, Y.; Xu, Z.; Wang, Z.; Lau, T.-C.; Zhu, G. A Photocaged, Water-Oxidizing, and Nucleolus-Targeted Pt(IV) Complex with a Distinct Anticancer Mechanism. *J. Am. Chem. Soc.* **2020**, *142*, 7803−7812.
(144) Bomben, P. G.; Robson, K. C. D.; Sedach, P. A.; Berlinguette, C. P. On the Viability of Cyclometalated Ru(II) Complexes for Light-Harvesting Applications. *Inorg. Chem.* **2009**, *48*, 9631−9643.
(145) Zeng, X.; Wang, Y.; Han, J.; Sun, W.; Butt, H.-J.; Liang, X.-J.; Wu, S. Fighting against Drug-Resistant Tumors Using a Dual-Responsive Pt(IV)/Ru(II) Bimetallic Polymer. *Adv. Mater.* **2020**, *32*, 2004766.
(146) Lin, Q.; Huang, Q.; Li, C.; Bao, C.; Liu, Z.; Li, F.; Zhu, L. Anticancer Drug Release from a Mesoporous Silica Based Nano-photocage Regulated by Either a One- or Two-Photon Process. *J. Am. Chem. Soc.* **2010**, *132*, 10645−10647.
(147) Liu, P.; Li, B.; Zhan, C.; Zeng, F.; Wu, S. A Two-Photon-Activated Prodrug for Therapy and Drug Release Monitoring. *J. Mater. Chem. B* **2017**, *5*, 7538−7546.
(148) Chaudhuri, A.; Mengji, R.; Venkatesh, Y.; Jana, A.; Pradeep Singh, N. D. An Improved Tumor-Specific Therapeutic Strategy by the Spatio-Temporally Controlled *in Situ* Formation of a Cu(II) Complex, Leading to Prompt Cell Apoptosis *via* Photoactivation of a Prodrug. *Chem. Commun.* **2020**, *56*, 4559−4562.
(149) Zhao, L.; Peng, J.; Huang, Q.; Li, C.; Chen, M.; Sun, Y.; Lin, Q.; Zhu, L.; Li, F. Near-Infrared Photoregulated Drug Release in Living Tumor Tissue *via* Yolk-Shell Upconversion Nanocages. *Adv. Funct. Mater.* **2014**, *24*, 363−371.
(150) Yao, X.; Li, M.; Li, B.; Xue, C.; Cai, K.; Zhao, Y.; Luo, Z. Tumor-Targeted Upconverting Nanoplatform Constructed by Host-Guest Interaction for Near-Infrared-Light-Actuated Synergistic Photodynamic-/Chemotherapy. *Chem. Eng. J.* **2020**, *390*, 124516.
(151) Ahmad, W.; Wang, J.; Li, H.; Ouyang, Q.; Wu, W.; Chen, Q. Strategies for Combining Triplet−Triplet Annihilation Upconversion Sensitizers and Acceptors in a Host Matrix. *Coord. Chem. Rev.* **2021**, *439*, 213944.
(152) Huang, L.; Zhao, Y.; Zhang, H.; Huang, K.; Yang, J.; Han, G. Expanding Anti-Stokes Shifting in Triplet−Triplet Annihilation Upconversion for *in Vivo* Anticancer Prodrug Activation. *Angew. Chem., Int. Ed.* **2017**, *56*, 14400−14404.
(153) Lv, W.; Li, Y.; Li, F.; Lan, X.; Zhang, Y.; Du, L.; Zhao, Q.; Phillips, D. L.; Wang, W. Upconversion-Like Photolysis of BODIPY-Based Prodrugs *via* a One-Photon Process. *J. Am. Chem. Soc.* **2019**, *141*, 17482−17486.
(154) Wang, H.; Lv, B.; Tang, Z.; Zhang, M.; Ge, W.; Liu, Y.; He, X.; Zhao, K.; Zheng, X.; He, M.; Bu, W. Scintillator-Based Nanohybrids with Sacrificial Electron Prodrug for Enhanced X-Ray-Induced Photodynamic Therapy. *Nano Lett.* **2018**, *18*, 5768−5774.
(155) Li, Y.; Gong, T.; Gao, H.; Chen, Y.; Li, H.; Zhao, P.; Jiang, Y.; Wang, K.; Wu, Y.; Zheng, X.; Bu, W. ZIF-Based Nanoparticles Combine X-Ray-Induced Nitrosative Stress with Autophagy Management for Hypoxic Prostate Cancer Therapy. *Angew. Chem., Int. Ed.* **2021**, *60*, 15472−15481.
(156) Geng, J.; Zhang, Y.; Gao, Q.; Neumann, K.; Dong, H.; Porter, H.; Potter, M.; Ren, H.; Argyle, D.; Bradley, M. Switching on Prodrugs Using Radiotherapy. *Nat. Chem.* **2021**, *13*, 805−810.
(157) Shi, Z.; Wu, J.; Song, Q.; Göstl, R.; Herrmann, A. Toward Drug Release Using Polymer Mechanochemical Disulfide Scission. *J. Am. Chem. Soc.* **2020**, *142*, 14725−14732.
(158) Huo, S.; Zhao, P.; Shi, Z.; Zou, M.; Yang, X.; Warszawik, E.; Loznik, M.; Göstl, R.; Herrmann, A. Mechanochemical Bond Scission for the Activation of Drugs. *Nat. Chem.* **2021**, *13*, 131−139.
(159) Li, G.; Lin, P.; Wang, K.; Gu, C.-C.; Kusari, S. Artificial Intelligence-Guided Discovery of Anticancer Lead Compounds from Plants and Associated Microorganisms. *Trends Cancer* **2022**, *8*, 65−80.
(160) Vamathevan, J.; Clark, D.; Czodrowski, P.; Dunham, I.; Ferran, E.; Lee, G.; Li, B.; Madabhushi, A.; Shah, P.; Spitzer, M.; Zhao, S. Applications of Machine Learning in Drug Discovery and Development. *Nat. Rev. Drug Discovery* **2019**, *18*, 463−477.
(161) Mizera, M.; Lewandowska, K.; Miklaszewski, A.; Cielecka-Piontek, J. Machine Learning Approach for Determining the Formation of β-Lactam Antibiotic Complexes with Cyclodextrins Using Multispectral Analysis. *Molecules* **2019**, *24*, 743.
(162) Xiong, F.; Ling, X.; Chen, X.; Chen, J.; Tan, J.; Cao, W.; Ge, L.; Ma, M.; Wu, J. Pursuing Specific Chemotherapy of Orthotopic Breast Cancer with Lung Metastasis from Docking Nanoparticles Driven by Bioinspired Exosomes. *Nano Lett.* **2019**, *19*, 3256−3266.
(163) Wang, L.; Jing, P.; Tan, J.; Liao, C.; Chen, Y.; Yu, Y.; Zhang, S. "One-Stitch" Bioorthogonal Prodrug Activation Based on Cross-Linked Lipoic Acid Nanocapsules. *Biomaterials* **2021**, *273*, 120823.
(164) Miller, M. A.; Mikula, H.; Luthria, G.; Li, R.; Kronister, S.; Prytyskach, M.; Kohler, R. H.; Mitchison, T.; Weissleder, R. Modular Nanoparticulate Prodrug Design Enables Efficient Treatment of Solid Tumors Using Bioorthogonal Activation. *ACS Nano* **2018**, *12*, 12814−12826.
(165) Zhang, Y.; Cui, H.; Zhang, R.; Zhang, H.; Huang, W. Nanoparticulation of Prodrug into Medicines for Cancer Therapy. *Adv. Sci.* **2021**, *8*, 2101454.
(166) Dong, X.; Brahma, R. K.; Fang, C.; Yao, S. Q. Stimulus-Responsive Self-Assembled Prodrugs in Cancer Therapy. *Chem. Sci.* **2022**, *13*, 4239−4269.

(167) Hou, B.; Zhou, L.; Wang, H.; Saeed, M.; Wang, D.; Xu, Z.; Li, Y.; Yu, H. Engineering Stimuli-Activatable Boolean Logic Prodrug Nanoparticles for Combination Cancer Immunotherapy. *Adv. Mater.* **2020**, *32*, 1907210.

https://doi.org/10.1021/acsnano.2c05379
ACS Nano 2022, 16, 13513−13553